Tesis Verimliliğinin Arttırılması Amacıyla Delme-Patlatma Optimizasyonu

Stephen Chanda

YÜKSEK LİSANS TEZİ

Maden Mühendisliği Anabilim Dalı

Mayıs 2019

Mine-to-Mill Optimisation for Increased Throughput and Profitability

Stephen Chanda

MASTER OF SCIENCE THESIS

Department of Mining Engineering

May 2019

Mine-to-Mill Optimisation for Increased Throughput and Profitability

A thesis submitted to Eskişehir Osmangazi University
Graduate School of Natural and Applied Sciences in partial
fulfillment of the requirements for the degree of Master of Science in
in Discipline of Mining Engineering of the Department of Mining Engineering
by

Stephen Chanda

Supervisor: Prof. Dr. Melih İphar

May 2019

APPROVAL OF THE THESIS

This thesis titled "Mine-to-Mill Optimisation for Increased Throughput and Profitability" and submitted by Stephen Chanda has been accepted as satisfactory in partial fulfillment of the requirements for the degree of Master of Science in Mining Engineering.

Supervisor **:** Prof. Dr. Melih İphar

Second Supervisor **:** -

Examining Committee Members:

Member : Prof. Dr. Melih İphar

Member : Prof. Dr. Mahmut Yavuz

Member : Dr. Öğr. Üyesi Erkan Özkan

Graduation of Stephen Chanda was approved by the Graduate School Board Decision on ..... with the decision number of .....

Prof. Dr. Hürriyet ERŞAHAN
Director of the Institute

ETHICAL STATEMENT

I hereby declare that this thesis study titled “Mine-to-Mill Optimisation for Increased Throughput and Profitability” has been prepared in accordance with the thesis writing rules of Eskişehir Osmangazi University Graduate School of Natural and Applied Sciences under academic consultancy of my supervisor Prof. Dr. Melih Iphar. I hereby declare that the work presented in this thesis is original. I also declare that, I have respected scientific ethical principles and rules in all stages of my thesis study, all information and data presented in this thesis have been obtained within the scope of scientific and academic ethical principles and rules, all materials used in this thesis which are not original to this work have been fully cited and referenced, and all knowledge, documents and results have been presented in accordance with scientific ethical principles and rules. 20/05/2019

Stephen Chanda

Signature

ÖZET

Sentinel Madeni (Kalumbila Madeni olarak da bilinir), First Quantum Minerals'e ait ve Kuzey-Batı Zambiya eyaletindeki Solwezi kasabasıdan yaklaşık 150 km uzaklıktaki Kalumbila şehrinde Kalumbila Minerals Limited tarafından işletilen büyük ölçekli bir bakır ocağıdır. Delme-patlatma ve zenginleştirme işlemlerinin performansını arttırmak amacıyla söz konusu bakır madeninde ocaktan-tesise (M2M) olarak adlandırılan bir optimizasyon çalışması yapılmıştır. Madencilik faaliyetleri ile cevher hazırlama süreçlerinin birbiri ile ilişkili olmasından dolayı her bir sürecin performansı bir diğerini etkilemektedir ve bu iki süreç birbiri ile uyum içerisinde olmalıdır. Ocaktan-tesise optimizasyon çalışması, madencilik faaliyetleri ve cevher hazırlama işlemlerinin performanslarını arttırmak amacıyla bu süreçlerin birbirleriyle ilişkili olan aşamalarını optimize etmek için bu iki süreci birbirine bağlamaktadır. Bu araştırmada, kapsamlı bir bilimsel ve mühendislik yöntembilimi kullanılmıştır. Bu yöntembilim, ocaktan-tesise stratejileri hakkında bilgi sahibi olabilmek amacıyla karşılaştırmalı değerlendirme çalışmalarını içermektedir. Ayrıca, maden yatağının jeolojik oluşumunu anlayabilmek amacıyla cevher karakterizasyonu yapılmış ve cevher yatağı farklı cevherleşme zonlarına ayrılmıştır. İncelenen bakır ocağında, sorunların neden kaynaklandığını ve bu sorunlara karşı alınabilecek önlemlerin belirlenebilmesi amacıyla cevher zenginleştirme tesisindeki ufalama devresi ile ilgili bir inceleme yapılmıştır. Bu ilk aşamada elde edilen sonuçlar; optimum kırma-eleme için gereken P_{80} değeri dikkate alınarak, delme parametrelerini optimize eden parçalanma modellerini geliştirmek amacıyla kullanılmıştır. Optimize edilmiş delme tasarımının uygulanması sonucunda meydana gelecek parçalanmanın tahmininde Kuz-Ram, Kırılmış Zon ve Swebrec Modelleri kullanılmıştır. Her bir P_{80} değeri için spesifik kırma enerjisini tahmin etmek için Morrel tarafından önerilen model kullanılmıştır. Son olarak, önerilen değişikliklerin uygulanması durumunda karşılaşılabilecek kazanç veya zararın parasal değerinin belirlenmesi için bir maliyet analizi yapılmıştır. Geliştirilen model; önerilen değişiklikler uygulandığı takdirde, kırıcı ve değirmen veriminde % 13'lük bir artış sağlanacağını ve kırılan ton başına maliyette 0,05 dolarlık tasarruf sağlanacağını göstermiştir.

Anahtar Kelimeler: Ocaktan-tesise, delme patlatma, parçalanma, Kuz-Ram modeli, Swebrec fonksiyonu, Kırılmış zon modeli, optimizasyon, Sentinel Madeni.

ABSTRACT

Sentinel Mine (also referred to as Kalumbila Mine) is a large scale copper mine owned by First Quantum Minerals and operated by Kalumbila Minerals Limited in Kalumbila, about 150km from Solwezi town in the North-western province of Zambia. A Mine-to-Mill (M2M) optimisation study was undertaken at the mine in order to enhance the performance of drilling and blasting and the comminution processes. Because the process of mining and mineral beneficiation is interlinked, the performance of the one affects the other, there is need to integrate the operation of the two. M2M links these two processes in order to optimise the combined stages of mining and processing with the aim of enhancing the performance of mining and mineral processing activities.

A comprehensive scientific and engineering methodology was used in this research. This included undertaking benchmarking studies to get acquainted with the M2M strategies, and ore characterization to understand the ore geology resulting into dividing the orebody into ore domains. A survey of the comminution circuit in the mineral processing plant was undertaken to identify the sources of bottlenecks and opportunities at the studied copper mine. The results obtained from these initial phases were used to develop fragmentation models that optimised the drilling parameters with respect to the P_{80} value needed for optimal crushing and milling.

The Kuz-Ram, Crushed Zone Model and the Swebrec Model were used to model and predict fragmentation that would result from the optimised drilling pattern. Morrel's model was used to predict the specific comminution energy for each P_{80} value produced. Finally, a cost analysis was conducted to attach a monetary value to the saving or loss that can be encountered in case of the proposed changes are applied. The developed model showed that if the proposed changes are applied there will be a 13% increase in the crusher and mill throughput and there will be an overall saving of $0.05 per tonne crushed.

Keywords: Mine-to-Mill, drilling and blasting, fragmentation, Kuz-Ram model, Swebrec function, Crushed zone model, optimisation, Sentile Mine.

ACKNOWLEDGMENT

I wish to thank my project supervisor Prof. Dr Melih İphar for support and guidance rendered during my research. Despite his busy schedule and being in two different continents during the research period, he always found time to attend to me.

I wish to express my gratitude to the Turkish government for offering me the sponsorship to pursue my studies.

Special thanks go to all my lecturers despite not being proficient in the language of instruction, they were patient with me and ensured that I understand what they were teaching. *Allah razi olsun!*

I thank Eng. George. B. Keyser and the management of First Quantum Kalumbila Minerals Limited for allowing me to do this research at their company.

I wish to convey special thanks to Eng. Jaco Botha, the Technical Manager at Kalumbila Mine for the technical support, guidance and motivation rendered to me.

I thank Eng. Bwalya Kasonde, who played a pivotal role during my entire time I was at KML and for being a true friend.

To my friends, course mates and TÖMER mates, I wouldn't have had done it without you guys.

Special appreciation goes to my family for their moral support and for allowing me to leave home for a long period of time to pursue my studies.

This work is dedicated to my late father Mr Stephen Chanda (SNR) and my loving and caring mother Mrs Febby. K. B. Chanda.

TABLE OF CONTENTS

Page

TABLE OF CONTENTS (Continued)

Page

TABLE OF CONTENTS (Continued)

Page

LIST OF FIGURES

Figure **Page**

LIST OF FIGURES (continued)

Figure **Page**

LIST OF TABLES

Table **Page**

LIST OF ABBREVIATIONS

Abbreviation	Description
AG	Autogenous mill
ANFO	Ammonium Nitrate and Fuel Oil
AEISG	Australian Explosives Industry And Safety Group Inc.
ASTM	American Society for Testing and Material
B	Burden
BI	Blastability Index
BME	Bulk Mining Explosives
CZI	Crush Zone Index
DTH	Down the hole hammer
EDD	Electronic delay detonator
FQML	First Quantum Minerals Limited
HF	Rock hardness factor
ISRM	International Society for Rock Mechanics
JKMRC	Julius Kruttschnitt Mineral Research Centre
KCO	Kuznetsov – Cunningham – Ouchterlony Model
KML	Kalumbila Minerals Limited
M2M	Mine-to-Mill
MMPT	Metso Minerals Process Technology Asia-Pacific & South America
MMU	Mobile mixing Unit
OTA	Ore type A
OTB	Ore type B
OW_i	Operating work Index
PETN	Pentaerythritol tetranitrate,
PIO	Process Integration and Optimisation
RDI	Rock density influence
RDM	Rock mass description
ROM	Run of Mine
RQD	Rock Quality Designation
S	Spacing

LIST OF ABBREVIATIONS (continued)

Abbreviation	Description
SABC	SAG/Ball/Pebble Crushing
SAG	Semi-Autogenous mill
SD	Subdrill
SDOB	Scaled depth of burial
St	Stemming
TSF	Tailings storage facility
UCS	Uniaxial Compressive Strength
ZCCM-IH	Zambia Consolidated Copper Mines-Investment Holding

1. INTRODUCTION AND PURPOSE

Drilling and Blasting are considered to be the first unit process of mining. In the mining and minerals industry, blasts are designed with the aim of fracturing and breaking the insitu rock for excavation and eventual transportation. This Run of Mine (ROM) is considered well fragmented when it is loose and fine enough for efficient mucking and loading operations. Hence mining optimisation strategies focuses on minimising the total cost of mining while maintaining optimal fragmentation size of the run of mine. Therefore, the designing of production blasts is aimed at achieving optimal swell and shape of the muckpile and fragmentation size that will result in increased productivity of the shovels and the trucks. In addition to this, these blasts should also produce minimum dilution and minimum negative effects on the adjacent pit walls and floor of the pit. (Jankovic and Valery, 2002). However, this approach ignores the impact that fragmentation size has on ore comminution. Results of several researches has shown that blast designs that are done to provide a run of mine fragmentation to optimize crushing and grinding operations results in enhanced overall efficiency, and an increase in productivity and reduction in the costs.

It is against this background that this research was sanctioned so as to develop a strategy that will satisfy both the loading and hauling fragment requirement and the crushing and grinding passing percentage that will optimize the overall operation costs.

The objective of Mine-to-Mill (M2M) optimisation is to develop and implement integrated mining and processing strategies tailored to the operation in order to minimize the overall cost per tonne treated and maximize company profit in a sustainable manner. Part of the strategy focus on modelling blasting operations (blast designs, charging and blasting practices) with the effect it has on the comminution process in mind. The other part deals with modelling of the crushing and milling operation with the aim of reduce electricity and water consumption, thus reducing the cost of treatment per ton of ore treated. Mine to mill relies on the fact that comminution is usually a site-specific process and that blasting is more efficient at breaking rock than grinding. These strategies are thus aimed at enhancing the performance of mining and downstream activities (Jankovic and Valery, 2002). Research

has demonstrated that by manipulating blast designs, explosive quality and type, a finer fragmentation from blasting could be achieved.

Kalumbila Minerals (Sentinel Mine) has been facing challenges with blast fragmentation. Despite a lot of effort by the technical and production teams at Sentinel mine to optimise the drilling and blasting operation so as to achieve an optimal fragment size, challenges still remain. This is partly because the ore deposit is contained within a rock with different geotechnical properties, making blast modelling hard. This can also be attributed to that fact that separate or independent optimisation work is done by the mining and the processing teams, thus neglecting the effect that one process has on the other. This has affected the mining operation productivity, crusher and milling throughput. Thus, it contributes to a higher cost of operation. In order to increase the productivity and efficiency in the mining phase, the crushing and milling throughput and the entire comminution processing, this research was justified. Not only will this research provide a working site-specific operation mine-to-mill strategy, it will also provide the basis of such strategy for the Zambian mines, and the world at large.

The main objective of this research is to develop a working site-specific Mine-to-Mill strategy, that will result in increasing the crusher and milling throughput and a reduction in the overall operating costs, through modelling, simulation and optimisation of blasting. Through a comprehensive literature review and industrial practice, a M2M strategy was developed. This research had the following sub-objectives:

1. To undertake an all-inclusive review of sources and types of bottlenecks in mine to mill operations.
2. To conduct a rock characterization exercise so as to establish the qualities of the rock and ore that influence blasting and comminution performance. This is because rock characterisation is very important to blastability and grindability of ore. This characterization results will be used to define and characterize the rock domains.
3. To investigate the effect of the rock domains on the blastability and grindability of the rock.
4. To develop blast fragmentation prediction models. The rock characteristics will be used to develop a blasting model for easier blast modelling. This model will be

compared to the current blasting models and will be validated. The validated fragmentation model will be used to optimize blasting operations for improved rock fragmentation.

5. To incorporate a “cost” component in the drill and blast model that will be developed so that an estimation of the costs of drilling and blasting can be made even before the actual execution of the design.

In order to successfully address the aforementioned problems, and to achieve the research objectives, this research seeks to address the following questions:

1. What is the current drilling practice at the mine?
2. What is the current blasting practice at the mine?
3. How is the implementation of the current drilling and blasting plans, is it accurate or not?
4. What is the current crushing and milling trend to the mine? What is the current throughput for the primary and secondary crushers and for the Ball mils?
5. What is the cost associated with blasting and milling?
6. What are the opportunities to improve in operation efficiency that can result in cost saving?

2. LITERATURE REVIEW

2.1. Introduction

Mine to Mill (M2M) strategies have been developed and utilized in several mines as a way of improving operation efficiency. This chapter gives a review and the summary of M2M works that have been carried out and resulted in positive gains to mine companies. A review of research on the effect of delay timing on fragmentation and prediction of comminution specific energy is also given.

2.2. Literature Reviews

In his book 'What is Mine to Mill', McKee (2013), defines Mine to Mill as an "*operating strategy for mining operations to enhance the performance of mining and downstream processing activities*". He went on to highlight some of the benefits that has proved to occur when a proper Mine to Mill strategy is implemented. He states that productivity gains in the range of 10-20% have been achieved while reducing the overall operating costs. This is possible by utilizing effort and cost at the most critical parts of the production chain to achieve overall productivity and cost optimisation. Another benefit of Mine to Mill optimisation is improvement in the predictability and hence consistency of both mining and processing performance by providing performance benchmarks for the range of ore types present in every mining operation. By means of such predictability, operations have the opportunity to identify when performance goes below the set benchmark, allowing them to commence corrective measures. McKee (2013) further highlights the technical and non-technical keys to a successful Mine to Mill optimisation. Some of the non-technical elements of Mine to Mill are listed as follows:

- The site general manager and higher level cooperate members need to show a positive drive and support to this process.
- In order to develop and implement a successful and suitable M2M strategy, a dedicated team of mining and metallurgical engineers should be constituted.

- For successful implementation of the strategy, there should be a pool of skilled supervisors and operators at the field level.
- Since people tend to resist change, there must be a wiliness to change from the already working practice to this new strategy.
- In order to track the change, there should be put in place a monitoring and evaluation system that is effective and able to report the production and cost of the new system.

When these non-technical keys are in place, the technical expert can come in and implement a M2M process that will result in substantial gains to the company.

Esen et al. (2007) describes the Process Integration and Optimisation (PIO) methodology that had been developed by Metso Minerals Process Technology Asia-Pacific & South America (MMPT). MMPT has undertaken several works at different mining sites that has resulted in positive gains for the mines (Lam et al., 2001; Valery et al., 2007; Gomes et al., 2010; Valery et al., 2011; Rybinski et al., 2011; Isokangas et al., 2012; Hart et al., 2011; Hakami et al., 2015; Valery et al., 2016). This methodology is used for optimising blasting and comminution processes in terms of fragmentation. A successful PIO involves stages like scooping, rock characterisation and domain definition, measuring current and proposed parameters, modelling and simulation of both blasting and comminution process and where needed material tracing is undertaken. The overall objective of a PIO strategy is to minimise the total operating cost of the entire mining and processing, leading to a positive effect on the entire mining operation. By evaluating and considering process constraints such as ore dilution, characteristic of muckpile, size and make of mining equipment, and installed power of crushing and milling equipment and other process bottlenecks in blast designs, increase in production, generating typically 5 to 20% higher milling throughput has been achieved.

Renner et al. (2006) investigated and implemented a M2M process at Ashanti AngloGold mine in Ghana. In a bid to reduce and optimise the cost of operation and increase SAG mill throughput, AngloGold Ashanti contracted METSO minerals to undertake an optimisation works at their mine. In order to achieve this, METSO undertook an extensive study with the work including ore body characterization, through blasting practice, blast fragmentation, crushing and milling optimisation. Several blasting scenarios with different

drill pattern parameters were conducted. This modelling resulted in the adoption of higher powder factor for 6 m and 9 m bench heights, giving an improved overall comminution performance. Due to the reduced drilling pattern size, an increase in rock fragmentation was recorded at the mine and the usage of the rock breaker for secondary breaking of big boulders was reduced by 75%. SAG throughput increases of 21% and 32.4% and utilization increase from 61% to 62.1% and 61 to 64% was achieved with the 6 m and 9 m PIO blasts, respectively. Blockage at the crushing plant was also reduced, resulting in 10% decrease downtime. The reduction in milling circuit load resulted in reduction in wear on pumps, pipes and cyclone. Further downstream, an improvement in F_{80} to the leach was recorded which resulted in recovery improvement from 91.2% to 91.65% (6 m PIO) and 91.2% to 92.05% (9 m PIO). Overall, there had been positive impacts on most aspects of the operations with a modest increase in drilling and blasting cost.

Burger et al. (2007) describes a comprehensive model that has been developed by PT Newmont Nusa Tenggara (PTNNT)and MMPT-AP for forecasting and optimising throughput at the Batu Hijau operation. The mechanistic models of blast fragmentation, ore crushing, and milling were used as the basis for developing an optimisation model. The ore domains that were defined during ore/rock characterization and their properties (e.g. lithology, Point Load Index, Rock Quality Designation, Bond Work Index, design and operating conditions), formed the main characteristic input into the model. Due to improvement in the blasting practice, increase in the fragmentation of harder rock was achieved with a 2-7% increase in milling throughput since late 2013 when the project was implemented. This increase in throughput resulted in an increase in flotation feed size from 200 to 240 µm, with minor snags in the floatation recovery.

Compamia Minera Antamina mine, located in the central Peruvian Andes, is predominantly a copper and zinc mine with molybdenum and lead/bismuth/silver concentrates produced as concentrate by-products. The mine wanted to increase the throughput of the SAG mill through integration and optimisation of blast fragmentation, crushing and grinding of the M4/M4A (CuZn) ores which is harder than other ore domains. Rybinski et al. (2011) reports that in order to achieve these goals, the mine contracted Metso Process Technology and Innovation (PTI) to undertake a complete mine to mill optimisation of the mine operations. The Antamina mining complex consists of six different ore types

that are processed on the basis of grinding and flotation requirements. The M4/M4A copper/zinc ore zone presented challenges and limited the throughput to just half of that achieved from the M1/M2 predominantly copper ore. This throughput was just in the range of 2,000-2,500 tph for the M4/M4A vs. 4,000-5,000 tph for the M1/M2. It was reported that in order to achieve a more stable feed grade for the downstream separation process, the M4/M4A ore types are blended. Therefore, concentration was set on the increasing of milling throughput of the harder M4/M4A ore type. In order to achieve the objectives, the Metso PIO methodology was implemented. This included reviewing of the current operating practice at the mine, ore domain characterization into blocks with similar blasting/fragmentation properties, measurement of the outcome from blast design implementation, and defining process constraints such as wall stability. The current drilling and blasting operations were also reviewed and benchmarked. Material movement during blasting using SmartTag^{TM} system was also undertaken. In the comminution stage, a comprehensive survey and analysis of the milling circuits was done and finally M2M modelling and simulation were conducted to achieve an optimum operating strategy that were finally implemented. The results from the first phase showed an increase in the SAG throughput to 3600 tph against the budget of 2700 tph. The eventual target was set to be 4400 tph of hard CuZn ore by the end of the project implementation in 2010.

Porgera Joint Venture (PJV) located in Papua New Guinea and Dyno Nobel initiated a project to optimize drilling and blasting practices to improve the performance of downstream operations (Lam et al., 2001). After recognizing that the optimisation of drill and blast practices to maximize the productivity of mine and mill operations would contribute to its profitability, PJV and Dyno Nobel (explosive supplier) embarked on this project with the goal of optimizing fragmentation for downstream processes. The initial aim was to increase SAG mill throughput when milling hornblende diorite. After auditing and surveying the current performance, site specific models of the process from blasting to SAG milling were calibrated. These models were linked, and simulations performed to study the effect of blast fragmentation on SAG mill throughput.

A modified blast design at a higher powder factor was selected to produce a finer feed to the primary crusher and SAG mill. The modified blast of 4.5×5.5 with a powder factor of 0.8 kg/t was used. Two modified blasts were fired and an increase of 774 dmtph

or 15% in the mill throughput was measured. Mill simulation revealed that an opening smaller than 70 mm would be detrimental to SAG mill throughput. A smaller grate opening will result in lower throughput because critical size material will occupy more mill volume and not break efficiently. It was thus concluded that it is better to remove this material from the mill and crush it.

The Kinross Paracatu mine is a low-grade gold ore deposit (average 0.44 g/t gold) in Brazil. Since its commission in 2009, the mine was operating below the designed processing capacity. A decision was thus made to engage Metso PTI to review and optimize the mine's operating strategies so as the reach the SAG mill designed throughput and the size of the final grinding products (Gomes et al., 2010). By looking at the process variables, a complete survey of the milling circuit and a full mass balance via model fitting, a PIO strategy was implemented. This strategy also considered possible changes to the circuit and propose an alternative strategy of operation. The Kinross Paracatu consists of two processing plants: an old one that has 5 lines ball mill and a new SAG mill. The new circuit consists of one SAG mill with two ball mills which are in a closed circuit with the two cyclones having 18 units of clusters each. There is no pebble crusher in the circuit, thus the oversize from the SAG mill returns back to the mill while the undersize is discharged to the trommel screen which further provides the ball mill feed through its 12.5 mm aperture. Ore characterization was conducted on the ore samples via test such as Bond Ball Mill Work Index, Drop Weight and Point Load tests. The results of this characterisation were used as inputs to the analysis of the effect on throughput and final product size of the variability of ore in the circuit. Metso also undertook a complete survey of the milling circuit to observe and benchmark the operation conditions. The JKSimMet Software was used to validate the results obtained from the survey and also to estimate any flow rate data that could not be collected during the survey through mass balancing and modelling. Several simulations were conducted that ranged from playing with the feature of the SAG mill futures to an introduction of the third ball mill. After the successful implementation of this project, the SAG throughput increased to 3000 tph and the grind size returned on a 200µm reduced from 40% to 20%. However, in order to achieve the design capacity of 5087 tph, installation of a third mill was proposed. Due to the increase in SAG throughput and the reduction in grind size, gold recovery increased to 70% from about 40%.

Located to the North-East of Laos capital Vientiane is the Phu Kham copper-gold mine operated by Phu Bia Mining Limited. This deposit is extremely heterogeneous and is very complex in terms of mineralogy, geology and geotechnical. This complexity affects the plant throughput and performance. Expected increase in the ore strength and competent possess a potential limitation on the future throughput of the Phu Kham operations (Bennett et al., 2014). In order to ascertain how to maintain the current operating rate in terms of throughput, for the entire life-of-mine, the mine management, with the help of Metso conducted a thorough throughput forecasting and optimisation project. The project employed the Metso's PIO methodology. The long-term objective of identifying future opportunities for increasing throughput and the overall comminution process was done. This was in addition to short term goal of identifying what is required with regards to secondary crushing in order to maintain the current throughput. Ore characterization resulted in the identification and grouping of the orebody into 9 ore domains. These domains were defined such that after blasting, ore enclosed in a domain will produced similar fragmentation from a given blast design. Metso's PTI blast fragmentation model was used to model and simulate fragmentation of the current ore blocks and of that which would be encountered as the pit goes dipper. The data obtained in the ore characterization stage was used to calibrate the model while the results from the image analysis were used to calibrate the coarser end of the fragmentation function. Primary crusher cut samples were used in validating the model. Correlation between the predicted and measured values demonstrated the accuracy of the prediction model. Using the results from the 6 simulations, it was showed that tightening the blast pattern leading to an increase in the powder factor resulted into a notable increase in the amount of generated fines. The new blast designs also included a reduction in the stemming height, thus an increase in the amount of explosives near the collar. This resulted in an increase in the fragmentation and a reduction in large borders in this region, too. Comminution modelling and simulation was also conducted. The integrated simulation showed that by increasing the powder factor would result in a 4%-6.55% increase in SAG throughput.

Several researches on the effect of timing on fragmentation have been conducted (Stagg and Nutting, 1987; Stagg and Rholl, 1987; Otterness et al. 1991; Katsabanis and Liu, 1996; Katsabanis et al., 2006; Johansson and Ouchterlony, 2013). These researches involved both theoretical and experimental tests. Katsabanis and Omidi (2015) conducted

experimental investigations into the effect of delay time on fragmentation. They used small-scale experiments of blocks made of grout in their analysis. Despite small scale test being criticised (Rossmanith, et al., 2009) for their boundary effects, the tests conducted in this experiment were considered large enough to draw a conclusion on the effect of timing on fragmentation.

Katsabanis et al. (2014a, 2014b) reviewed the timing requirements for optimised fragmentation. In their test, test samples made from commercial high strength grout with the dimension of 60×40×25 cm test samples were used in these tests This grout had a UCS of 60 MPa, density of 2.34 g/cm^3 and a P-wave velocity of 4000 m/s, making it generally ideal for the tests. Using 7.5cm burden and 10.5cm spacing dimensions, boreholes were drilled in the grout using a wooden dowel. Two strand of detonating cords with an equivalent 4.89 g Pentaerythritol Tetranitrate (PETN) charge were used as explosive. Delays corresponding to 2.5, 5 and 10 ms/m of burden were used. The results for unlined tests showed that short delay (less than 1 ms) produced finer fragments while longer delay (more than 1 ms) showed an increase in the median size of the fragments. It was also shown that fragmentation is not only affected by delay time but also geological condition that is not homogeneous even within the same bench.

Johansson (2011) conducted small-scale tests to ascertain the effects of confinement and initiation delay on fragmentation. He used 650/660×205×300 mm blocks drilled with two rows of 10 mm diameter hole, with 5 holes per role. The burden and spacing of 110 mm and 70 mm was used. The results showed that if delay is set such that there is wave interaction there is no major difference in the fragment size. However, there was a decrease in the mean fragment size by 20% at a delay time of 1 ms/m of burden when compared to that of 2 ms/m. Armed with this background, it was further conducted some tests to determine the effect of wave collision on fragmentation (Johnson, 2014). Having a dimension of 38×19×19 cm masonry blocks wrapped in geotextile fabric and a wire mesh fragments containment were used so as to enable analysis of the in situ tensile crack formation. Short and instantaneous delay was used to provide shock waves which were analysed. Simulations using ANSYS Autodyn was conducted and the comparisons between simulated and experimental results were done. The result showed that wave collision from single blast hole denotation had a positive effect on fragmentation and material flow, thus, a

reduction in the fragment size resulted. The other conclusion made was that the angle of shock front contributes largely to the reflection of the shock waves.

Hettinger (2015) investigated the effect of short hole-to-hole delays on rock fragmentation. Unlike many test carried out on this subject, Hettinger's tests were conducted in an operating mine, and thus they took into consideration the effect of geology on fragmentation. A granite quarry in Talbotton, was used as a test site were 5 blasts were conducted. For each test blast, the bench was divided into three different zones of timing, allowing the evaluation of multiple delay times in each shot while providing visual comparison for movement of the face and material throw. Using the 16 and 5 ms delays as baseline times, hole to hole delay of 0 ms, 1 ms, 4 ms, and 10 ms were used. Highspeed camera was used for blast monitoring during all the tests and WipFrag was used for fragmentation analysis using still photographs. The results showed that the 10 ms and 25 ms inter-hole delay times resulted in finer fragmentation while the 1 ms delay produces coarser rock fragments. It can be concluded that there was wave interaction when 10 ms and 25 ms delay was used, agreeing with the conclusion made by several other researchers (Rossmanith, 2003; Yamamoto et al., 1999). An analysis of the 0 ms delay results showed that significant amount of oversize (60 in.) were present and digging was harder and tight. This was because the burden was pushed out in a single mass. It can thus be seen that shooting all of the holes at once at 0 ms does not allow for pre-stressing of the hole by the preceding blast holes as blasting progress. This pre-stressing of the rock mass is very important and influences fragmentation (Johansson and Ouchterlony, 2013). Thus, short inter-hole delay does not improve rock fragmentation in full bench blasting.

Several theories for estimating the energy required in size reduction of rock has been proposed. The three classical comminution theories have been put forward by Bond (1952), von Rittinger (1867), and Kick (1885). These three proposed empirical equations for size reduction, which have been presented by Walker et al. (1937).

$$\mathrm{d}E = -C\,\frac{d_x}{x^n} \tag{2.1}$$

Where:

E = Net energy requirement per unit weight,

x = Size distribution index, e.g.P_{80},

n = Order of process exponent,

C = Constant relating the material properties and the units chosen.

von Rittinger (1867) proposed that the surface area that is produced during crushing of rock is proportional to the energy consumed during crushing. This equation is in actual sense a solution to Walker's equation when n is equated to 2, thus:

$$E_{Rittinger} = C_{Rittinger}\left[\frac{1}{P_{80}} - \frac{1}{F_{80}}\right] \tag{2.2}$$

Where:

$E_{Rittinger}$ = The energy input,

$C_{Rittinger}$ = Material constant,

P_{80} = Particle size equal to 80% of the product passing,

F_{80} = Particle size equal to 80% of the feed passing.

In 1885, Kick proposed a theory that states that the reduction in volume of the particle is proportional to the work that is required to break this material. Thus:

$$E_{kick} = -C_{kick}\left(\frac{P_{80}}{F_{80}}\right) \tag{2.3}$$

Bond (1952) introduced a formula that relates the total energy consumed to the particle size. This equation is what has come to be known as the 'Third Theory of Comminution'. He stated that the total energy used for crushing/grinding is inversely proportion to the square root of the mean particle size. This total energy become to be known as the Bond Work Index (BWi):

$$E_{bond=}C_{bond}\left(\frac{1}{\sqrt{P_{80}}} - \frac{1}{\sqrt{F_{80}}}\right) = BW_i = \left(\frac{10}{\sqrt{P_{80}}} - \frac{10}{\sqrt{F_{80}}}\right) \tag{2.4}$$

If plant data is used, the above equation is rearranged and referred to as the Operating Work Index (OW_i), otherwise, if the plant data is not available, the work index is determined in the laboratory:

$$OW_i = 1/10\left(\frac{10}{\sqrt{P_{80}}} - \frac{10}{\sqrt{F_{80}}}\right) \quad (2.5)$$

Due to this fact, Bond developed rod and ball mill tests, giving him the operating work indices. During his test, he assumed that the energy consumption per evolution of the test mill is constant. However, Levin (1992) state that this energy is far from being constant and estimated its vale as 198.4 kWh/rev×10^{-7}. This value was used by Bond (1961) in his equation for determining the work index for ball mills, using full-scale mill data. This developed equation estimated the value of the ball mill work index using laboratory test mill as:

$$W_i \frac{49}{P_1^{0.23}(Gbp)^{0.82}\ 10\left(\frac{1}{\sqrt{P}} - \frac{1}{\sqrt{F}}\right)} \quad (2.6)$$

Where;

W_i = Bond laboratory ball work index (kWh/t),

P_1 = Closing screen size in µm,

Gbp = Net grams of screen undersize per mill revolution,

P = 80% passing size of the product in µm,

F = 80% passing size of the feed in µm, and F<P.

Bond (1961) further developed rod mill and crushing laboratory tests, recommending that these tests generate a similar product size to that of a proposed full circuit, thus reducing the error associated with the use of an incorrect exponent. After realising that the Bond equation steadily becomes more inaccurate, he introduced a number of correction factors to use during such situation. These have been modified and expanded to carter for the current change in comminution circuit design, precisely in Ag and SAG mills (Rowland and Kjos, 1978; Barratt and Allan, 1986).

Hukki (1962) pointed out that the above three equations (Rittinger, Kick and Bond) are just a special form of Walker et al. (1937) equation. These equations are obtained by equating *n* to 2, 1.5 and 1. Hukki thus concluded that these three equations are only applicable to a relatively narrow size distribution, and that the equation by Walkers et al. has the wrong form of the exponent, which is not a constant but varies with the size of the size

distribution index, *x*. Thus, the general differential equation which is more appropriate was proposed as:

$$dE = -C\frac{dx}{x^{f(x)}} \tag{2.7}$$

Where;

x = Size of the size distribution index,

C = Constant related to the breakage properties of the material,

f(x) = Variable function.

Napier-Munn et al. (1996) proposed a classical model that links the energy consumption and breakage as:

$$dE = -K * \frac{dx}{x^n} \tag{2.8}$$

Where *K* is comminution constant and *x* is the feed size.

Morrel (2004a) proposed an alternative energy-size relationship to that of Bond. He suggested that because data from pilot and full-scale AG and SAG ball mill circuits have proved that Bond's equation is not effective for the particle size range 100 mm + 0.1 mm, there is need to develop a new relationship for predicting energy requirements for milling and gridding circuits. He analysed data from pilot AG/SAG mill programs to see whether Bond Work Index remains constant, as postulated by Bond (1952). The results of this test showed that BW_i was not constant but declined as the product size becomes finer. This test also showed that, despite the product of the AG/SAG being fed to the ball mill, the work indices of the AG/SAG circuits were higher than that of the associated ball mill. This finding is contrary to the assertion that the overall specific energy to grind a specific feed size F_{80} to a specific product size P_{80} is similar within ±5%, provided the circuits are operated under optimal conditions.

Morrel (2004a) proposed that instead of using a constant exponent of -0.5, a variable exponent, such as that proposed by Hukki, is more appropriate. Thus:

$$W = M_i.K\left(x_2^{f(x_2)} - x_1^{f(x_1)}\right) \tag{2.9}$$

Where;

W = Specific energy (kWh/t),

K = Constant chosen to balance the units of the equation,

M_i = Index related to the breakage property of an ore (kWh/t) determined experimentally using a bond grinding test or ROM the plant data,

x_2 = 80% passing size for the product,

x_1 = 80% passing size for the feed.

The function $f(x)$ is given by $f(x)= -(a+x^b)$; where a, b = constants; x = 80% passing size. This function can also b expressed as:

$$f(x) = -(0.295 + \frac{x}{1{,}000{,}000}) \tag{2.10}$$

Morrel (2004b) developed a rock breakage characterization test, that uses small quantities of samples to generate a strength index (DW_i) that can be used to predict specific energy of AG and SAG mills. This index can be used in ordering and/or with power based techniques. Because it presents a good correlation with the JK rock breakage parameters (A and b), it is fit for use in modelling. For power-based calculations, the following equation was proposed:

$$\text{Specific Energy} = K.F_{80}^{a}.DW_i^{b}.\left(1 + c\left(1 - \mathrm{e}^{-dj}\right)\right)^{-1}.\emptyset^{\mathrm{e}}.f(A_r) \tag{2.11}$$

Where; F_{80} is 80% passing size of the feed; DW_i is the strength index; J is the volume of balls (%); $\emptyset$ is the mill speed (% of critical); $f(Ar)$ is a function of mill aspect ratio (length/ diameter); a, b, c, d, e are the constants; K is the function whose value is dependent upon whether a pebble crusher is in-circuit.

The specific energy calculated can be used to predict the power of a mill of given dimensions, ball load and speed. This equation can be used both during design stage of greenfield projects and optimisation of existing projects. In the situation of design, a specific target throughput will be specified and using this data, the mill dimension can be adjusted until the required power draw is achieved. In instances of optimising an existing Ag/SAG

circuit, the throughput can be predicted by dividing the power draw by the specific energy. This method has been extended to cater for High Pressure Grinding Rolls and tumbling mills (Morrel 2008; 2009).

2.3. Conclusion

This chapter presents some of the literature that was considered in this research and had a major impact on the direction taken. Mine to Mill projects that have been undertaken, mostly by Metso PIO and resultant outcomes have been highlighted. It was shown that throughput gain in the range of 5 to 30% has been achieved on these sites. The chapter went on to highlight some of the research that has been done in blast delay timing determination with emphasis on short delay. It was shown that short inter-hole delays do not necessary result in improved fragmentation as opposed to medium delay. However, delays should be timed such that there is wave collision between the holes which will result in pre-stressing of the rock mass by preceding holes as the shot progresses. The literature review showing the relationship between energy requirement and particle size are also given. These equations form the basic understanding of energy consumption in comminution. Methods and models used to predict specific energy have also been reviewed, with the model proposed by Morrel (2004b) being the most outstanding and widely used model.

3. MATERIALS AND METHODS

3.1. Introduction

This chapter gives a detailed description of Sentinel mine where the research was conducted, giving a corporate background of the mine and the geological and metallurgical properties of the mine. The scope of work, the materials and the methodology used in this research are then discussed. A comprehensive methodology that included a desk study and engineering and scientific testing was applied. The scope of work involved a scoping study, ore characterization, modelling, simulation and validation. Through the use of these methods, the research questions were answered, and the objectives were achieved.

3.2. Corporate Background

First Quantum Minerals Limited (FQML) operates Kansanshi and the Trident Project in Zambia. FQML has 80% share in Kansanshi Mine with the other 20% being controlled by Zambia Consolidated Copper Mines-Investment Holding (ZCCM-IH), a Zambian government agency. The company wholly owns the Trident Project, through its subsidiary Kalumbila Minerals Limited (KML). Kansanshi Mine is located in Solwezi, about 180 km from Chingola Town of the Copperbelt Province of Zambia. The Trident Projects comprises of three mines, namely; Sentinel, Intrepid and Enterprise. As part of the Trident project, KML has developed the Sentinel open pit mine to exploit copper sulphide ores located at the western end of the Zambian Copperbelt.

3.3. Research Location

Kalumbila Minerals is located some 140 km west of the Solwezi Town in the North-Western Province of Zambia in Central Africa. The Sentinel Mine is a relatively new operation, having begun production in February 2015. The Sentinel project will generate approximately 55 Mt per annum of copper sulphide ores from the approximately 6.5 km long, 3 km wide, 375 m deep open pit over a 20-year life. KML license covers an area of

248.07 km^2 over the Sentinel deposit, processing plant and supporting infrastructure and is valid for 25 years, expiring in April 2036. Figure 3.1 shows the location of Kalumbila relative to Zambia, while Figure 3.2 shows the mine license area for the Trident Project.

Figure 3.1. Location of Kalumbila Minerals Limited (Sentinel Mine).

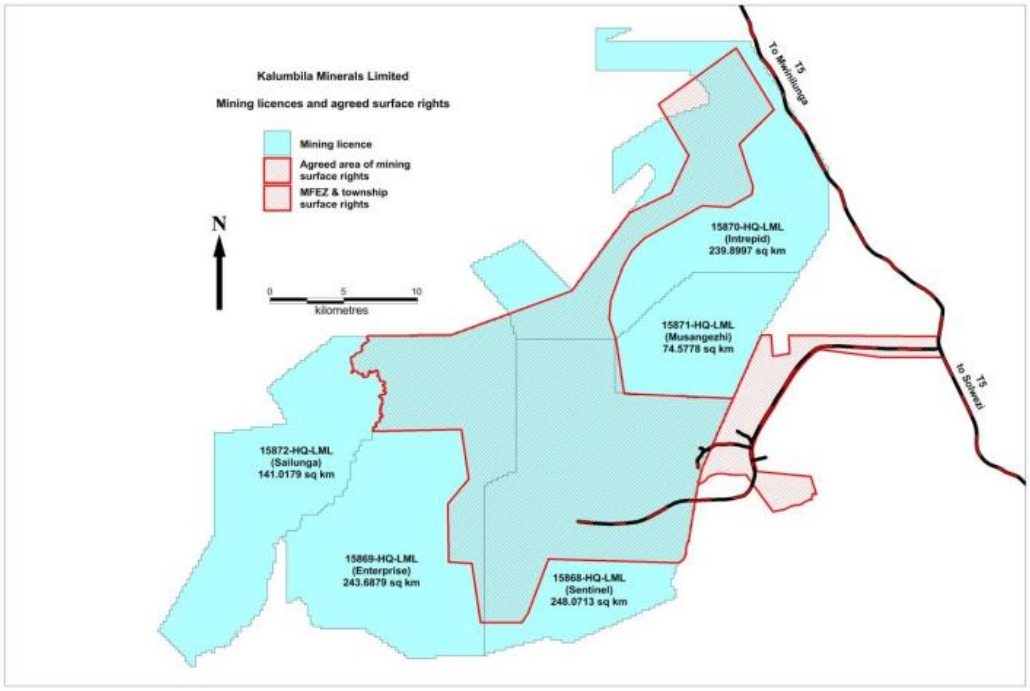

Figure 3.2. Areas showing mining licenses and surface rights (Xstract, 2012).

3.4. Geology and Mineralization

3.4.1. Regional geology

The Trident Project is located on the western end of the Lufilian Arc which extends from northern Zambia, across the Katanga Province of Democratic Republic of Congo, and into northeast Angola. It lies on the margins of the Mesoproterozoic Kapombo Dome, one of several antiformal basement inliers in northwest Zambia, within a thick succession of Neoproterozoic sedimentary rocks of the Katanga Supergroup. Figure 3.3 shows the regional geology of the Zambian Copperbelt that spans from the DRC to Angola.

3.4.2. Geology of Sentinel Mine

The Sentinel copper deposit is a structurally modified sediment hosted copper deposit with a strike extent of about 11 km and a dip extent of approximately 800 m. Copper mineralisation is hosted within a phyllite package and occurs as a series of layered continuous sheets having a northerly 20° to 30° dip. Copper mineralisation is dominated by chalcopyrite which occurs as fine to coarse disseminations and or veinlets. It is hosted within

the structurally thickened, northwest dipping carbonaceous meta-pelitic rocks known as ‘Kalumbila phyllite’. Compositionally, the Kalumbila phyllite is very fine grained, with quartz, muscovite, biotite, and iron sulphides being the dominant minerals. Total organic carbon test-work has confirmed graphite content between 1-5% (CSA, 2012).

The hanging-wall and foot-wall rocks are both quartz-feldspar-biotite schists, displaying strong petrographic similarities. Interpretation of diamond drill core drilled within and proximal to the Trident Project area suggests the hanging-wall schist immediately north of Sentinel represents the Mwashya subgroup into grand Conglomerate, with the thin footwall schist and silt-sand-stone packages to the south representing the Upper Roan Group. Overburden and regolith across the deposit is typically 0-5 m, with insitu laterite and saprolitic layers underlying woodland and tall grassland. Figure 3.4 shows a generalised stratigraphy of the Sentinel deposit.

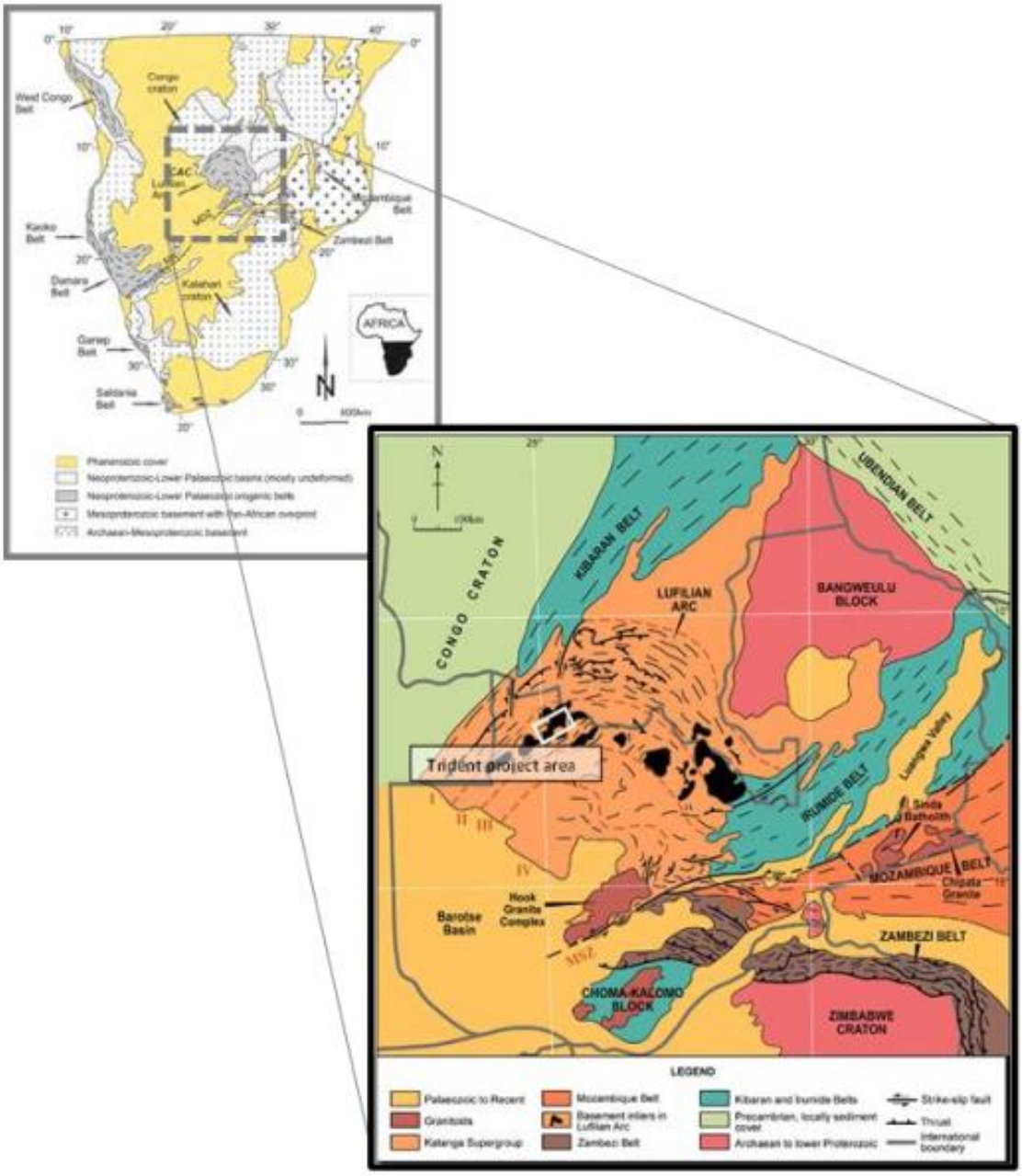

Figure 3.3. Regional geology of the Trident Project (CSA, 2012).

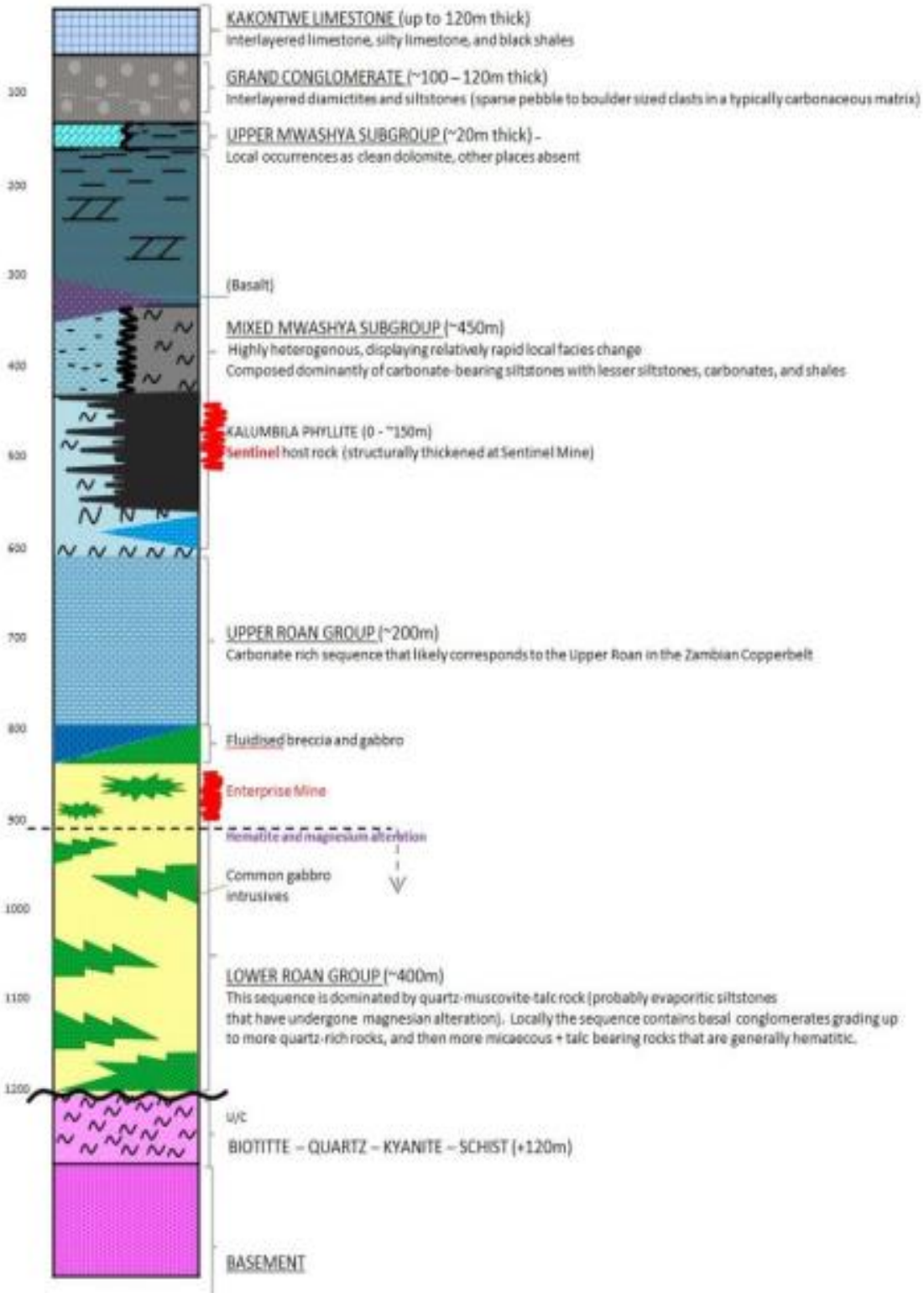

Figure 3.4. Generalised stratigraphy of the trident area (CSA, 2012).

3.5. Mineralisation

The Sentinels copper mineralization is a low-grade mineralization. Limited to the strongly fortified phyllite unit, it extends into the foot and hanging-wall for only 1-2 meters. Striking east-west, the orebody extends approximately 11 km long and the mineralised horizon dips parallel to the dominant foliation between 20° and 30° in a northerly direction. Occurring within the foliation/bedding parallel to the quartz-kyanite-carbonate veinlets, chalcopyrite is the dominant copper-bearing mineralisation. The veinlets tend to be thicker, blebby and more irregular within the folded zones and usually contains higher chalcopyrite proportion. Less common are disseminated, blebby or late sulphide- bearing cross-cutting veinlets. Figure 3.5 shows a cross-section through the Sentinel deposit.

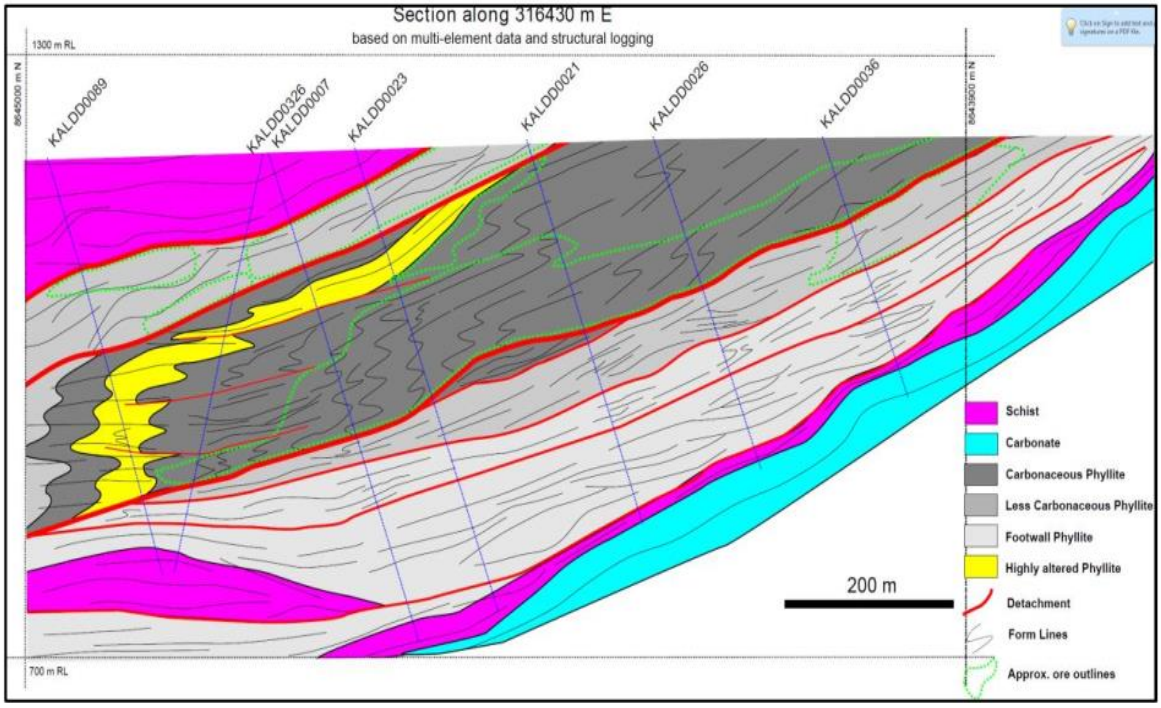

Figure 3.5. Cross section through the Sentinel deposit (Gray et al., 2015).

For a depth of approximately 70 m, the oxidized horizon contains non-primary sulphide copper minerals, predominantly tarnished chalcopyrite and chalcocite. The top 5-15 m from surface contains trace oxide minerals and mixed refractory copper because it is leached.

Occurring as discreet horizon within the footwall phyllite, the Nickel-Cobalt mineralization occurs in the form of cobalt-pentlandite with traces of vaesite. It also occurs

as rare sporadic meter-scale lenses. This footwall phyllite is the lowermost phyllite portion that tends to have very low mineralization of copper or barren. The north east extension of the deposit, proximal to the Kalumbila Faults, is where the Nickel-Cobalt mineralization tends to be best developed (CSA, 2012).

3.6. Mineral Resource Estimates

Sentinel Mineral Resource estimates have been classified according to drill grid spacing, geological confidence and confidence in the panel grade estimate as well as consideration of the sampling and preparation methods, analytical techniques and the associated data quality. Additional data and confidences have provided a 4% increase in copper metal for the measured and indicated resource categories due to a 4% increase in grade. Increased confidences have upgraded previous Indicated Mineral Resources into the measured category by 44%. The resulting Mineral Resources have been reported using a copper cut-off grade of 0.2% as at May 2015, as per Table 3.1. Reported Mineral Resources are inclusive of Mineral Reserves (Gray et al., 2015).

Table 3.1. Sentinel mineral resource

Classification	**Material**	**Tonnes (Mt)**	**Density**	**TCu (%)**	**Cu Metal (kt)**
Measured	Non-primary sulphide	78.7	2.75	0.47	372.2
Measured	Primary sulphide	661.8	2.80	0.57	3,748.2
Measured Subtotal		**740.5**	**2.79**	**0.56**	**4,120.5**
Indicated	Non-primary sulphide	19.0	2.75	0.45	84.5
Indicated	Primary sulphide	268.2	2.80	0.46	1,239.9
Indicated Subtotal		**287.2**	**2.79**	**0.46**	**1,324.3**
Measured & Indicated Subtotal		**1,027.7**	**2.79**	**0.53**	**5,444.8**
Inferred	Non-primary sulphide	6.9	2.78	0.29	19.7
Inferred	Primary sulphide	129.1	2.80	0.38	486.5
Inferred Subtotal		**136.0**	**2.80**	**0.37**	**506.2**

The above Mineral Resource estimate based on a $3.00/lb ($6,613.87 per tonne) copper price, was reported at a 0.2% Cu cut-off grade and included mining tonnage dilution of an additional 5% (at zero grade) and mining recovery losses of 5%.

3.7. Mineral processing summary

In-pit crushing is utilized at Sentinel mine. Overland conveys are used to transport the crushed ore from the pit to the stockpile ahead of the two milling circuit. The milling circuit comprises of Semi-Autogenous (SAG) mill and a single Ball mill. Each milling train consists of two parallel banks of flotation cells, with each bank comprising seven cells operating in series. Using dedicated concentrate handling facility, a 24% grade copper final concentrate is generated after being filtered and thickened. The recommended metallurgical parameters for mine planning are 92% recovery for primary sulphide, and 70% recovery for the relatively smaller proportion of near surface non-primary sulphide (FQML, 2013). This process flowsheet and metallurgical design are similar to those that are found elsewhere on the Zambian Copperbelt that treat predominantly chalcopyrite ores. Figure 3.6 shows a diagrammatic flowsheet.

The Sentinel processing flowsheet comprises of:

- Crushing, conveying and ore stockpiling (making use of in-pit crushing and conveying).
- Secondary crushing by use of two Metso secondary crushers, utilised one at a time.
- Crushed ore stockpile reclaim and milling in a SABC (SAG/Ball/Pebble crushing) circuit.
- Flotation circuit on a bleed stream from cyclone underflow.
- Rougher, scavenger and cleaner flotation.
- Concentrate deslime and concentrate handling.
- Tailings disposal.
- Reagent mixing, storage and distribution.
- A water and power supply.

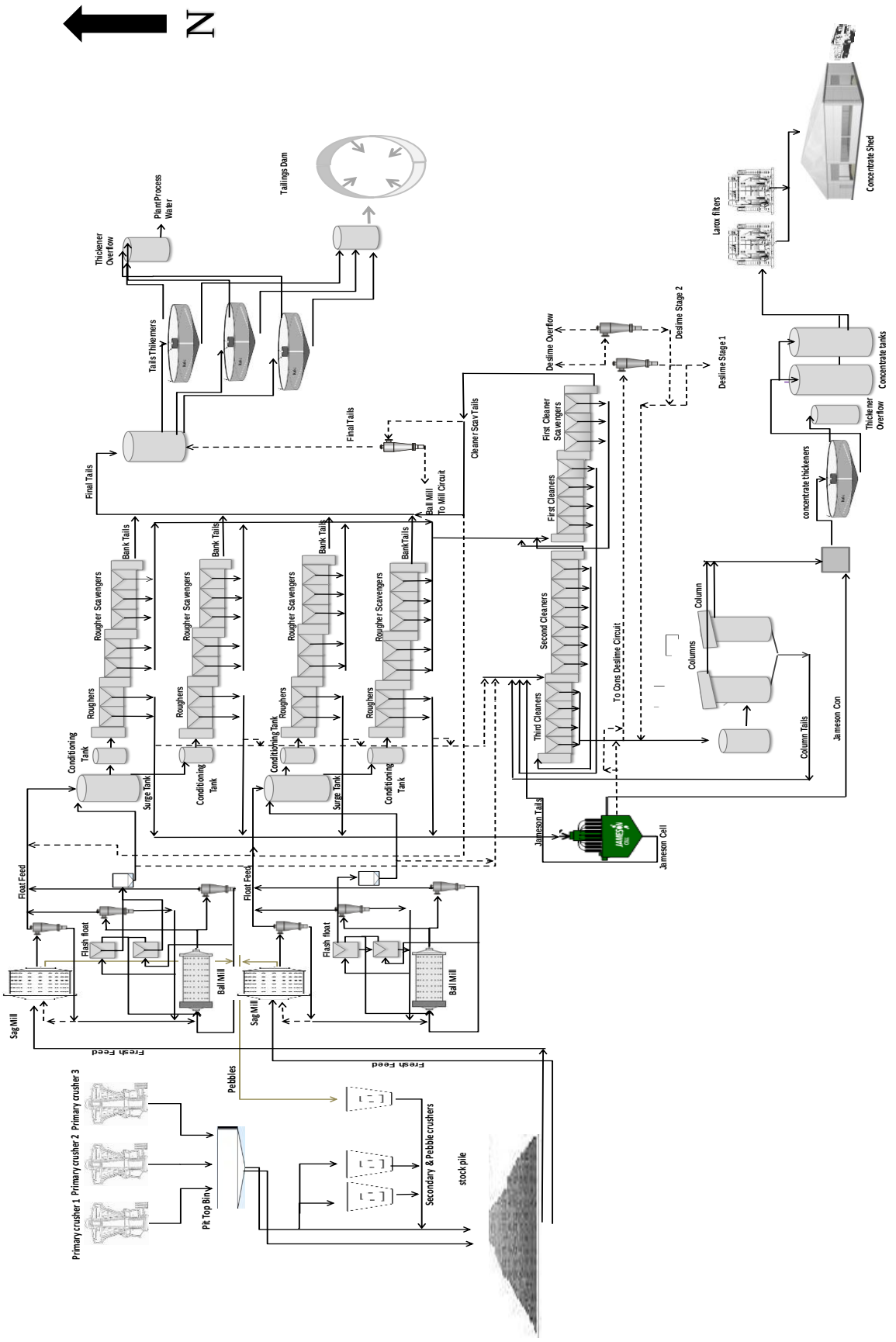

Figure 3.6. Processing flowsheet (FQML, 2013).

A 1,000 million tonnes capacity tailings storage facility (TSF) has been designed for the life of the mine to receive tailings from both the Sentinel and Enterprise processing circuits. The circular tailings storage facility is 5.5 km in diameter and is designed to reach a maximum height of around 40 m. The TSF stage 1 earthfill embankment provides an initial 15 months of storage capacity. The tailings will be deposited from spigots along the top of the embankment. Over time the tailings storage facility will be upstream raised with tailings.

3.8. Scope of the Work

The scope of work for this research included:

1. Scoping

   The scoping work involved an extensive auditing of the current drilling and blasting operation practices. Blast designs, implementation and initiation sequences were studied. Surveys of the crushing and grinding circuits were conducted and provided necessary data that was used to model the comminution stages. These data and information were used to identify problems, bottlenecks -in both the mining and comminution process-, and opportunities for improvements.

2. Ore Characterisation

   Ore characterization was undertaken in order to have a detailed understanding of breakage characteristics of the ore. The characteristic of ore for blasting breakage and for crushing and grinding breakage are different. For example, the rock mass structure and strength are important for blasting, whereas the micro fracture network, grain size, grain characteristics and breakage resistance may be important for crushing and grinding.

3. Modelling and Simulation

The collected data under bench marking and ore characterization stages was used to develop models. These models were then used to predict the operating conditions such as blast fragmentation via multiple simulations.

4. Validation and Implementation

The modelling and simulation stage provided optimisation strategies that are based on mining and processing constraints and a cost/benefit analysis. These results were used to determine the alternative designs and operating strategies for each process to improve the overall efficiency of the operation. These models were validated and proposed for implementation, key performance indicators were identified and measured to quantify improvements, and fine tune the recommendations.

3.9. Methodology

3.9.1. Data collection

A desk study to review current literature relating to the topic was conducted. Special attention was paid to reports and article highlighting mines at which the mine to mill strategy has successfully been implemented and yielding results. A review of the current operation practice at the mine was also carried out so as to identify and understand the bottleneck in the processes. A survey of the comminution process to establish current operation trends and identify bottlenecks that can be eliminated for improved efficiency was conducted. Ore comminution theories and models with specific interest to those applied to predicting specific energy were also reviewed.

3.9.2. Scientific and engineering tests

Because natural rock contains discontinuities such as joints, bedding planes, folds, sheared zones and faults which render its structure discontinuous, it is important to consider the effect of these discontinuities when determining the engineering properties of rock masses. Palmström (2002) notes that because the rock engineering properties depends on the geological defects within the rock mass as opposed to the intact rock strength of the rock mass, the knowledge of the joint type and their frequency is far more important than the knowledge of the type of rock involved. This entails that a careful mapping of the rock mass joint characteristic must be done. For this reason, a wide range of scientific tests to determine rock properties were done, otherwise the data from consultants engaged by the mine firm was used for rock and Run of ore mine (ROM) characterization. These tests include rock strength tests (e.g. Point Load Index, Uniaxial Compressive Strength (UCS), and Drop Weight Test) and rock structures tests (e.g. Rock Quality Designation (RQD), image analysis, and fracture frequency).

3.9.2.1. Point load test

The Point Load Test (PLT) is a procedure that is used in rock mechanics to determine the rock strength index. This index can also be used to estimate other rock strength parameters (Rusnak and Mark, 2000). It is obtained by subjecting a rock sample to an increasing point loading force delivered through a truncated pair of platens until failure occurs. The failure load is used to calculate the point load strength index and to estimate the Uniaxial Compressive Strength (UCS). The uniaxial compression test is used to determine compressive strength of rock specimens, but it is a time-consuming and expensive test that requires specimen preparation. Therefore, in order to reduce the time and costs associated with the UCS tests, during field work alternative methods like point load tests are used instead.

A point load tester, as shown in Figure 3.7, consists of a loading system that has a loading frame with a plate-to-plate allowance that allows testing of rock samples of different size as per requirement; a measuring system, -for example a load cell or a hydraulic pressure

gauge- for indicating load, *P*, (required to break the specimen); and a means for measuring the distance, *D*, between the two platen contact points.

Figure 3.7. GCTS Point Load Tester (ASTM, 1995).

The testing procedure for drill core samples is as follows:

1. Several test samples are collected. A core specimen is inserted into the test device and the platens are closed to make contact along a core diameter. One has to ensure that the distance, *L*, between the contact points and the nearest free end is at least 0.5 times the core diameter. Figure 3.8 illustrates these dimensions, where D is core diameter and L is core length to the point of loading
2. Distances *D* and *L* are determined and recorded.
3. The load is steadily increased such that failure occurs within 10 to 60 s, and the failure load, *P* is recorded. The results are invalidated and rejected if the plane of fracture passes through just one plate of the loading plane.
4. The procedures in step 1-3 are repeated for each sample of the rock type.

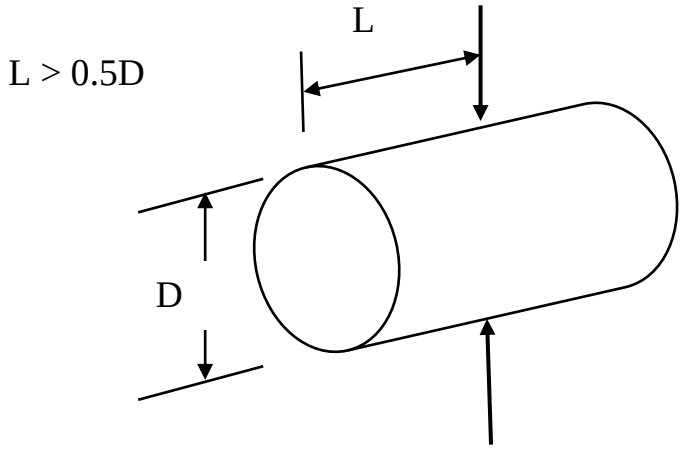

Figure 3.8. Load configurations and specimen shape requirement for the diametral test, (ASTM, 1995).

The uncorrected point load strength Index is calculated as:

$$I_s = \frac{P}{D^2} \text{ , MPa} \tag{3.1}$$

where: P= failure load (N) and D=core diameter (mm^2).

A size correction factor is introduced to obtain a unique point load strength value for the rock sample and one that can be used for purposes of rock strength classification. The size-corrected point load strength index $I_{s(50)}$, of a rock sample is the value of strength index that would have been obtained if the specimen had a diameter 50 mm. It is determined either by using a graph or empirically as per Equations 2.2 to 2.4.

$$I_{s(50)} = F \times I_s \tag{3.2}$$

Where F is the size correction factor given as:

$$F = \left(\frac{D_e}{50}\right)^{0.45} \tag{3.3}$$

Where De is the equivalent diameter of the drill core

For tests near the standard 50mm size diameter (*D*), only slight error is introduced and is corrected by using the approximate expression:

$$F = \sqrt{\frac{D}{50}} \tag{3.4}$$

The estimated UCS can be obtained by using the graph given in Figure 3.9 or using the following formula:

$$\sigma_{UC} = C \times I_{s(50)} \tag{3.5}$$

Where;

σ_{UC} = Uniaxial Compressive Strength,

C = Factor that depends on site-specific correlation between σ_{UC}C and $I_{s(50)}$,

$I_{s(50)}$ = Corrected point load strength index.

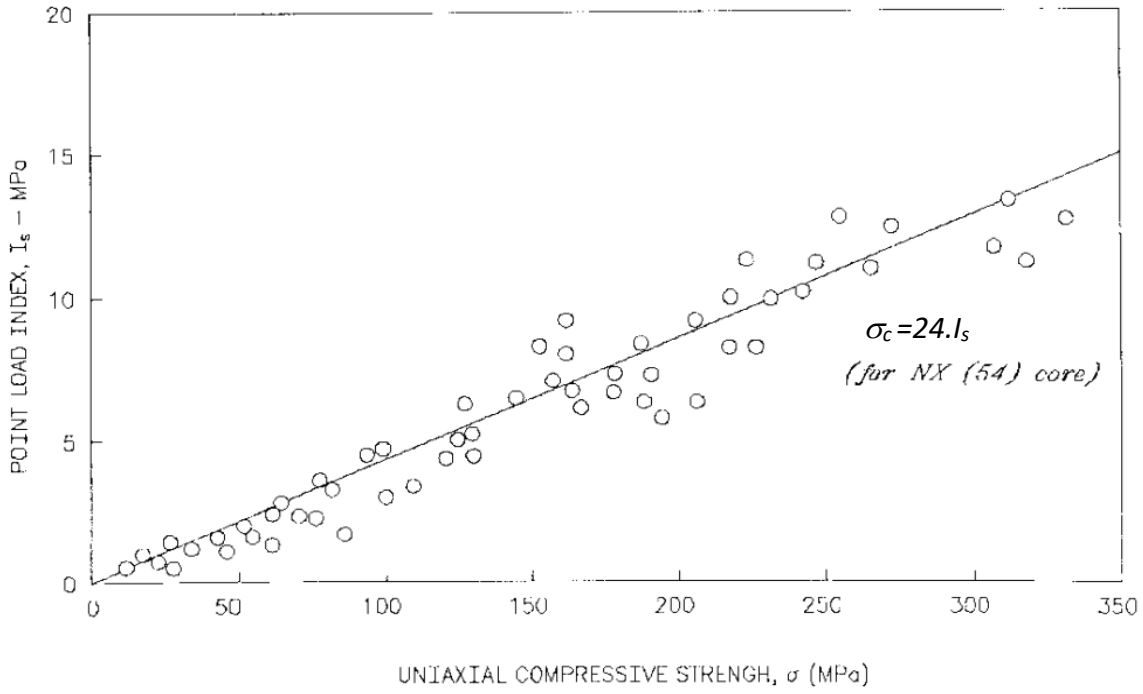

Figure 3.9. Relationship between Point Load Strength Index and UCS.

3.9.2.2. Rock quality designation (RQD)

RQD was proposed by Deere in 1964 (Deere, 1964) to provide a simple and inexpensive general indication of rock mass quality to predict tunnelling conditions and support requirements. The RQD is defined as the ratio (in percentage) of the total length of sound core pieces that is 100mm or longer to the length of the core run. It is thus calculated

by summing all the pieces of intact rock core equal to or greater than 100 mm (4 in.) long and dividing by the total length of the core run.

The American Society for Testing and Material (ASTM, 1996) outlines the procedure for determining the RQD in Designation: D6032,-96. Despite the researcher not having conducted these tests, the procedure is outlined below:

1. All core piece lengths that are intact and greater than 100 mm to the nearest 1 mm are measured and the values record on a RQD data sheet. These measurements must be done along the centreline of the core.
2. The top and bottom depths of each core run are recorded.
3. The core feature such as natural fractures, drilling breaks, lost core, or areas of high weathered pieces, are sketched to give a full vision of the condition of the core.
4. The sum of intact core pieces longer than 100 mm long are recorded and the Value of RQD calculated for the core run being evaluated as:

$$RQD = \frac{[\sum of\ intact\ core\ pieces > 100mm] \times 100\%}{total\ core\ run} \tag{3.6}$$

During the determination of RQD pieces of core that contain numerous pores, are moderately or intensely weathered, or are friable, are not included in the summation of pieces greater than 100 mm. However, any rejected piece of core is still included as part of the total length of core run and should be indicated in the report. Only those pieces of rock formed by natural fractures (that is, joints, shear zones, bedding planes, or cleavage planes that result in surfaces of separation) are considered for RQD purposes. Remarks concerning judgement decisions such as whether a break in a core is a natural fracture or a drilling break or why a piece of core longer than 100 mm was not considered to be intact should be included on a log sheet (ASTM, 1996). Figure 3.10 shows an illustration of core logging and calculation of RQD.

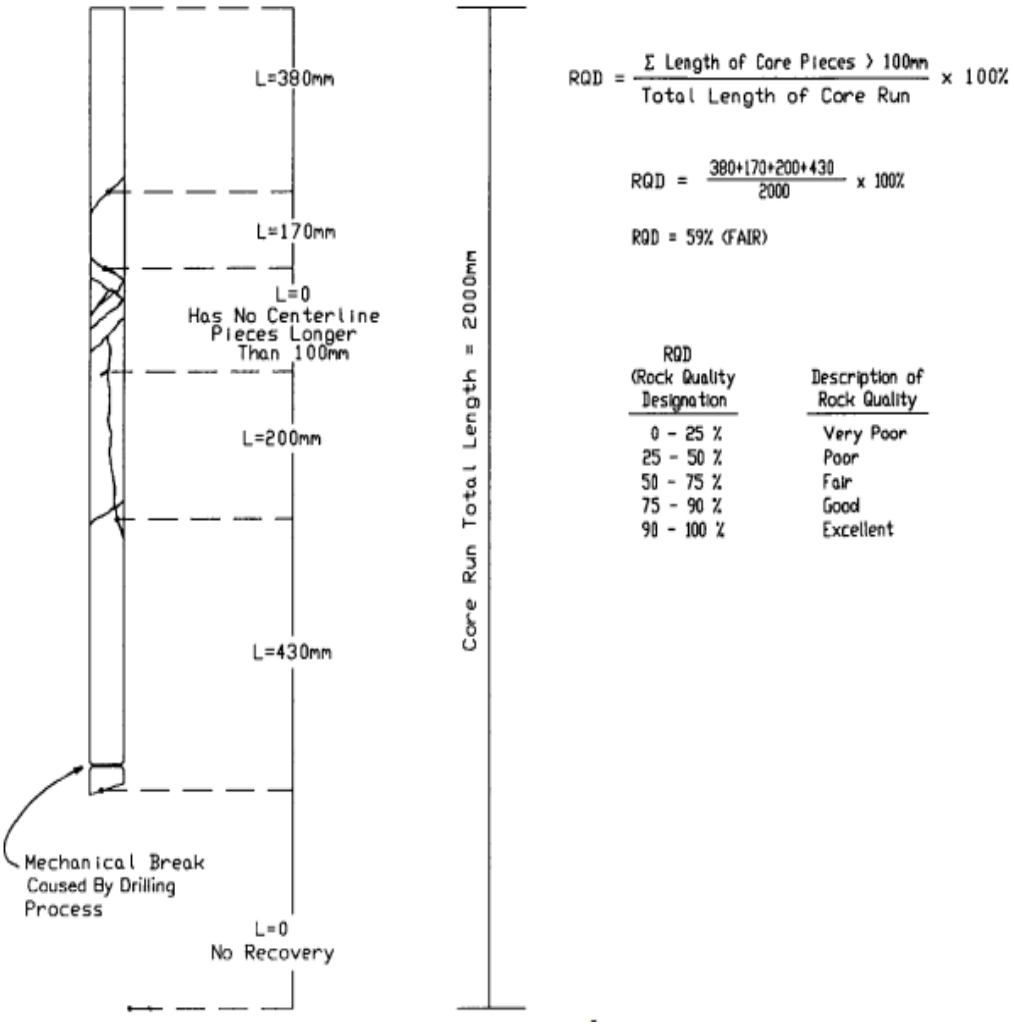

Figure 3.10. RQD logging and calculation of RQD (ASTM, 1996).

Apart from using the direct method for determining RQD from coring, different indirect methods are also available for evaluating RQD. These methods include;

a) <u>Discontinuity frequency</u>:

Hudson and Harrison (2000) observed that discontinuity frequency, which is defined as the number of fractures per meter, was a mean spacing reciprocal. This discontinuity spacing parameter can also be used to classify rock mass (Wines and Lilly, 2002). Discontinuity spacing measurements are classified into three types:

1. *Total spacing*: This is the distance between two adjacent discontinuities. It is generally measured along a line of general with location and orientation having been specified.

2. *Set spacing*: This is defined as the spacing between two adjacent discontinuities from a particular discontinuity set, measured at a specified location and orientation along a line.
3. *Normal set*: This is spacing is the set spacing measured along a line that is normal to the mean orientation of a particular set.

Thus, the discontinuity frequency method applies the correlations between RQD and linear discontinuity frequency. Priest and Hudson (1976) derived the following relationship between RQD and linear discontinuity frequency λ:

$$RQD = 100e^{\lambda t}(\lambda t + 1) \tag{3.7}$$

Where λ is linear discontinuity frequency and *t* is the length threshold.

Sen and Kazi (1984) derived an expression for determining the RQD for short sampling line of length *L*, with a length threshold *t* as:

$$RQD = \frac{100}{1-e^{-\lambda L}-\lambda L e^{-\lambda L}}\left[e^{-\lambda L}(\lambda t + 1) - e^{-\lambda L}(\lambda L + 1)\right] \tag{3.8}$$

Where λ is linear discontinuity frequency and *t* is the length threshold and *L* is sampling length.

b) <u>Seismic velocity measurement</u>:

This method compares the P-wave velocity of in situ rock mass with laboratory P-wave velocity of intact drill core obtained from the same rock mass in estimating the RQD (Deere et al., 1967). Thus:

$$RQD = \left(\frac{v_{pF}}{v_{pO}}\right)^2 x100\% \tag{3.9}$$

Where; v_{pF} is the P-wave velocity of in situ rock mass, and v_{pO} is the P-wave velocity of the corresponding intact rock.

c) Correlation between RQD and volumetric discontinuity frequency:

The estimation of RQD using this correlation is achieved as (Palmström, 1974; ISRM, 1978):

$$RQD = 115 - 33\lambda_v \tag{3.10}$$

Where; λ_v is the volumetric discontinuity frequency which is defined as the sum of the number of discontinuities per unit length for all discontinuity sets, which can be determined from the discontinuity set spacing within a volume of rock mass.

The use of volumetric discontinuity frequency λ_v for estimating RQD provides a quite useful way in reducing the directional dependence of RQD. It is also possible to do core boring, scanline sampling and/or wave velocity measurements at different directions and then evaluate the overall RQD of the rock mass (Zhang, 2016).

3.9.2.3. Drop weight tests

This test involves dropping a known mass (steel weight) on a fragment of rock sample of known mass from a known height as shown in Figure 3.11. In this way, the specific energy imparted on the particle can be calculated. The fragments from the smashed particle are collected and sieved, permitting analysis of the relationship between specific impact energy and particle size (Napier-Munn et al., 1996).

The potential energy on impact is calculated as:

$$Ep=mg\Delta h \tag{3.11}$$

Dividing the impact energy by the mass of the sample gives the specific average comminution energy imparted on the sample.

$$E_{is} = \frac{E_p}{w} \tag{3.12}$$

Where: E_P = potential energy (j); m = drop weight mass (kg); g = acceleration due to gravity; Δh = drop height (m); E_{is} = specific energy (J/kg); w= mean particle mass (kg).

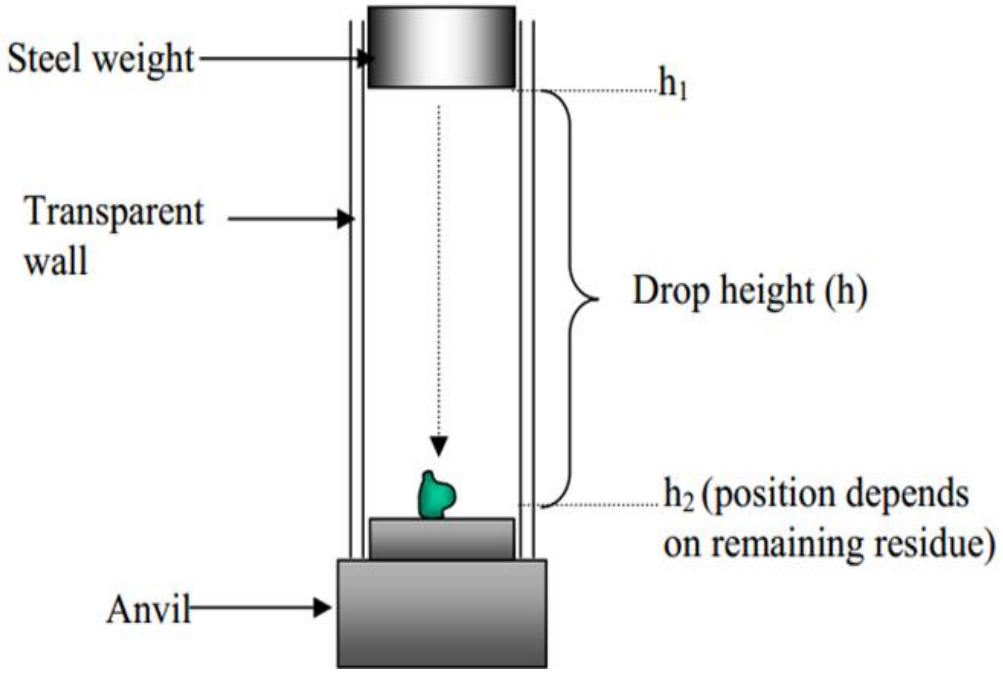

Figure 3.11. Schematic of a drop weight test.

a) <u>JK drop weight test</u>:

The drop weight test is used to determine the breakage characteristic of ore sample in the Autogenous (AG) and Semi-Autogenous (SAG) mill. Two main breakage mechanisms are involved in rock breaking in an AG/SAG mill; these are the impact breakage, utilizing high energy, and low energy abrasion breakage. The JKTech Pyt company is one of the leading companies that undertakes comprehensive Drop Weight Tests. These tests are done at JKMRC at University of Queensland in Australia. The tests measure the abrasion and impact parameters of a specific rock sample. The abrasion breakage parameter (t_a) is measured using a tumbling test while the JK Drop Weight tester, which is a breakage device that uses high impact energy, is used for determining the impact breakage parameters *A* and *b* These indexes are later used in optimising the crushing/milling models.

b) Impact breakage test:

This test involves sizing the 100 kg sample into five size fractions: -63 +53 mm, -45 +37.5 mm, -31.5 +26.5 mm, -22.4 +19 mm, -16 +13.2 mm. In order to obtain fifteen size/energy combinations for each size fraction, the particles between 10mm and 30mm are broken at each of three energy levels under impact at the required energy level using the JK Drop Weight Tester. The breakage products of all particles for each size/energy combination are collected and sized. The size distribution produced is normalised with respect to original particle size. The t_{10} which is the percentage passing one-tenth of the original particle size is used in the JKTech convention. Figure 3.12 shows a JK Drop Weight tester.

Figure 3.12. The JK Drop Weight Tester (JKTech, 2019).

The geometric mean of the size range e.g. -63 +53 = 57.8 mm, is used to estimate the original particle size for the size fractions. In this way, a set of t_{10} and specific energy (E_{cs}) values are produced for the 15 energy/size combinations. The following equation relates of the amount of breakage, t_{10}, to the specific energy, E_{cs} (kWh/t):

$$t10=A(1-e^{-b \cdot Ecs}) \tag{3.13}$$

Using the 15 energy/size combination data values, the best fit *A* and *b* parameters are calculated using a minimisation of error squared routine. The resulting *A* and *b* parameters

are related to the resistance of the ore to impact breakage. The product of *A* and *b* is a measure of the resistance to impact breakage of ore. It is gives as the gradient of the curve at E_{cs} = 0 kWh/t. By comparing these values with other samples having lower values the hardness of the ore can be established via the use of these parameters (JKTech, 2019).

c) Abrasion breakage test:

The tumbling test is used in characterising the abrasion breakage. A laboratory mill 305 mm in length by 305 mm in diameter is used as a standard tumbling test. During this test, a 3 kg sample of -55 +38 mm particle size is tumbled at 70% critical speed for 10 minutes. The t_{10} value of the product is determined by sizing the product from the tumble.

For an original size fraction -56 +38 mm the particle size geometric mean is 46.13 mm. The t_{10} size is the calculated as one tenth of 45.7 mm, giving 4.57 mm. The abrasion parameter, t_a, is then defined as: $t_a = \frac{t_{10}}{10}$.

3.9.2.4. Bond index test

ALS Metallurgy undertook metallurgical tests on 12 samples from the Sentinel mine (ALS, 2018). One of these tests was the Bond Work Index test, using a closing screen of 300µm. The result from this test was used in this research when calculating and modelling the comminution parameters.

ALS outlines the test procedure as follows (ALS, 2018):

1. After being stage crushed to 100% passing 3.35 mm, then each sample was divided into portions by rotary splitting.
2. Using a standard mill, 700 mL of the crushed portion was ground for a number of revolutions. The material was then screen at 300µm so as to remove the material that is <300µm.
3. In order to achieve the original test weight, a fresh sample feed is added to the >300µm.
4. During each cycle, the number of the revolution of the mill was adjusted so as to achieve a stable load recirculation.

5. The work index is calculated as:

$$Wi_B = \frac{44.5}{(P_1)^{0.23} \times (Gbp)^{0.82} \times \left(\frac{10}{\sqrt{P_{80}}} - \frac{10}{\sqrt{F_{80}}}\right)} \times 1.102 \quad (3.14)$$

Where:

Wi_B = Work index value expressed in kWh/t,

P_1 = Grindability test aperture (micrometres),

Gbp = Mean of equilibrium grindability values (g/rev),

P_{80} = 80% passing size of the equilibrium product (micrometres),

F_{80} = 80% passing size of the feed to period 1 (micrometres).

3.9.3. Application of modelling theories

Fragmentation models were reviewed and applied to blast designs in benchmarking the current blasting practice and in predicting the percentage passing for each blast pattern that was analysed. The models used are Kuz-Ram model, Crush Zone Model, Swebrec Model and the Kuznetsov – Cunningham – Ouchterlony (KCO) Model. These models are discussed in detail in Chapter four.

3.9.4. Developing fragmentation models

An ideal fragmentation model that can be used to determine the drilling and blasting parameters for the mine was developed to achieve a certain fragmentation. This model combines both the Kuz-Ram and the KCO models.

The above explained methodology is simplified in the algorithm in Figure 3.13

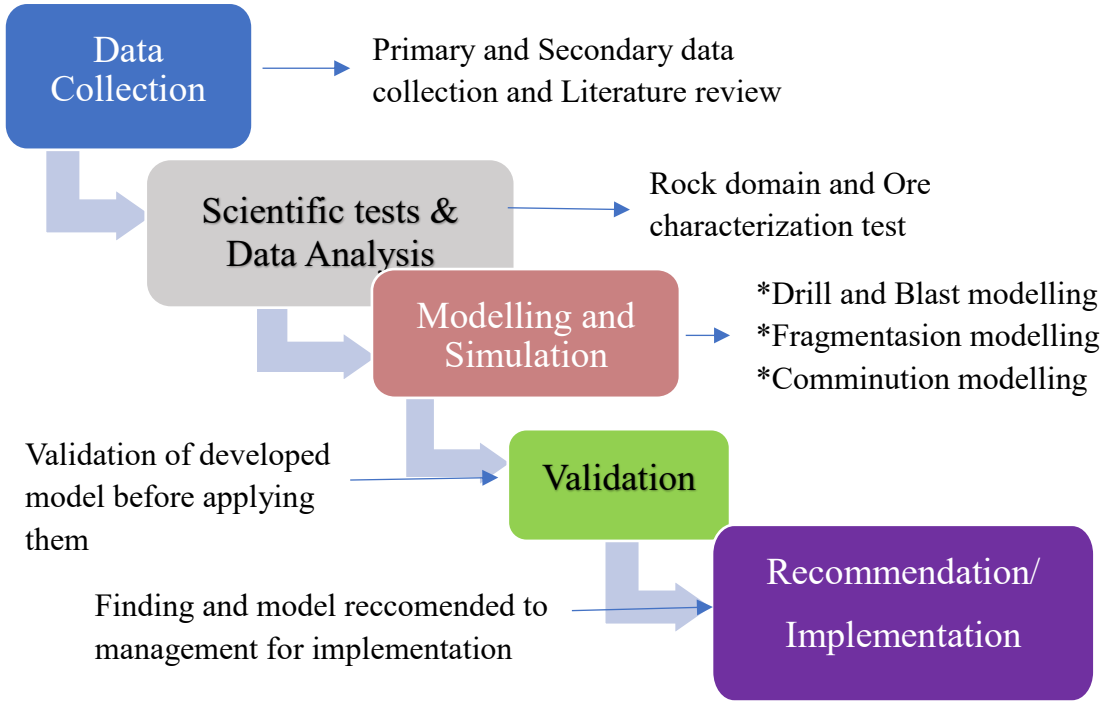

Figure 3.13. Methodology flow chart.

3.10. Conclusion

This Chapter has provided a brief background of mine to mine optimisation. It has also provided insight into the project location, which is some 140 km west of Solwezi Town in the North-Western Province of Zambia in Central Africa. KML is 100% owned by FQML and production at the Sentinel Mine begun in February 2015. After introducing the topic, the problem statement, justification of the research and the hypothesis is given. It has also provided information about geology of the Sentinel deposit. An overview of the mineralization and metallurgical characteristics of the project location has also been provided. The technical reports by CSA Global (UK) Ltd., (2012) and Gray et al.(2015) are the primary source of the information in this section because geological, geotechnical and other data about Sentinel mine is very limited.

This chapter has further highlighted the scope of the work that encompassed this research. The methodology that was employed has also been discussed and a visual flow chart provided. This methodology involved primary and secondary data collection models.

Secondary data involved a comprehensive literature review, both local and international literature was accessed. Primary data collection method involved scientific test and analysis to determine the rock blastability and grindability qualities. Test to define the blastability and breakage (e.g. Point Load Test and RQD); and test to define ore crushability and grindability such as the Bond Work Index were applied.

4. FRAGMENTATION MODELS

4.1. Introduction

Quantification of blast fragmentation requires the assessment of the blast performance and size distribution. The blast outcomes are affected by a number of parameters. These are grouped as controllable and non-controllable parameters (Jimeno et al., 1995). The controllable parameters are those that deal with basic blast design and can be varied by the blast designer. These parameters are grouped into three categories:

Group A- Geometric; these deals with the geometry of the blast pattern and include drill hole diameter, burden, spacing, charge length etc.

Group B -Physicochemical parameters, which pertain to the explosive chemistry and includes type, strength and energy of the explosive, priming system.

Group C relates to the timing part of blasting and involves timing delay and initiation system and sequence.

The uncontrollable factors relate to the rock geological and geotechnical characteristics that are outside the control of the blast engineer (Hustrulid, 1999).

Measuring fragmentation size is achieved using either direct or indirect methods. Sieving analysis is the only direct fragment size quantification method. Even though this method is the most accurate technique, it is very expensive and time consuming, thus limiting its application in the industry. Because of the foregoing reason, indirect fragment size quantifying methods have been developed. These methods are usually observation, empirical and digital (Esen and Bilgin, 2000).

Prediction of fragmentation before a blast is fired is very important in mining and comminution optimisation. Fragmentation measurements taken after a blast is of less importance as limited remedy options can be taken. The only mediation is to use a rock

breaker if large boulders are produced. If finer material is generated, seldom is there remediation methods, but the product is regarded as waste.

Several methods of predicting rock fragmentation by blasting have been developed and applied in the industry. These methods include rock engineering-based models, numerical approach, statistical analysing and purely empirical models (Jimeno et al., 1995; Cho and Kaneko, 2004; Monjezi et al., 2009; Faramarzi et al., 2013). This chapter discusses these methods in detail.

4.2. Kuz-Ram Model

The Kuz-Ram fragmentation model developed by Cunningham in 1983 is one of the widely used fragmentation prediction model. The Kuz-Ram model is based on the modification of the Kuznetsov's empirical equation for estimating the mean fragment size (X_{50}) and the Rossin-Rammler equation for the entire size distribution description. This model is thus a three-parameter question consisting of the Kuznetsov's equation, the Rosin-Rammler equation and Cunningham's Uniformity index (n). Since its inception, the Kuz-Ram model has been updated to accommodate new thoughts and advancement in technology, like the effect of Electronic Delay Detonators (EDDs), better ways of determining the rock factor, A, and that of calculating the explosive strength (Cunningham, 1987 and 2005).

4.2.1. Kuznetsov's equation

Kuznetsov developed an equation for determining the characteristic fragmentation size (Mean size), given by (Kuznetsov, 1973):

$$\bar{X} = A\left(\frac{V_O}{Q}\right)^{0.8} \times Q^{\frac{1}{6}} \tag{4.1}$$

Where:

$\bar{X}$ = The mean fragment diameter (cm),

A = Rock factor,

V_O = Volume of blasted rock per hole (m^3),

Q = Weight of explosives of TNT equivalent explosives per hole (kg).

Because TNT is no longer in use, Equation 4.1 is modified. If Q_e is the equivalent mass of explosive per blast hole and E is the Relative Weight of this explosive to ANFO, the Relative Weight Strength (*RWS*) of TNT is 115, then;

$$\text{Qe} \times \text{E} = \text{Q} \times 115 \tag{4.2}$$

Solving for Q:

$$Q = Q_e \frac{E}{115} \tag{4.3}$$

Replacing Equation 4.3 into 4.1 gives:

$$\bar{X} = A\left(\frac{V_0}{Q_e}\right) \times Q_e^{\frac{1}{6}} \left(\frac{E}{115}\right)^{-\frac{19}{30}} \tag{4.4}$$

But $\left(\frac{V_0}{Q_e}\right)$ is the powered factor, K, and replacing E with *RWS*, Equation 4.4 can be simplified as:

$$\bar{X} = AK^{-0.8} \times (Q_e)^{\frac{1}{6}} \times \left(\frac{115}{RWS}\right)^{\frac{19}{30}} \tag{4.5}$$

The rock factor A is determined as:

$$\text{A} = 0.06\ (\text{RMD} + \text{RDI} + \text{HF}) \tag{4.6}$$

Where: *RMD* = Rock mass description, *RDI* = Rock density influence; and *HF* = Hardness factor.

These parameters are measured and determined through geological and geotechnical logging.

Rock Mass Description: A number is assigned for according to the rock condition. If powdery/friable, *RMD* = 10; massive formation *RMD*= 50; but if the rock is vertically jointed, *RMD* is derived as jointed rock factor (*JF*) as follows:

$$JF = (JCF \times JPS) + JPA \tag{4.7}$$

Where;

JCF = Joint condition factor,

JPS =Joint plane spacing factor,

JPA = Joint plane angle factor.

Values are assigned to the *JCF* as 1 for tight joints, 1.5 for relaxed joints 1.5 and 2 for gouge-filled joints.

The values of *JPS* are assigned depending on the size and are relative to the absolute joint spacing. Thus; joint spacing < 0.1 m, *JPS* = 10; joint spacing between 0.1–0.3 m, *JPS* = 20; joint spacing = 0.3 m to 95% of *P*, *JPS* = 80; joint spacing > *P*, *JPS*=50 (*P* being the reduced pattern factor relating burden and spacing as: $P = (B \times S)^{0.5}$).

The values for the vertical *JPA* are defined as dip out of face 40; Strike out of face 30; dip into face 20.

Rock Density Influence: It is calculated as: $RDI = (25 \times \rho_{rock}) - 50$. Where ρ_{rock} is the in-situ density of the rock.

Hardness factor: The *HF* is given as a function of *UCS* and Young's Modulus as:

$$HF = \frac{Y}{3} \text{ if } Y < 50; \quad HF = \frac{UCS}{5} \text{ if } Y > 50;$$

Where;

Y = Elastic modulus (GPa),

UCS = Unconfined compressive strength (MPa).

The elastic modulus is used because it will be meaningless to determine the *UCS* of a weak rock mass.

An adjustment was made to the Rock Factor *A*, by introducing a rock correction factor *C*(*A*). This factor varies between 0.5 and 2 and is applied if there are indications that the rock factor needs to be changed, instead of tweaking the entire algorithm. Thus:

$$A = 0.06\,(RMD + RDI + HF) \times C(A) \tag{4.8}$$

After the incorporation of the effects of *EDDS*, timing scatter and the rock factor correction factor (Cunningham 2005), the Kuznetsov's equation for mean size estimation had been adjusted to as:

$$x_m = AA_T \frac{Q^{\frac{1}{6}}}{K^{0.8}} \times \left(\frac{115}{RWS}\right)^{\frac{19}{30}} \times C(A) \tag{4.9}$$

Where:

X_m= Mean fragment size,

A = Rock factor;

A_T = Timing factor (incorporating the effect of inter-hole delay on fragmentation),

K = Powder factor,

RSW = Relative Weight Strength of the explosive being used,

$C(A)$ = Correction for rock factor.

4.2.2. Rosin-Rammler equation

The Rosin-Rammler equation is used for determining the percentage passing (Lilly 1986). As stated by Faramarzi, et al. (2013), this equation is important in characterizing or describing the muck pile size distribution. It is given as:

$$R = e^{-\left(\frac{X}{X_c}\right)^n} \tag{4.10}$$

Where:

R = Proportion of material retained on screen size x,

x = Screen size,

x_c = Characteristic size,

n = Uniformity index

This equation has however been adapted by Cunningham (2005) and thus presented as:

$$R_x = e^{\left[-0.693\left(\frac{x}{x_m}\right)^n\right]} \quad (4.11)$$

Where:

R_x = Mass fraction retained on screen opening x, x= Screen opening,

x_m= Characteristic size, n = Uniformity index (between 0.7 and 2).

4.2.3. Cunningham's uniformity index (n)

The Cunningham Uniformity Index (n) uses the controllable parameters of blast design. This index defines the uniformity of the fragment size. The value of n determines the shape of the curve. It is given as:

$$n = \left[2.2 - 14\left(\frac{B}{D}\right)\right]\left[0.5\left(1 + \frac{S}{B}\right)\right]^{0.5}\left[1 - \frac{W}{B}\right]\left[\frac{L}{H}\right] \quad (4.12)$$

However, this formula had been modified to incorporate deck charging, thus:

$$n = \left[2.2 - 14\left(\frac{B}{D}\right)\right]\left[0.5\left(1 + \frac{S}{B}\right)\right]^{0.5}\left[1 - \frac{Z}{B}\right]\left[0.1 + \text{Abs}\left(\frac{(BCL_b - CCL_t)}{L}\right)\right]^{0.1}\left[\frac{L}{H}\right]C(A) \quad (4.13)$$

Where: B = burden, m; S = spacing, m; D = hole diameter, mm; W or Z = standard deviation of drilling precision, m (3 cm/m acceptable); L = charge length, m; BCL_b = bottom charge length, m; CCL_t = column charge length, m; H = bench height, m; $C(A)$= Corrected rock factor.

The value of n ranges from 0.5 to 2.2 if n=0.6, it means the muckpile is not uniform and if n=2.2, it means the fragments are uniform and the majority of the fragments are close to the mean size x_m.

4.2.4. Shortcomings of the Kuz-Ram model

The Kuz-Ram model has shortcoming. Firstly, the model over-estimates the mean size of the fragment. This is because Cunningham assumed that the passing 50% (P_{50}) is the same as the mean size from the Rosin-Rammler equation. However, this is not true as shown by Spathis (2004). This resulted in the modification given in Equation 4.7. Secondly; the model underestimates the fines, this has been corrected in the Swebrec model as will be shown in Section 4.4. Also, the *S*/*B* ratio should be less than 2 and initiation and timing should be such that no cut-offs or misfires results. The rock geotechnical structures must be assessed carefully to give a good input into the model (Kwangmin, 2006).

4.3. Crush Zone Model

During the detonation an explosive inside a blast hole, a rapidly expanding gas is formed that fills the entire blast hole. The continuous expansion of this gas leads to the formation of blast induced damages around the hole peripheral. Zones of failure are formed that can be grouped into elastic deformation zone, fracture zone and crushed zone, as shown in Figure 4.1. In the crushed zone module, rock around the blast hole is turned into fines.

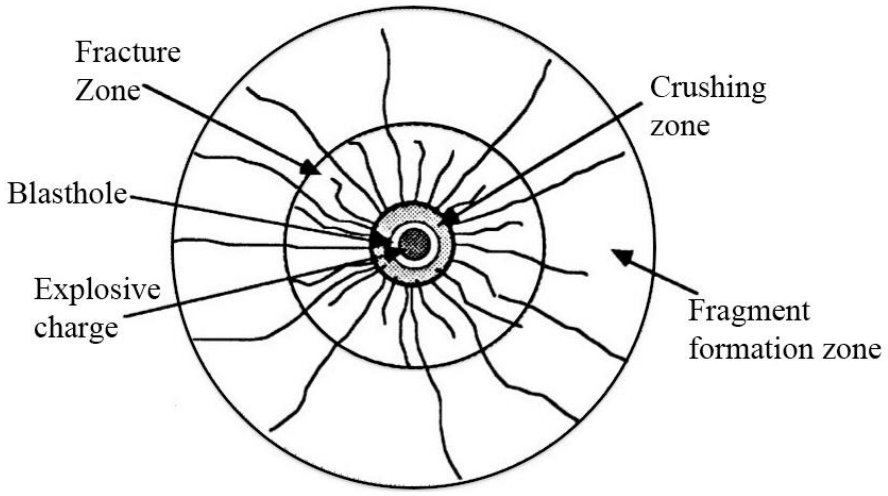

Figure 4.1. Formation of crushing zone, fracture zone and fragment zone in a blast hole.

Several methods to determine the extent of the crush zone near a blast hole has been proposed. Among them are those developed by II'yushin (1999), Vovk et al., (1973) and Szuladzinski (1993, as cited in Esen et al., 2003), and Lu et al. (2016). However, these

methods do not consider the effect that cavity expansion and the in-situ stress and compressive hoop stress have on fragmentation.

Esen developed a model that is used to determine the extent of the crush zone after a blast (Esen et al. 2003). After analysing some of the already existing models, he conducted tests on 92 samples to measure the extent of the crushed zone. This lead to the introduction of the Crush Zone Index (*CZI*), which is a dimensionless parameter. This index measures the potential of crushing of a charged hole and, it is a function of the pressure of detonation, *UCS*, Poisson's ratio and the dynamic Young's modulus. Through these experiments, it was shown that the radius of the crush zone depends on the *CZI* and the blast hole diameter. Application of dimension analysis leds to the derivation of two dimensionless indices:

$$\pi_1 \frac{r_0}{r_c} \text{ and } \pi_2 = \frac{(P_b)^3}{(K) \times \sigma_c^2} = \text{CZI} \tag{4.14}$$

Where:

r_c = Crush zone radius (mm),

r_o = Radius of the blast hole,

P_b = Borehole pressure (Pa),

K = Rock stiffness (Pa),

σ_c = Uniaxial compressive strength (Pa).

Rock stiffness (K) is determined as:

$$K = \frac{E_d}{1+\nu_d} \tag{4.15}$$

Where:

ν_d = Dynamic Poisson's ratio,

E_d = Dynamic Young's modulus (GPa).

The borehole pressure (P_b) which is defined as the pressure of the explosive gases expanded to the initial volume of the borehole, is determined as:

$$P_b = \frac{P_{CJ}}{2} \quad (4.16)$$

P_{CJ} is the ideal detonation pressure calculated from the principal of Ideal detonation as:

$$P_{CJ} = \frac{\rho_0 D_{CJ}^2}{\gamma+1} \quad (4.17)$$

Where:

P_{CJ} = Ideal detonation pressure (Pa),

ρ_0 = Density of the ungassed explosive (kg/m^3),

D_{CJ} = Velocity of detonation (m/s),

γ = Specific heat ratio.

By applying ideal detonation pressure, all the assumption of ideality apply (Fickett and Davis, 1979).

Applying regression analysis to Equation 4.14 the crushed zone radius is defined as;

$$r_c = 0.812 \times r_o \times (CZI)^{0.219} \quad (4.18)$$

Where:

r_c =Crush zone radius (mm),

r_o = Radius of the blasthole (mm),

CZI = Crush Zone Index.

The crushed zone model by Esen et al. (2003) has been discussed in more detail because it has been applied and incorporated into the fragmentation prediction model.

There are other models for determining the radius of the crushed zone. A summary of two of these is given hereof:

Djordjevic (1999) developed a Two-Component model that is based on the Griffith failure criterion. In his model, the radius of crushing is given as:

$$r_c = \frac{r_o}{\sqrt{\frac{24T}{P_b}}} \tag{4.19}$$

Kanchibotla's model assume that the crushing zone radius depends on the detonation pressure, UCS and the borehole diameter (Kanchibotla et al., 1999). Thus:

$$r_c = r_0\sqrt{\frac{P_d}{\sigma_c}} \tag{4.20}$$

Where:

r_o = Borehole radius (mm),

T= Rock material's tensile strength of the (Pa),

P_d= Borehole detonation pressure (Pa),

σ_c =Rock's unconfined compressive strength (Pa).

Lu et al. (2016) argues that dividing the final blast induced damage area into three zones is erroneous because it assumes that the hoop stress around the fractured zone is equal to zero. This phenomenon, presented in the existing models, dictated that the region between the elastic deformation zone and the crushed zone is completely damaged by radial cracking. This simply entails that the rock between these two zones can only transit radial stress and do not support any hoop stress, thus equating the hoop stress to zero. However; because the fracture zone connects the crushed zone and the elastic deformation zone, the rock cannot be completely destroyed. He therefore proposed that the fracture zone be divided into two distinct zones: inner fracture zone (fracture zone I) and the outer fracture zone (fracture zone II). This idea is shown in Figure 4.2.

Thus, the final area of damage is divided into four zones as opposed to three and determined as follows.

1. The crushed zone $a(t) \leq r \leq b\times(t)$
2. The fractured zone I : $b\times(t) \leq r \leq b_I(t)$

3. The fractured zone II : $b_I(t) \leq r \leq b_{II}(t)$
4. The elastic deformation zone: $b_{II}(t) \leq r \leq \infty$

Where: $a(t)$ is the expanding cavity radius; $b\times(t)$ is the crushed zone radius; $b_I(t)$ is fractured zone radius I; and $b_{II}(t)$ is the fractured zone II radius, all in mm.

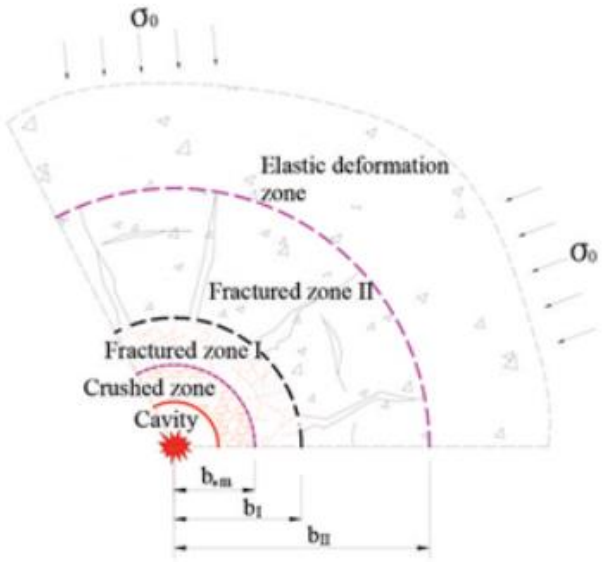

Figure 4.2. Damage zone surrounding a blast hole as proposed by Lu et al. (2016).

Thus, the proposed radius of the crushed zone is given as:

$$b_m = \begin{cases} r_b \left(\frac{P_b}{\sigma_s} K \frac{\sin\theta}{1+\sin\theta}\right)^{\frac{1}{2\gamma_1}} K^{-\frac{1}{2}} & a_m \leq r_k \\ r_b \left(\frac{P_b}{\sigma_s} K \frac{\sin\theta}{1+\sin\theta}\right)^{\frac{1}{2\gamma_2}} \left(\frac{r_k}{r_b}\right)^{\frac{\gamma_1-\gamma_2}{\gamma_2}} K^{-\frac{1}{2}} & a_m > r_k \end{cases} \quad (4.21)$$

Where: b_m = Radius of the crushed zone,(mm); r_b = Blast hole radius (mm); P_b = Explosion pressure (Pa); σ_s = Compressive strength (Pa); γ_1 and γ_2 = Adiabatic isentropic exponents; r_k = Explosive critical radius (mm); $K = a_m$ = Maximum cavity radius (mm); θ = Internal friction angle.

4.4. Swebrec Function

The Swebrec function is another method used to predict the amount of fines in rock fragments. It was developed by Ouchterlony of the Swedish Blasting Research Centre in

2005. Since then this method has found wide application and it is improving the way fragment distribution prediction. The Swebrec function has three parameters; x_{max}, x_{50} and the curve undulation exponent b. This function is given as:

$$P_x = \left[\frac{1}{1+\left[\frac{\left(In\frac{x_{max}}{x}\right)}{\left(In\frac{x_{max}}{x_{50}}\right)}\right]^b}\right] \tag{4.22}$$

$$b = \left[2In2In\left(\frac{x_{max}}{x_{50}}\right)\right]n \tag{4.23}$$

Where: P_x = Fraction smaller than size x; x_{max} = Minimum among values of in situ block size, Spacing or Burden. It limits the fragment size; x_{50} = Median or size of the 50% passing; b = Curve undulation exponent; n = Cunningham's uniformity index.

4.5. Kuznetsov – Cunningham – Ouchterlony (KCO) Model

The Swebrec function removes the drawbacks of the Kuz-Ram model. When an extended version is applied together with the Kuz-Ram, the model becomes to be known as Kuznetsov – Cunningham – Ouchterlony (KCO) Model (Ouchterlony, 2005 and 2010; Spathis, 2013). This model is as a result of replacing the Rosin-Rammler equation in the Kuz-Ram model with the Swebrec function. Thus, the KCO model can be stated as:

$$P_x = \left[\frac{1}{1+\left[\frac{\left(\mathrm{In}\frac{x_{max}}{x}\right)}{\left(\mathrm{In}\frac{x_{max}}{x_{50}}\right)}\right]^b}\right] \tag{4.24}$$

$$x_{50} = \frac{g(n).A.Q^{\frac{1}{6}}.\left(\frac{115}{S_{ANFO}}\right)^{\frac{19}{30}}}{q^{0.8}}, \quad \text{where g(n)=1 or } (\mathrm{In}2)^{\frac{1}{2}}.\Gamma(1+\frac{1}{n}) \tag{4.25}$$

$$b = \left[2\mathrm{In}2\mathrm{In}\left(\frac{x_{max}}{x_{50}}\right)\right]n \text{ or}$$

$$2In2.In\left(\frac{x_{max}}{x_{50}}\right)\left(2.2-\frac{0.0148B}{d}\right)\left(1-\frac{SD}{B}\right)\left(\sqrt{\frac{1+\frac{S}{B}}{2}}\right)\left(\frac{|L_b-L_c|}{L_{tot}+0.1}\right)^{0.1}\left(\frac{L_{tot}}{H}\right) \quad (4.26)$$

Xmax= min(in situ block size, *B* or *S*)

Where: P_x = Fraction smaller than size *x*; x_{max} = Minimum among values of in situ block size, Spacing or Burden; x_{50} =Median or size of the 50% passing; *b* = Curve undulation exponent; *n* = Cunningham's uniformity index; *S* = Spacing; *B* = Burden; *d* = Drill hole diameter; *SD* = Standard deviation of drilling; L_c = Length of column charge; L_b = Length of bottom change; L_{tot} = Total charge length; S_{ANFO} = Specific weight of an explosive relative to ANFO; *Q* = Explosive charge quantity; *H* = Bench height; and Γ= Gamma function.

4.6. Conclusion

This chapter has given a detailed description of some of the common fragmentation prediction model. Of particular interest to this research is the modified Kuz-Ram model, the Crushed zone model by Esen et al. (2003) and the Kuznetsov-Cunningham- Ouchterlony model. The modified Kuz-Ram model has continued to be applied in the industry (Adebola et al., 2016) because of its ease to use. However; by replacing the Rosin-Rammler equation with the Swebrec function, the KCO model has increased the prediction accuracy and thus has been applied to this research. In order to do a dual diligence, a comparison of the three models, the modified Kuz-Ram with *g(n)*=1, the modified Kuz-Ram with *g(n)* calculated and the KCO model were done.

5. DATA COLLECTION

5.1. Introduction

The unit of operations employed at Sentinel mine is unique to that used in the copper mines in Zambia. This is because in-pit crushing is used at the mine as opposed to the traditional hauling method. This unit of operations can be summarised as drill-blast-load-haul-In-pit crush-convey-mill. This chapter discusses the data that was collected during the research and gives a detailed description of the drilling and blasting and the comminution operations of Kalumbila mines.

5.2. Rock characterization

The Sentinel pit is divided into 8 ore domains based on the major rock lithology, as shown in Table 5.1

Table 5.1. Ore domains of Sentinel mine

Domain	Type	Unit Weight (kN/m^3)	RQD (%)	UCS (MPa)	RMR_{76}	Young's Modulus (GPa)
Meta-carbonate	Fresh Weathered	28.0 -	96 -	75 -	77 -	42.2 7.5
Phyllite	Fresh Weathered	27.5 26.5	88 38	78 37	73 43	31.6 5.6
Phyllite-carbonaceous	Fresh Weathered	27.5 26.0	87 36	85 36	73 43	31.6 5.6
Schist	Fresh Weathered	27.5 26.5	93 57	97 27	77 47	42.4 -

During planning and drilling, the ore domains in Table 5.1 are demarcated in the pit and are provided as a geological input to the drilling planning team. The rate of penetration from production rotary-circulation drilling is used to deduce which domain the bench lies in and to determine the rock hardness. Figure 5.1 shows a dig map illustrating main ore domain demarcation.

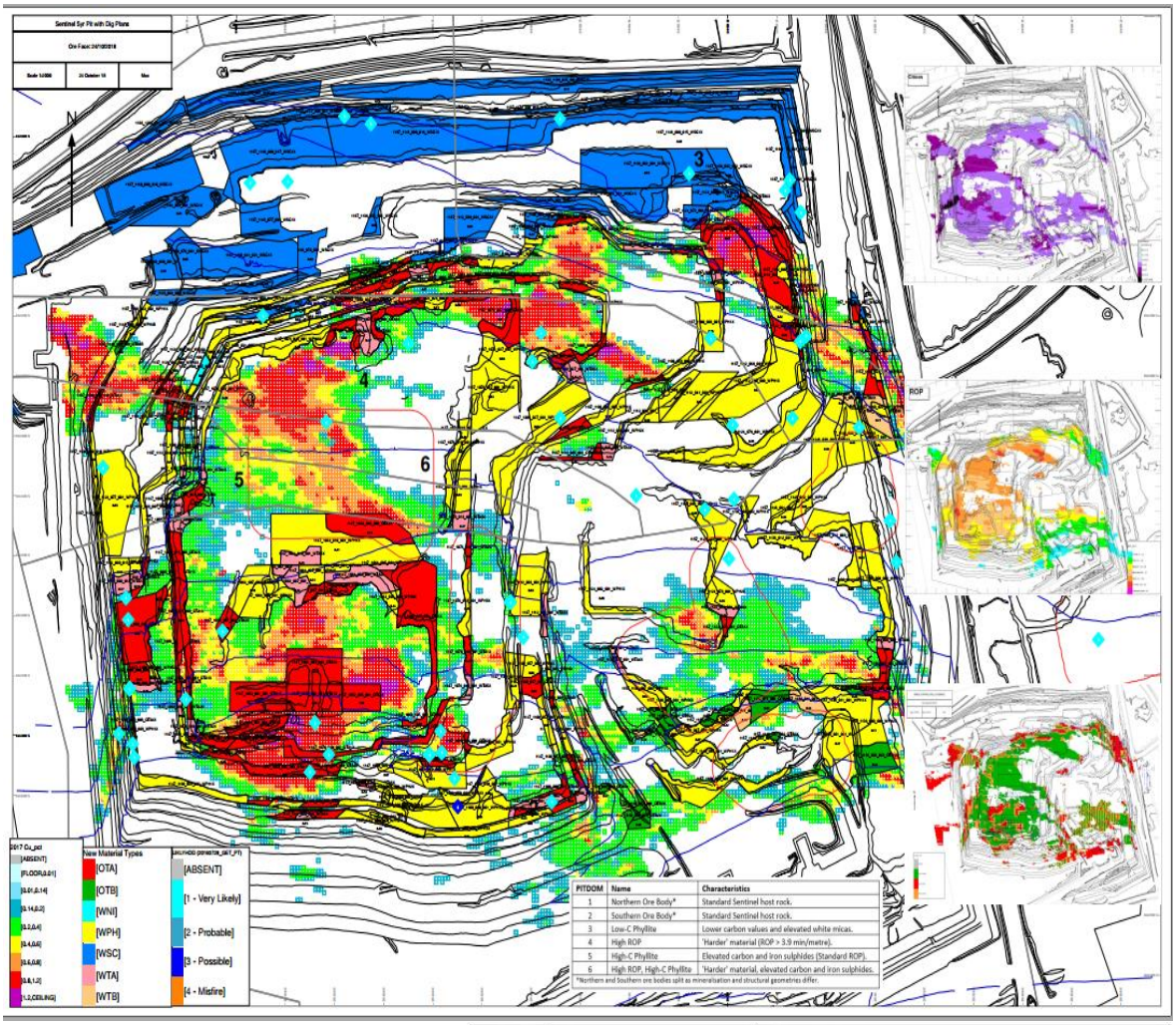

PITDOM	Name	Characteristics
1	Northern Ore Body*	Standard Sentinel host rock.
2	Southern Ore Body*	Standard Sentinel host rock.
3	Low-C Phyllite	Lower carbon values and elevated white micas.
4	High ROP	'Harder' material (ROP > 3.9 min/metre).
5	High-C Phyllite	Elevated carbon and iron sulphides (Standard ROP).
6	High ROP, High-C Phyllite	'Harder' material, elevated carbon and iron sulphides.

*Northern and Southern ore bodies split as mineralisation and structural geometries differ.

Figure 5.1. Example of ore domain demarcation.

5.3. Drilling

Drilling equipment can be classified depending on three major parameters. Dey (1995) classified them as follows:

1. Depending on the method of drilling. Thus,
    a. Percussive Drilling,
    b. Rotary Drilling,
    c. Rotary-percussive Drilling.

2. Depending on the tramming mechanism and operating power source. Thus,
    a. Diesel driven drilling machine,
    b. Electrically driven drilling machine.

3. Depending on the power transmission mechanism:
    a. Pneumatically operated machine,
    b. Hydraulically operated machine,
    c. Electrically operated machine,
    d. Combination with hydraulic and pneumatic system.

Kalumbila mine has a fleet of drill rigs that comprises both percussion and rotary drills that are both diesel and electrically operated. These are: Cat MD 6640, Epiroc Pit Vipers 271, Sandvic D25k, Furukawa DCR-20.

CAT MD 6640 is electric powered rotary drill rig. They are used to drill 290 mm diameter production holes. Because they are fitted with modular system (Modular, 2019), they have a high collaring and drilling accuracy.

The EPIROC Pit Vipers drills 270 mm drill holes, utilising rotary drilling mechanism. They are also electric powered. Collaring is done manually, as they are yet to be fitted with modular intelligent system.

SANDVIC D25K has a 469 kW diesel powered DTH drill rig. The D25K rigs utilise Down-the-hole-hammer (DTH) drilling technique and are used to drill 270 mm production holes, mostly near the pit walls and in areas were the electric powered rigs cannot access. The DKs have a maximum drilling depth of 25 meters.

The Furukawa DCR-20 is diesel driven roto-percussion drilling rig. They are used to drill 165 mm drill holes, which are mostly for presplit purposes. They are also used to drill boulders for secondary blasting in instances where the rock breaker cannot be used. In some cases, a combination of the DKs and DCRs is used in a trim blast, but mostly the big drills (MDs and PVs) are used as they provide the advantage of bigger blast holes and higher productivity. Visual presentations of these rigs are given in Appendix A.

Kalumbila mine uses 12-meter benches drilled with a predetermined sub-drill for preconditioning the next bench in very hard and hard domains. In sensitive areas and on bench slopes, a negative sub-drill is used.

Empirical formulas suggested by Ash (1963) compiled by Hustrulid (1999) are used to determine the drilling parameter. The formulae are:

- Burden (*B*) = 20 to 40 × Hole diameter (*D*),
- Hole depth ratio = 1.5 to 4 × *B* (typically 2.5),
- Spacing (*S*) = 1 to 2 × *B*,
- Subgrade (*Su*) = 0.3 × *B* (as a minimum),
- Stemming length (*St*) = 0.5 to 1 × *B* (0.7 average).

Other industrial recommendation "*rule of thumb*" includes those proposed by industrial blasting leaders Dyno Nobel and Orica (Dyno Nobel, 2010; Orica 2013a, 2015). These are:

- Bench Height (*BH*) = 2 to 4 × *B* or 40 to 60 × *D*,
- Hole diameter in mm (*D*) = 8 to 15 × *BH* in m (for small diameter holes),
- Burden (*B*) = 20 to 40 × *D*,
- Spacing (*S*) = 1.1 to 1.4 × *B*,
- Stemming length (*St*) = 20 to 30 × *D*,
- Subgrade (*Su*) = 8 to 12 × *D*.

5.3.1. Stemming

Stemming in a blast hole provides explosive confinement and prevents the escaping of the high-pressure gasses resulting from explosion of an explosive. Stemming also prevents flyrock and noise. In order to provide successful fragmentation in the stemming region and to reduce the potential of flyrocks and air-blasts, a proper stemming height should be selected.

Chiappetta and Treleaven (1997) established the theory of the Scaled Depth of Burial (SDOB). They conducted crater experiments and found that flyrock is affected by the length

of explosive charge below the stemming and the depth of burial. They also found that the potential of flyrock is a function of the distance from the surface to the center of defined charge crater (*d*), and the explosive weight of the explosives just below the stemming, (*w*), as shown in Figure 5.2.

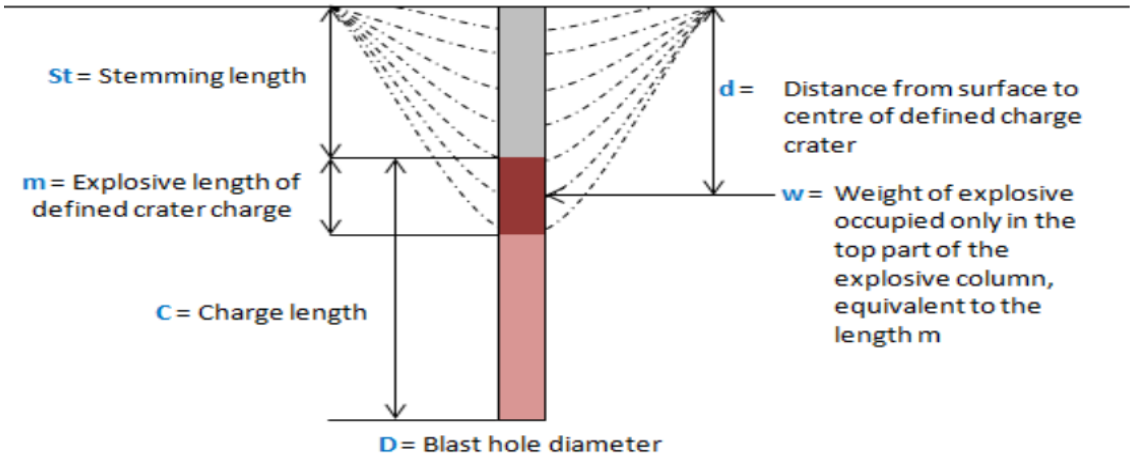

Figure 5.2. Concept of scaled depth of burial (Chiappetta and Treleaven, 1997).

SODB is determined as:

$$SDOB = \frac{d}{w^{\frac{1}{3}}} = \frac{St+0.0005mD}{0.00923\left(dD^3\times\rho_{explo}\right)^{\frac{1}{3}}} \quad (5.1)$$

Where:

St = Stemming length (m),

m = Contributing charge length factor,

$m = \frac{1000c}{D}$, "*m*" has a maximum value of 8 for blast hole diameter less than 100 mm, and a maximum value of 10 for a blast hole diameter greater than or equal to 100 mm (ISEE Blasters' Handbook™, 2011),

D = Blast hole diameter (mm),C = Charge length (m),

ρ_{explo} = Explosive density (g/cc),

As the SDOB is indirect proportional to the risk and severity of flyrock, noise and airblast (Figure 5.3), maintaining a SDOB between 0.92 and 1.40 m/kg⅓, will result in insignificant flyrock and noise, and good fragmentation. Thus, a SDOB of 1.62 m/kg⅓ is used.

Rearranging equation 5.1, the stemming height is determined as:

$$St = (0.00923\ SDOB \times (mD^3 \times \rho_{explo})^{1/3}) - (0.0005Dm) \quad (5.2)$$

The Subdrill is determined by using the empirical formula: Su=8 to 12 × D.

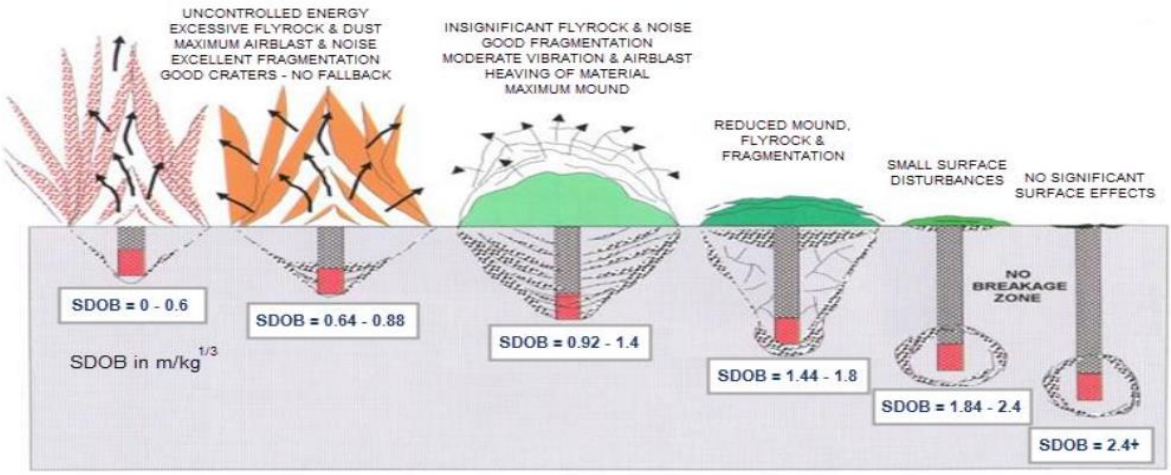

Figure 5.3. Scaled depth of burial values (Chiappetta and Treleaven, 1997).

Based on these formulas, the drilling parameters for the mine, depending on the rock hardness is given in Table 5.2.

Table 5.2. Kalumbila mine drilling pattern parameter

Hole diameter: 270mm					**Hole diameter: 251mm**			
Parameter	Ore Hardness				Ore Hardness			
	Very Hard	Hard	Medium	Soft	Very Hard	Hard	Medium	Soft
Burden	5.4	6.3	7.0	7.5	5.2	6.1	6.8	7.2
Spacing	6.2	7.2	8.1	8.6	6.0	7.0	7.8	8.3
Sub-drill	4.0	4	3.0	3.0	4.0	4.0	3.0	3.0
Stemming	5.5	5.5	5.5	5.5	5.0	5.0	5.0	5.0

Table 5.3. Kalumbila Mine drilling pattern parameter (continued)

Hole diameter: 229mm					**Hole diameter: 165mm**			
Parameter	Ore Hardness				Ore Hardness			
	Very Hard	Hard	Medium	Soft	Very Hard	Hard	Medium	Soft
Burden	5.0	5.8	6.4	6.9	4.0	4.5	5.0	5.5
Spacing	5.8	6.7	7.4	7.9	4.6	5.2	5.8	6.3
Sub-drill	4.0	4.0	3.0	3.0	3.0	3.0	3.0	3.0
Stemming	4.5	4.5	4.5	4.5	4.0	4.0	4.0	4.0

5.4. Blasting

Blasting is the primary and most effective way of breaking and fragmenting in-situ rock. Different types of explosives are used to achieve this task. An explosive is defined as any compound or mixture susceptible (by heat, shock, friction or other impulse) to a rapid chemical reaction, decomposition or combustion with the rapid generation of heat and gases with a combined volume much larger than the original substance. Generally, explosives and their accessories are classified into 3 classes. These are:

1. Class A explosives - High explosives. These are any material possessing detonating properties, such as dynamite, nitro-glycerine, fulminate of mercury, black powder, blasting caps, and detonating primers.

2. Class B explosives - Low explosives. These are materials that cannot explode, but rather possess flammable hazard. These include black powder, safety fuses, igniters, igniter cords, fuse lighters, except for bulk salutes, and some special fireworks.
3. Class C explosives - Blasting agents. These include ammonium nitrate-fuel oil and certain water gels.

The Zambian government divides explosives in 7 classes (Explosive act, 1995). These are:

Class 1. *Gunpowder*. Gunpowder includes blasting powder that consists of an intimate mixture of chemicals like saltpetre (potassium nitrate), sulphur and charcoal, saltpetre containing potash perchlorate in greater quantity than one percent.

Class 2. *Blasting agents*. A blasting agent is any nitrate mixture which cannot be normally detonated without the use of a nitro-compound primer or booster when used for blasting purposes.

Class 3. *Nitro-compound*. These are chemical compound or mechanically mixed mixture consisting wholly or partly of nitro-glycerine, or other liquid nitro-compound, and used for the purpose of blasting.

Class 4. Chlorate mixture - any explosive containing a chlorate.

Class 5. *Fulminate*. These are defined as any chemical compound or mechanical mixture that can be used for initiating a detonation because they have a high susceptibility to detonation.

Class 6. *Detonators*. They are defined as a device enclosing a sensitive explosive and prepared so as to be used for initiating the detonation of less sensitive explosives.

Class 7. *Blasting initiator*. These include any fuse or device that can be used to ignite a plain detonator.

Kalumbila Minerals has contracted Bulk Mine Explosives (BME) to conduct blasting. The contractor has an onsite emulsion manufacturing company. This gives an advantage to tailor the emulsion to customer needs and satisfaction, in terms of energy content. Emulsion is transported into the pit by the mobile mixing units (MMU) and chemical mixing (gassing/sensitising) is done on the ground. Charging is achieved by either pumping or augering. Three types of explosives are used at the mine, these are low energy INNOVEX™ 100, high energy INNOVEX™ Lateral and INNOVEX™ 207. INNOVEX™ 207 is a high-energy blended emulsions containing 70% emulsion and 30% ammonium nitrate prill.

Electronic blasting is used at the mine. AXISIS Electronic Delay Detonators (EDD) are used for initiation while 400 g Viper boosters are used for priming. Magnum megamite is used in pre-splitting and in secondary blasting (BME, 2019). V echelons and centre-lifts

are used as firing sequence. Orica's ShotPlus software is used for drill and blast design. The technical properties of these explosives are given Table 5.3. Appendix B gives a visual presentation of the explosives and accessories used at Sentinel mine.

Table 5.4. Types of explosive used at KML

Product Name	Normal Bulk Density (g/cm^3)	In-hole Density (g/cm^3)	Relative Weight Strength	Relative Bulk Strength	Velocity of Detonation (m/s)
INNOVEX™ 100	1.47-1.51	0.9-1.2	84	126	3500-5000
INNOVEX™ Lateral	1.46-1.50	0.95-1.25	81	121	2500-4000
INNOVEX™ 207	-	1.15	90	134	3500-5000

5.4.1. Reactive ground

Reactive ground is a term used in the mining industry to describe ground in which the reaction between sulphide bearing rock/soils like iron, zinc and copper sulphides with ammonium nitrate based explosives, leads to an auto-catalysed process which can lead to an exothermic decomposition and unwarranted explosion (Orica 2013b; Botha, 2014; Hariparsad,2015; Krause, 2016).

During natural weathering process of iron containing rocks, ferrous ions and acid is formed. This process is exacerbated by drilling and loading activities that increases the surface area of the sulphide fines for reaction. This reaction is given as:

Iron sulphides + atmosphere (H_2O + air) = ferrous ions + sulphuric acid

When nitrates (found in explosives), is introduced in the equation heat is formed among other products:

Nitrates + iron sulphides + ferrous ions + sulphuric acid = nitrous oxide + ferrous ions + heat.

This reaction can slowly, but gradually, intensifies until a violent reaction that can lead to an explosion occurs.

Treatment of reactive grounds has been discussed at length in literature (AEISG, 2007; Van Jaarsveld and Van Greunen, 2013; Simmons, 2015; Krause, 2016). These include on the block temperature testing, bucket testing, geothermal logging and blast hole sleeving. Kalumbila mines regular conducts laboratory test to establish and map reactive grounds. These tests are usually conducted by expert contractors (Orica or BME) who are suppliers of explosives to the mine. BME also conducted test as a way of keeping the key performance indicators (KPIs) for their explosive. Sleeving of blastholes has been adopted at the mine site. This method provides a barrier between the explosives and the ground thus reducing the chances of contact and reaction occurrence. Figure 5.4 shows the use of a blast liner.

Figure 5.4. Use of blast hole liner to prevent the contact of ammonium nitrate and sulphides.

5.5. Load and Haul

Loading at Kalumbila mine is achieved via the use of electric-powered rope shovels (face shovels), and electric or diesel-powered front end loader. A fleet of dump trucks hauls the ore from the blasted area to the location of the in-pit crushers and low grade ore to low-grade stockpiles while waste is taken to the dumps. The use of in-pit crushing and

conveyance (IPCC) has greatly reduced the cost of material handling and has resulted in low carbon emission by the mine, unlike ordinary load and haul operations.

5.6. Crushing

The operation of the crushers is within a performance envelope that consists of material throughput, size and of the product and power consumed. The design parameters of the equipment dictate the overall shape of the envelope. These parameters are the Mechanical Design Variables (MDV), Machine Operating Variables (MOV) and the Feed Material Variables (FMV).

The MDV's do not change with time and the represent the material flow and the energy that need to be applied to the material inside the crusher. These include: cavity design, angle of the cone head, eccentric throw, and the speed of the cone head. MOV's are those variables that the user can change with time. These include the feed rate and the closed side setting of the crusher.

The FMV's include: strength of feed material, feed size, feed grading (and hence bulk density), choke feed level, and the moisture content of the feed. These variables can easily change significantly over small periods of time and controlling them can be difficult.

Time dependency in crushing involves variables that are encompassed in the operating envelopes above. Of interest to this research is the feed rate and feed material type and grading. Thus, this research worked to establish a constant feed rate with well fragmented material.

Three in-pit Gyratory crushers shown in Figure 5.5 (ThyssenKrupp KB 63 – 89) are used for primary crushing of blasted material at Kalumbila Mine. These crushers are strategically located on the North and South sides of the pit to reduce the haul distance from the pit. The crushers have a design throughput of 4000 tph and reduce the ROM ore from 800 mm down to 150 mm. The material from the in-pit crushers is transported to the processing plant via the pit top bin, by three overland conveyors, one from each crusher.

These crushers are “choke fed”. This feeding model has several advantages, among these are:

1. In order to ensure a development of a wear profile that is uniform,
2. It gives a product sizing that is more consistent,
3. It results in maximizing throughput,
4. It extends the life of the crusher liners,
5. It results in an improved cubicity of the product.

Figure 5.5. ThyssenKrupp KB63-89 gyratory crusher.

The material from primary crushers (mixed with secondary and pebble crusher product, if applicable) are stockpiled near the processing plant at the milling stockpile. Two shuttle conveyors from the primary crushers stockpile the material which is fed to the mills by 4 reclaim feeders per mill train which are located below stockpile.

Two Metso MP2500 cone crushers (Figure 5.6) located within the process plant are used for secondary crushing in case of need. This is particularly one when the ore feed is hard so as to generate finer material in the feed to the mills. These crushers operate separately and a throughput of 3700 tph and reduce primary crusher product down to 55 mm.

A Metso MP1250 pebble crusher (Figure 5.7) is also in the circuit and is used to reduce SAG mill reject pebbles down to 19 mm, which is later taken to the milling stockpile.

Figure 5.6. Metso MP2500 secondary crusher.

Figure 5.7. Metso MP1250 pebble crusher.

5.7. Milling

The material from the milling stock pile is fed into two SAG mills. The SAG mills are in series connection with two ball mills, with a total of 6 cyclone clusters. The SAG and ball mills with a design capacity of 5000 tph throughput have an installed power of 28 MW and 22 MW, respectively. The grinding media used in the SAG and ball mills are 125-140 mm and 65 mm, respectively. The milling circuit is shown in Figure 5.8.

Figure 5.8. Milling circuit showing the SAG and ball mills.

The crushing and milling data for a three months' period from September to November was studied to provide an insight into the operation situation of the comminution plant. This data is given in Table 5.4 -Table 5.7.

Table 5.5. Crusher data, August 2018.

	Primary Crusher	**Secondary Crusher**	**Pebble Crusher**
Total Crushed	121,857 dmt	55,709 dmt	9,876 dmt
Operating Time	14 hrs	20 hrs	9.65 dmt
Overall rate	3,865 tph	2,781 tph	1,024 tph
Power Draw	1,410 kW	1,422 kW	-
Specific Energy	0.36 kWh/t	0.51 kWh/t	-

Table 5.6. Crusher data, September 2018.

	Primary Crusher	**Secondary Crusher**	**Pebble Crusher**
Tonnes Crushed (ROM)	116,344 dmt	69,659 dmt	8,343 dmt
Operating Time	12.70 hrs	14.2 hrs	8.19 hrs
Overall rate	3,063 tph	4,893 tph	1,018 tph
Power Draw	2,183 kW	1,443 kW	818 kW
Specific Energy	0.23 kWh/t	0.29 kWh/t	0.80 kWh/t

Table 5.7. Crusher data, October 2018.

	Primary Crusher	**Secondary Crusher**	**Pebble Crusher**
Tonnes Crushed (ROM)	134,809 dmt	106,408 dmt	10,059 dmt
Operating Time	13.10 hrs	22.24 hrs	11.08 hrs
Overall rate	3,342 tph	4,784 tph	908 tph
Power Draw	6,146 kW	899 kW	897 kW
Specific Energy	0.64 kWh/t	0.19 kWh/t	0.99 kWh/t

Table 5.8. Milling data for three months.

	August 2018	September 2018	October 2018
Total Milled	150,086 dmt	143,989 dmt	138,636 dmt
Pebbles to Stockpile	13,952 dmt	8,998 dmt	10,921 dmt
Feed to Flotation	136,134 dmt	134,991 dmt	127,715 dmt
Overall rate	3,211 tph	3,291 tph	3,688 tph
Power Draw	81,345 kW	88,586 kW	81,853 kW
Specific Energy	12.69 kWh/t	13.34 kWh/t	10.93 kWh/t

5.8. Quality Control and Quality Assurance

Quality Control (QC) and Quality Assurance (QA) was conducted on all of the drilling and blasting operation. Drilling compliance for X, Y and Z measurements were done. A drilling tolerance of ±1 m has been adopted. If a hole is over-drilled, backfilling is done while if a hole is under-drilled, a redrill is done next to that under-drilled hole. However;

remedy for X, Y compliance is seldom done. Thus, deviation in collaring is avoided by means of using computerised locating methods via modular intelligent system. Rigs that are not fitted with this system depend on visual signals given to the operator by the assistance. This all is done to ensure that the final drill pattern is in tandem with the planned geometry.

Blasting QA/QC is done via measuring the amount of explosives being pumped in each hole. The explosive density is measured before charging is commenced. After gassing, and determining that the reaction rate is acceptable, charging is continued, otherwise abandoned. This measurement for density and gassing rate is done every after 15 holes. The charge mass is sometimes predetermined. However, because of variance in hole depth, this changes, and charging is just done up to the predetermined ungassed charging length, leaving an allowance for gassing before the final stemming height is achieved. This data is transferred directly to the BME server where it can be accessed and analysed for compliance. Charged holes are measured before being stemmed to determine if the final stemming length has been achieved. If the holes are under-charged, topping up with and extra charge mass is done, while if they are overcharged, the over-changed amount is pumped out.

5.9. Split Image Analysis

Online split system (Split, 2019) is used for fragmentation analysis using the image analysis feature. A number of cameras are mounted on the loading units, primary, secondary and pebble crusher, and along the conveyor belt. These cameras take real time photos and using the system software, the photos are analysed. The results are either processed as fragmentation curves or as an excel sheet which can then be analysed. This system gives real-time notification if large boulders are detected at loading, directing the haul truck operator to dump that material at the crusher stockpile where it can be broken down using a rock breaker instead of tipping the load into the crusher which can lead to crusher bridging. This system thus eliminates the need of taking photos in the field for subsequent analysis.

5.10. Conclusion

This chapter has provided a vivid picture of how the rock is drilled and how the material is moved up to the processing plant in Kalumbila mine, Zambia. The mine utilises

both electric-powered rotary drill rigs and diesel powered DTH drill rigs, with 270 mm 251 mm and 229 mm diameter holes used for production blasts while 165 mm holes are used in presplit or trim blasts. Three types of emulsion are used with viper boosters as primers. Electronic blasting is used at the mine site which provides the advantage of accuracy and less scatter, which is an important factor in fragmentation modelling. An overview of the crushing and grinding operation is also presented in this chapter.

6. FRAGMENTATION MODELLING AND OPTIMISATION

6.1. Introduction

A lot of factors are considered in order to have an optimal fragment size. Optimisation of fragmentation is achieved when all the operations that lead to blasting are optimised. These operations are primarily drilling and blasting. This chapter discusses how drilling and blasting was conducted to obtain an optimal fragment size. The used fragmentation prediction models are introduced and discussed. Also, the crushing and milling operations are highlighted.

6.2. Drilling

The blasting parameters used at the mine are given in Chapter 5. However, it was discovered that these parameters were not producing an optimal fragment size. This was made vivid by the amount of crusher bridging events that were reported at the mine. It should be noted that the mine had been working and implementing strategies to reduce the crusher bridging but most time or not, these strategies resulted in effecting negatively on the comminution process as they resulted in generating more fines than that of required. When these parameters were used with a high energy explosive, they tend to pulverise the fragments. For this reason, the drilling parameters were re-looked at to ensure that they will produce a fragment that is good both for materials handling and comminution process.

6.2.1. Determination of the drilling parameters

There are several documented formulas that are used to calculate the drilling parameters. Some of these are provided in Section 5.3 and are used to determine the current drilling patterns.

In order to determine the drilling pattern parameters (burden and spacing), one need to determine the Blastability Index (*BI*) of that area. The *BI* was first introduced by Lilly in 1986. It is defined as the measure of the ease with which a rock can be blasted. The

geological structure of the rock affects the *BI* (Chatziangelou and Christara, 2013) and thus there is need to do a thorough mapping of an area when determining the index. The BI is given by the following equation:

$$BI = 0.5\ (RMD + JPS + JPO + RDI + S) \tag{6.1}$$

Where; *RMD* is Rock Mass Description, *JPO* is Joint Plane Orientation, *JPS* is Joint Plane Spacing. These parameters can be determined via Table 6.1.

Table 6.1. BI parameters.

Parameter	Definition	Rating
Rock Mass Description	Powderly or friable	10
	Blocky	20
	Massive	50
Joint Plane Orientation	Horizontal	10
	Dip out of face	20
	Strike normal to face	30
	Dip into face	40
Joint Plane Spacing	Close (<0.1m)	10
	Intermediate (0.1m-1.0m)	20
	Wide (>1.0m)	50

RDI= Rock Density Influence, (Specific Gravity Influence, SGI) and S=Rock Strength Influence, are determined as:

$$RDI = 25\rho_{rock} - 50 \tag{6.2}$$

$$S = 0.05 \cdot UCS \tag{6.3}$$

Using the geotechnical data, the *BI* for Sentinel pit for all of the ore domains calculated. These figures are given in Table 6.2.

Table 6.2. BI values calculated for Sentinel mine.

Geotechnical domain	***RMD***	***JPS***	***JPO***	**Density (t/m^3)**	***CS* (MPa)**	***BI***
Meta-carbonate – Fresh	Blocky	Intermediate (0.1 – 1.0 m)	Horizontal	2.8	90	7.8
Phyllite – Fresh	Blocky	Intermediate (0.1 – 1.0 m)	Dipping out of face	2.8	100	2.5
Phyllite – Weathered	Friable	Close (<0.1 m)	Dipping out of face	2.7	45	9.9
Phyllite-carbonaceous – Fresh	Blocky	Intermediate (0.1 – 1.0 m)	Dipping out of face	2.8	110	2.8
Phyllite-carbonaceous – Weathered	Friable	Close (<0.1 m)	Dipping out of face	2.7	40	9.1
Schist – Fresh	Blocky	Intermediate (0.1 – 1.0 m)	Dipping out of face	2.8	125	2.5
Schist – Weathered	Friable	Close (<0.1 m)	Dipping out of face	2.7	40	9.8

Using the calculated *BI* (Lilly, 1994) values provided in Table 6.2, and the "*rule of thumb*" by Orica (2013a), and via multiple optimisation with respect to P_{80} and INNOVEX 2017 as the main explosive, new parameters were determined. The empirical formulae determined applied are:

Very rock hard domain: $B = 22D$, $S = 1.15B$, $SD = 15D$ and $St = 17D$

Hard rock domain: $B = 24D$, $S = 1.15B$, $SD = 15D$ and $St = 17D$

Medium rock domain: $B = 27D$, $S = 1.15B$, $SD = 12D$ and $St = 19D$

Soft rock domain: $B = 28D$, $S = 1.15B$, $SD = 12D$ and $St = 19D$

Table 6.3. Optimised drilling parameters.

Hole diameter: 270mm					**Hole diameter: 251mm**			
Parameter	Ore Hardness				Ore Hardness			
	Very Hard	Hard	Medium	Soft	Very Hard	Hard	Medium	Soft
Burden	5.9	6.5	7.2	7.7	5.5	6.0	6.7	7.2
Spacing	6.8	7.5	8.2	8.8	6.4	6.9	7.6	8.2
Sub-drill	4.1	4.1	3.2	3.2	3.8	3.8	3.0	3.0
Stemming	4.6	4.6	5.1	5.1	4.3	4.3	4.8	4.8
Hole diameter: 229mm					**Hole diameter: 165mm**			
Parameter	Ore Hardness				Ore Hardness			
	Very Hard	Hard	Medium	Soft	Very Hard	Hard	Medium	Soft
Burden	5.0	5.5	6.1	6.5	3.6	4.0	4.4	4.7
Spacing	5.8	6.3	7.0	7.5	4.2	4.6	5.0	5.4
Sub-drill	3.4	3.4	2.7	2.7	2.5	2.5	2.0	2.0
Stemming	3.9	3.9	4.4	4.4	2.8	2.8	3.1	3.1

6.3. Blasting

The ground at Kalumbila mine is reactive. Thus, special treatment is given during charging so as to avoid any incidents. This is achieved by means of sleeving all the blast holes with plastic liners and then the explosive is pumped inside these liners. In order to ensure that the primer is at least 1 m from the bottom of the blast hole, the charging horse is used to push the primer down as it is lowered, and charging/pumping is done from bottom while withdrawing the horse. Instead of pre-priming, all the priming is done when the Mobile Mixing Unit (MMU) is at that specific hole that need to be charged.

A performance analysis was done for INNOVEX^{TM} Lateral and INNOVEX^{TM} 207. Both being high energy explosives, it was illogical for the researcher that they both being continued to be used. A site visit to the Bulk Mining Explosive's emulsion making plant was conducted so as to understand the process of making these emulsions. It was discovered that these two emulsions can be replaced with the other but still produce the same effect.

6.4. Drilling and Blasting Modelling

Using the new drilling parameters and just using INNOVEX^{TM} 100 and INNOVEX^{TM} 207, fragmentation models were developed and applied to the blasts. Validation of the models was done through the use of old blast results and the fragmentation analysis provided by the split data and eventually 2 trial blasts were conducted. The results of these analyses are presented in the next chapter. The fragmentation models were prepared in Excel and the general interface is shown in Figure 6.1. The inputs to the model are: the drilling and blast parameters, the geological data, and the explosive properties. The P_{80} value and the percentage fine have paramount importance to this model. Also, since KML require a P99.9 of 1000 mm, this too was given attention to. Five different fragmentation prediction models (Original Kuz-Ram, Modified Kuz-Ram, Crushed Zone Model (CZM), Kuznetsov-Cunningham- Ouchterlony (KCO) model and KCO with the calculated value of *g(n)*) were used and comparisons to each other were made so as to increase the confidence in the predictive results, as shown in figure 6.2

Material Hardness	Very Hard	
Drill and Blast Parameters	**Units**	**Rule of Thumb**
Material density, ρ_{rock}	2.70 g/cc	
Hole Diameter, *D = (8 - 15) x BH*	270 mm	*23 x BH*
Bench Height, *BH = (40 - 60) x D*	12.0 m	*44 x D*
Burden, *B = (20 - 40) x D*	5.9 m	*22 x D*
Stiffness Ratio *SR = BH / B (1.5 - 4, <2 typical for OC metal)*	2.0	
Spacing, *S = (1.1 - 1.4) x B*	6.8 m	
Spacing factor = *S/B*	1.15	
Pattern Type (Square or Staggered)	Staggered	
Subgrade, *Su = (8 - 12) x D*	4.1 m	*15 x D*
Hole Angle, β	0 °	
Hole Length, *L = BH + Su*	16.1 m	
Stemming, *St = (20 - 30) x D*	4.6 m	*17 x D*
Charge Length, *C = L - St*	11.5 m	
Scaled depth of burial, *SDOB = 0.92 - 1.4*	1.03	
Volume of rock per hole, $V_r = B \times S \times BH$	487 m³	
Tonnes of rock per hole, $T_r = V_r \times \rho_{rock}$	1,315 tonne	
Drill productivity, $Drill_{Prod} = V_r / L$	30 m³/m	
Drill productivity, $Drill_{Prod} = T_r / L$	82 tonne/m	
Bulk Product	INNOVEX 207	
Volume of fines in breakage zone, V_b	21.35 m³	
Fragmentation parameters		
Fines inflection point (% fines <1 mm), f_c	7.4%	
Mean Fragment Size, $d_K = A \times (V_r/Q)^{4/5} \times Q^{1/6}$	22.9 cm	
Characteristic Size (Corrected), $x_c = d_K/\Gamma(1+1/n)$	258 mm	

Figure 6.1. Fragmentation prediction models input parameters

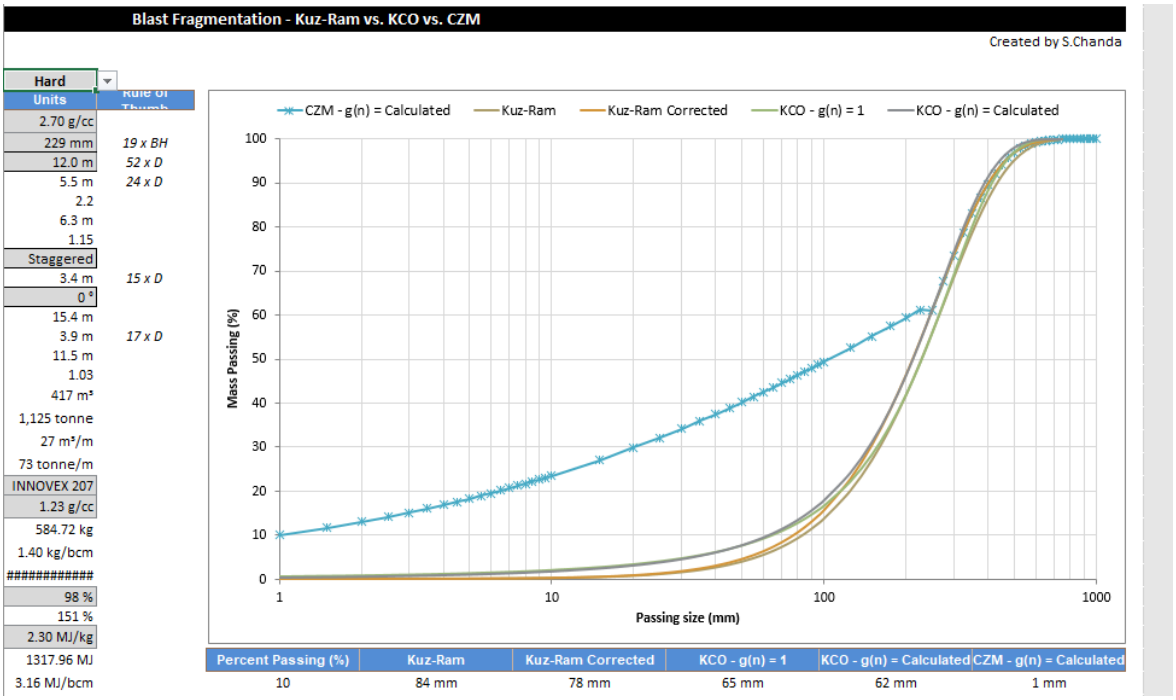

Figure 6.2. Fragmentation graphs

A cost analysis was done comparing the cost per tonne of the current cost of drilling and blasting using the current and the proposed parameters. This was presented as an interactive Excel spreadsheet. As shown in Figure 6.3.

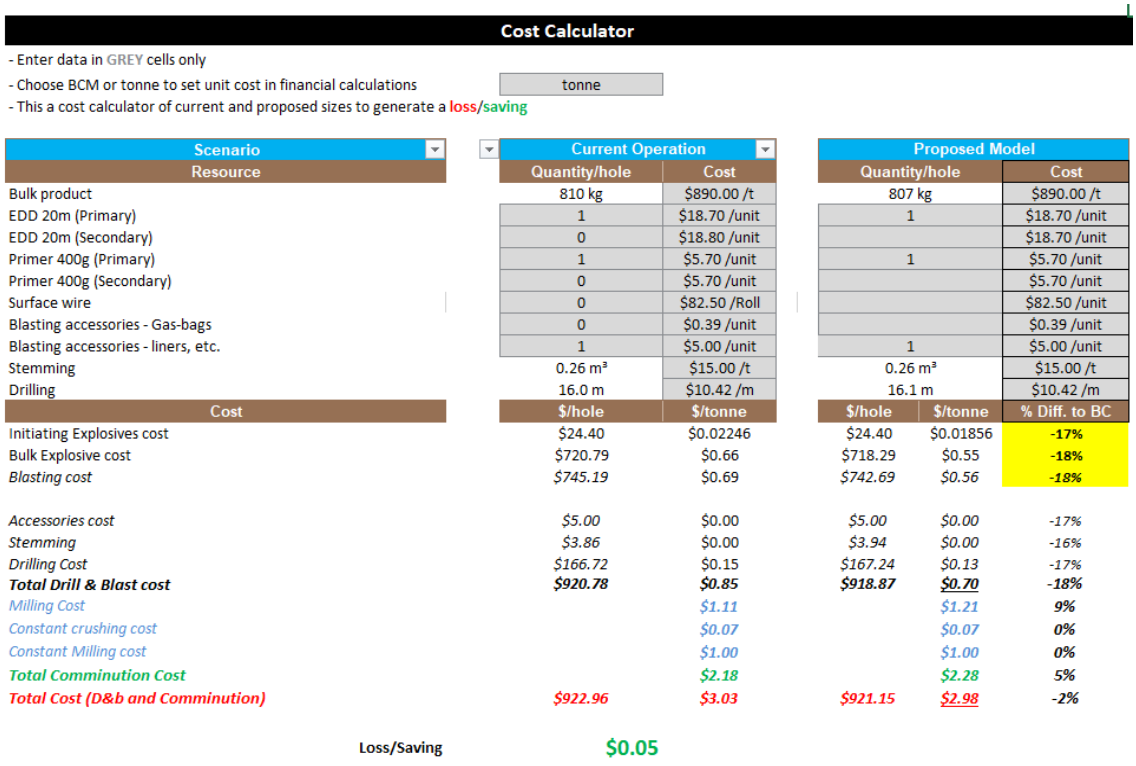

Figure 6.3. Cost modelling

6.5. Comminution Modelling

Several crusher modelling and performance prediction methods have been put forwarded in the literature. These can be broadly divided into fundamental models, classical models, black-box models, and empirical models.

Classical models are concerned with establishing the relationship that exists between energy consumption and the size reduction in a crusher. These include methods proposed by von Rittinger (1867), Kick (1885), Bond (1952) and Napier-Munn et al. (1996). These models have been modified of late to accommodate technological changes that have occurred since then.

Black box models are based on the theory that the crusher is a transformation media between the feed and the product size. They use the feed size distribution, operating conditions of the crusher and the characteristic of rock breakage in the crusher to predict the product size distribution. The Whiten model (Whiten, 1972) is the most generic black box model. Whiten assumed that the particle that enters the crusher can either be broken or dropped unbroken through the crusher chamber. This crushed material also faces the same choice of either dropping or being crushed and broken further. Thus, a cone crusher can be divided into two zones: a single breakage zone and a classification zone where the particles are rebroken or selected for exit. This model is illustrated in Figure 6.4.

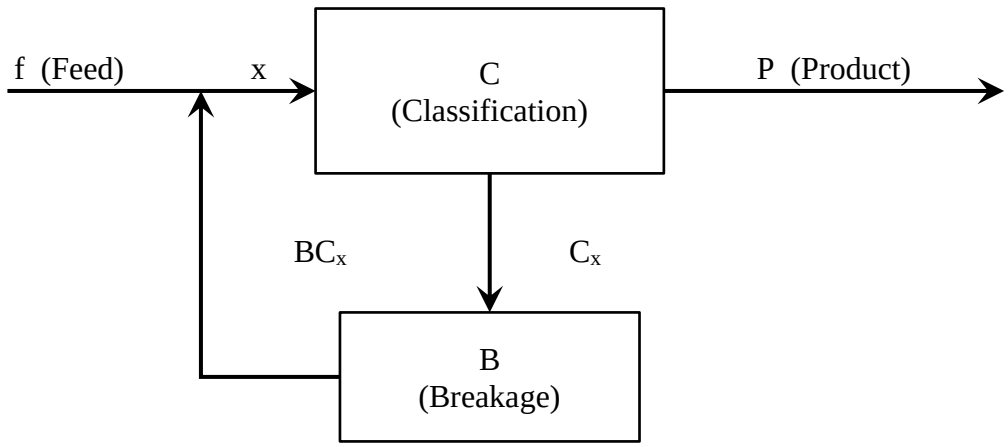

Figure 6.4. Schematic representation of the Whiten crusher model

Through mass balancing, node one mass balance gives $x=f+ BCx$ while node two gives $x=Cx+ p$. Solving the two equations give the 'Whiten model' of a crusher:

$$p= (I-C) (I-CB)^{-1}f \tag{6.4}$$

Where; p and f = products and feed flow rates, I = unit matrix, B =breaking matrix, C = classification function.

Empirical models have been developed based on multiple regression techniques to try and find the relationship between the machine variables in the operating envelop and the performance of the crusher. An example of such a model is that of Karrar (1982), which related the machine variables and the crusher performance – throughput and power consumption. He stated that:

$$Throughput = 1.663(Sin\theta)^{1.224}(throw)^{0.773}(CSS)^{0.507} \tag{6.5}$$

$$Power\ consumption = 19.547(Throughput)^{0.849}(P_{80})^{-0.984} \tag{6.6}$$

Where:

P_{80} = Particle size passing 80%,

θ = Vertical angle of mantle at closed-side setting and throw is the stroke of the mantle during rotation and nutation around the mantle shaft.

This is depicted in Figure 6.5, where *ES* is the rotational speed of the mantle.

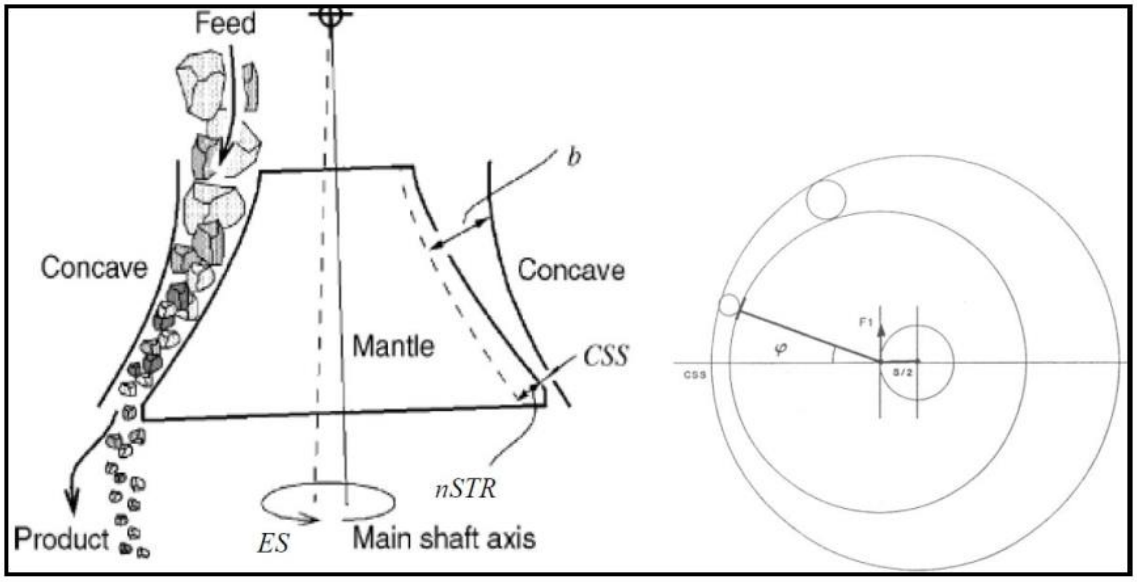

Figure 6.5. A cone crusher with the machine variables (Itävuo and Vilkko 2011).

In this 21st century computer based simulation software have become a norm of the day. These software are used to simulate and predict the performance of the plant subject to some already established parameters and operation constraints. Several commercial software are available on the market, notable among these are: JK Tech's SimMet, Metso's Bruno, Sandvik's Plant Designer, and King's MODSIM. The use of these software makes evaluation of multiple scenarios and the identification of operating condition that will be optimum and productive to the site easier and less tedious.

6.6. Prediction of Comminution Specific Energy

Morell's proposed methods where used in predicting the specific energy for each comminution stage (Morrel 2004b, 2008, 2009; SMC Testing, 2019a, 2019b). Since an ABC/SABC comminution is applied at Kalumbila mine, the following equations from 6.5 to 6.10 were adopted.

$$W_T = W_a + W_b + W_c \tag{6.7}$$

Where;

W_T = Total specific energy to reduce the crusher product to a final product,

W_a = Specific energy to grind coarser particles in tumbling mills,

W_b = Specific energy to grind finer particles in tumbling mills,

W_c = Specific energy for conventional crushing.

Coarse particle tumbling mill specific energy

$$W_a = 0.95 * M_{ia} 4 \left(X_2^{f(x_2)} - X_1^{f(x_1)} \right) \tag{6.8}$$

Where;

K_1 = 0.95 (Because the circuits have pebble crusher),

X_1 = P_{80} in µm of the product of the last stage of crushing before grinding,

X_2 = 750 µm,

M_{ia} = Coarse ore work index and is provided directly by SMC Test.

$$f(x_j) = -\left(0.295 + \frac{x_j}{1{,}000{,}000}\right) \tag{6.9}$$

Fine particle tumbling mill specific energy

$$W_b = M_{ib} 4 \left(X_3^{f(x_3)} - X_2^{f(x_2)} \right) \tag{6.10}$$

Where;

x_2 = 750 µm,

x_3 = P_{80} of final grind in µm,

M_{ib} = Provided by data from the standard Bond ball work index test using the following equation (Morrell, 2009):

$$M_{ib} = \frac{18.18}{P_1^{0.295}(Gbp)\left(P_{80}^{f(P_{80})} - f_{80}^{f(f_{80})}\right)} \tag{6.11}$$

Where;

M_{ib} = Fine ore work index (kWh/tonne),

P_1 = Closing screen size in µm,

Gbp = Net grams of screen undersize per mill revolution,

P_{80} = 80% passing size of the product in µm,

f_{80} = 80% passing size of the feed in µm.

Conventional crushers

$$W_c = K_2 M_{ic} 4 \left(X_2^{f(x_2)} - X_1^{f(x_1)} \right) \quad (6.12)$$

Where;

K_2 = 1.0 for all crushers operating in closed circuit with a classifying screen, If the crusher is in open circuit, e.g., pebble crusher in a AG/SAG circuit, K_2 takes the value of 1.19,

$x_1 = P_{80}$ in µm of the circuit feed,

$x_2 = P_{80}$ in µm of the circuit product,

M_{ic} = Crushing ore work index and is provided directly by SMC Test.

6.7. Conclusion

This chapter has presented the work done to optimise fragmentation. It has discussed and presented the drilling modelling that was done in order to determine the optimal drilling parameters. This was done by conducting a back analysis of the set P_{80} to deduce the optimal drilling patterns that can produce such a fragment. Using data from past blasts, the model was adjusted accordingly and validated so that it can produce accurate predictions. Split analysis data were also used in the development and validation of this model. Blasting operations were also optimised and several trials were done to determine the best explosive to be used. QA/QC works continued to be implemented and an eye was kept on the ground to look for any indication of ground reactivity of a hot hole. Theories of crusher and milling simulation has also been presented with the empirical models and software modelling being identified as the most reliable means of optimising crushing and milling operations.

7. RESULTS AND DISCUSSION

7.1. Introduction

This chapter presents the results of the research and interpretation of these results is given via an in-depth analysis and discussion. It is shown that the implementation of optimization strategy will resulted in a 42% reduction in drilling cost, a 18% decrease in the blasting cost per tonne and a 6% reduction in the overall cost. In addition, as 20% increase in the productivity of the drill rigs and a 15% increase in the crusher throughput will be attained. In the analysis of the milling cost, a constant milling cost was used, as cost of the consumables was not provided to the researcher.

7.2. Fragmentation Modelling

Three fragmentation models were applied to this analysis. The fragmentation parameters are given in Table 7.1. A detailed calculation of these values is given in Appendix C.

Table 7.1. Fragmentation model parameters

Parameter/Rock type	Very Hard	Hard	Medium	Soft
Kuz-Ram Parameters, after Cunningham (1983, 1987)				
Uniformity index, n (Eq. 4.13)	1.91	1.89	1.65	1.63
Energy per blasthole, Q (Eq. 7.1)	688.10	688.10	607.04	607.04
Mean fragment size, x_m (Eq. 4.5)	21.62	24.30	30.06	32.71
Characteristic size (Uncorrected), x_c (Eq. 7.2)	262.01	294.91	375.36	409.36

Table 7.1. Fragmentation model parameters (continued).

Parameter/Rock type	Very Hard	Hard	Medium	Soft
Kuz-Ram Parameters, after Spathis (2004)				
Characteristic size (Corrected), x_{c1} (Eq. 7.3)	216.23	243.04	300.70	327.19
Fragment size upper limit, x_{max}	700	700	700	700
Curve-undulation parameter, b (Eq. 4.23)	3.10	2.77	1.93	1.72
Swebrec Parameters, after Ouchterlony (2005)				
50% Passing size ($g(n)$) calculated (Eq. 4.25)	201.05	225.61	269.30	292.12
Curve-undulation parameter, b (Eq. 4.23)	3.30	2.97	2.19	1.98
JKMRC Crush Zone Model, after Esen et al. (2003) and Onederra et al. (2004)				
Rock stiffness, K (Eq. 4.15)	3.38×10^6	2.53×10^6	1.6×10^6	4.48×10^6
Borehole pressure, P_b (Eq. 4.16)	6.53×10^9	6.53×10^9	6.53×10^9	6.53×10^9
Crushing zone index, CZI (Eq. 4.14)	826.44	1,492.24	6,975.13	50,839.12
Radius of crush zone, rc (Eq. 4.18)	477.26	543.20	761.43	1,176.38
Volume of fines in crushed zone, V_c (Eq. 7.4)	7.54	9.97	17.84	43.37
Breakage Zone				
Pressure decay factor, φ (Eq. 7.5)	-1.42	-1.39	-1.38	-1.53
Equilibrium pressure, P_{eq} (Eq. 7.6)	1.09×10^9	9.43×10^8	5.98×10^8	2.40×10^8
Length of cracks, C_l (Eq. 7.7)	3,694	3,972	4,144	1,251
Dynamic tensile strength factor, f	6	6	6	6
Dynamic tensile strength, T_d (Eq. 7.8)	50×10^6	43×10^6	25×10^6	17.5×10^6
Adiabatic gas expansion coefficient, γ	1.20	1.20	1.20	1.20
Strain at borehole wall, $\mathcal{E}_s$ (Eq. 7.9)	0.07	0.09	0.12	0.20
Breakage Zone				
Number of near field radial cracks, C (Eq. 7.10)	9.38	13.40	30.76	75.11
Volume of fines in breakage zone, V_b (Eq. 7.11)	26.97	33.13	40.80	1.38

Table 7.1. Fragmentation model parameters (continued).

Parameter/Rock type	Very Hard	Hard	Medium	Soft
Fragmentation Parameters				
Fines inflection point (% fines <1 mm), f_c (Eq. 7.12)	0.07	0.07	0.08	0.05
Mean fragment size, x_m (Eq. 4.5)	21.62	24.30	30.06	32.71
Characteristic size (Corrected), x_{c1} (Eq. 7.3)	243.62	273.76	336.17	365.48
Uniformity index of coarse, n=n_c (Eq. 4.13)	1.91	1.89	1.65	1.63
Uniformity index of fines, n_f (Eq. 7.13)	0.42	0.40	0.36	0.43

$$Q = M_c \times \frac{RWS}{100} \times 0.87 \tag{7.1}$$

$$x_c = \frac{x_m}{log_e 2^{\frac{1}{n}}} \tag{7.2}$$

$$x_{c1} = \frac{x_m}{\Gamma\left(\frac{1}{1+n}\right)} \tag{7.3}$$

$$V_c = \left[\pi \left(\frac{r_c}{1000}\right)^2 - \pi \left(\frac{D}{2000}\right)^2\right] \times C_{leng} \tag{7.4}$$

$$\varphi = [(0.0083E) + 0.9955] \times \left(\frac{PW_v}{VOD}\right)^{-0.33} \tag{7.5}$$

$$P_{eq} = P_b \left(\frac{r_c}{\frac{D}{2}}\right)^{\emptyset} \tag{7.6}$$

$$C_l = \frac{D}{2} \times \left(\frac{T_S \times 1{,}000{,}000}{P_{eq}}\right)^{\frac{1}{\emptyset}} - r_c \tag{7.7}$$

$$T_d = T_s \times \mathrm{f} \tag{7.8}$$

$$\varepsilon_s = \frac{P_b \times (1-\upsilon)}{2\{[(1-2\upsilon)] \times (1000 \times \rho_{rock}) \times PW_v^2\} + [3P_b \times \gamma \times (1-\upsilon)]} \tag{7.9}$$

$$C = \frac{P_b}{T_d} \tag{7.10}$$

$$V_b = \left\{\left[\left|\frac{\left(\left(cos\left(\frac{360}{2C}\right) \times \left(\frac{r_c}{1000}\right)\right) \times \left(sin\frac{320}{2C} \times \frac{r_c}{100}\right)\right)}{2}\right| + \left[\frac{\left(\left(\left(sin\left(\frac{360}{2C}\right) \times \frac{r_c}{1000}\right) \times \left(\frac{C_l + r_c}{1000}\right)\right) - \left(cos\left(\frac{360}{2C}\right) \times \left(\frac{r_c}{1000}\right)\right)\right)}{2}\right]\right] \times \left(\frac{r_c}{1000}\right)^2\right\} \times CL \tag{7.11}$$

$$f_c = \frac{V_c + V_b}{V_r} \tag{7.12}$$

$$n_f = \frac{LN\left[\frac{-LN(1-f_c)}{LN(2)}\right]}{LN\left[\frac{0.001}{\frac{x_m}{100}}\right]} \tag{7.13}$$

Where; *Mc* = Mass Charge per hole, *RWS* = Relative Weight Strength, *Γ* = Gamma function, *D* = Blasthole diameter, C_{Leng} = Charge length, PW_v = P-Wave velocity, *VOD* = Velocity of Detonation, T_S = Tensile strength, ρ_{rock} = rock density, V_r = Volume of rock per hole, and *LN* = Natural logarithm.

7.3. Drilling

The following drilling modelling was done using annual production targets of 55,000,000 Bank Cubic Meter (BCM) of material (ore and waste), and 270mm drill holes drilled using CAT MD 6640 in very hard rock formation, with an average penetration rate of 25m/operating hour. Drill availability and utilization are pegged at 90% and 80%, respectively. The mine operates 8 hours' three shifts per day with a 352 operating days in a year. This gives the total annual operating hours of 8,448. At 72% of utilization of availability, the total annual operating hours per drill are calculated as 6,083. A detailed calculation of drill productivity is given in Appendix D. The modelled results for drilling operations using this data and the optimised drilling parameter show that:

1. Number of holes per pattern will decrease by 0.3%.
2. The material (Bank Cubic Meter, BCM) produced per drill will increase by 20.3%.
3. Required blast holes will reduce by 17.1%.
4. Required drill meters will reduce by 16.9%.
5. Cost per drilled hole will increase by 0.3%.
6. Drilling cost per tonne will reduce by 17.1%.
7. Tonne of rock per hole will increase by 20.6%.
8. Drill productivity will increase by 20.3%.

These results will be obtained because using an increased burden and spacing (expanded pattern) will result in drilling fewer holes on a block as compared to a small burden and spacing pattern thus the required meters per pattern will increase. Because the total hole depth will increase due to an increase in the subdrill, the amount of BCM or tonnes

per hole will increase. This increase in the tonnes per hole will translate to an increase in drills productivity per hole. Despite a 0.31% increase in the drilling cost per hole, the drilling cost per tonne will reduce by 17.1%, thus the overall cost per pattern will reduce. Figure 7.1 shows these achievements.

Drilling Parameters	Current Operations	Proposed Model	
Scheduled work hours	8,448 hours	8,448 hours	
Availability, *A*	90%	90%	
Utilisation, *U*	80%	80%	
Utilisation of Availability, *UofA = A x U*	72%	72%	
Drill Operating Hours	6,083 ophrs/drill	6,083 ophrs/drill	
Redrill allowance	5%	5%	
Penetration rate	25 m/ophr	25 m/ophr	
Number of holes/drill	9,504 holes	9,474 holes	*-0.3%*
Number of meters/drill	159,667.20 m	159,667.20 m	*0.0%*
Material produced/drill, bcm	3,818,327 bcm	4,592,276 bcm	*20.3%*
Material produced/drill, tonne	10,309,483 tonne	12,399,145 tonne	*20.3%*
Required material production, bcm	55,000,000 bcm	55,000,000 bcm	
Required material production, tonne			
Required blast holes	136,898 holes	113,471 holes	*-17.1%*
Required drill meters	2,299,881 m	1,912,275 m	*-16.9%*
Number of drills required (Exact)	14.4	12.0	*-16.9%*
Number of drills required (Rounded up)	15	12	*-20.0%*

Design Parameters	Value	Value	Rule of Thumb
Material density, ρ_{rock}	2.70 t/m³	2.70 t/m³	
Hole Diameter, *D = (8 - 15) x BH*	270 mm	270 mm	*23 x BH*
Bench Height, *BH = (40 - 60) x D*	12.0 m	12.0 m	*44 x D*
Burden, *B = (20 - 40) x D*	5.4 m	5.9 m	*22 x D*
Stiffness Ratio *SR = BH / B (1.5 - 4, <2 typical for OC metal)*	2.2	2.0	
Spacing, *S = (1.1 - 1.4) x B*	6.2 m	6.8 m	
Spacing factor = *S/B*	1.15	1.15	
Pattern Type (Square or Staggered)	Staggered	Staggered	
Subgrade, *Su = (8 - 12) x D*	4.0 m	4.1 m	*15 x D*
Hole Angle, β	0 °	0 °	
Hole Length, *L = BH + Su*	16.0 m	16.1 m	
Stemming, *St = (20 - 30) x D*	4.5 m	4.6 m	*17 x D*
Charge Length, *C = L - St*	11.5 m	11.5 m	
Scaled depth of burial, *SDOB ≈ 0.92 - 1.4*	1.02	1.03	
Volume of rock per hole, $V_r = B \times S \times BH$	402 bcm	485 bcm	*20.6%*
Tonnes of rock per hole, $T_r = V_r \times \rho_{rock}$	1,085 tonne	1,309 tonne	*20.6%*
Drill productivity, $Drill_{Prod} = V_r / L$	2511.0%	3020.0%	*20.3%*

Figure 7.1. Drill productivity.

Using the five models (Original Kuz-Ram, Modified Kuz-Ram, Crushed Zone Model (CZM), Kuznetsov-Cunningham- Ouchterlony (KCO) model and KCO with the calculated value of *g(n)*) it can be seen that the expanded patterns will be able to achieve the optimal fragment size, P_{80} of the primary crusher. The current P_{80} for the primary crusher is 800mm. It should be noted that this modelling was done with respect to both P_{80} and P_{100}. The fragmentation analysis from these models is shown in Figure 7.2.

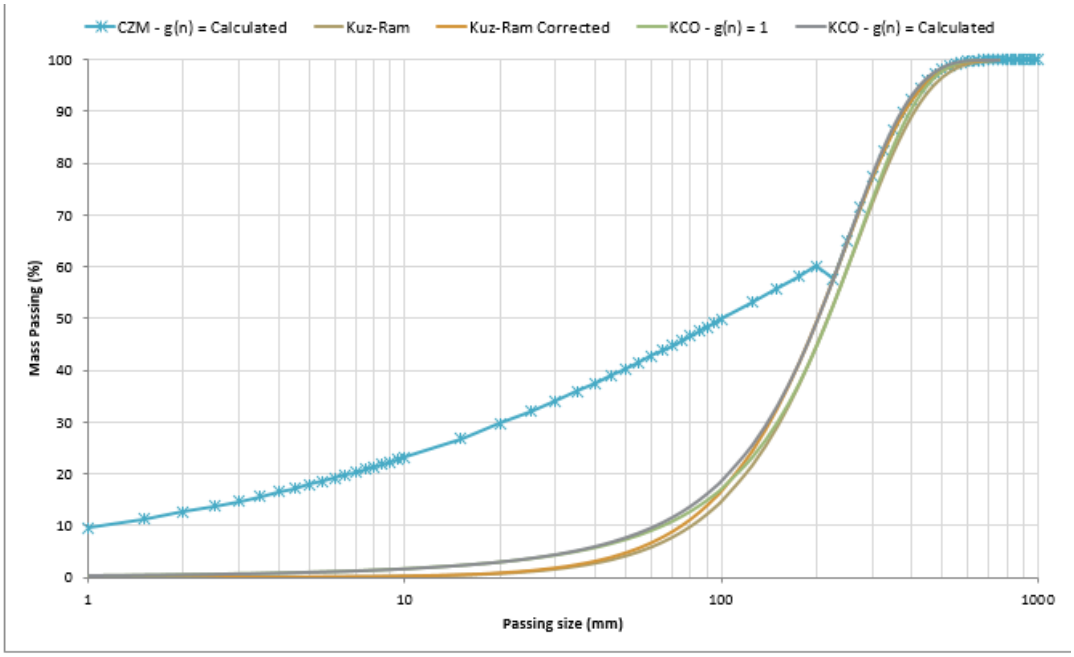

Percent Passing (%)	Kuz-Ram	Kuz-Ram Corrected	KCO - g(n) = 1	KCO - g(n) = Calculate	CZM - g(n) = Calculate
10	80 mm	75 mm	64 mm	62 mm	1 mm
20	119 mm	111 mm	112 mm	105 mm	7 mm
30	153 mm	142 mm	150 mm	139 mm	21 mm
40	184 mm	171 mm	184 mm	171 mm	49 mm
50	216 mm	201 mm	216 mm	201 mm	101 mm
60	250 mm	233 mm	250 mm	232 mm	198 mm
70	289 mm	269 mm	286 mm	267 mm	269 mm
80	336 mm	313 mm	330 mm	309 mm	313 mm
90	406 mm	377 mm	392 mm	369 mm	377 mm
99.5	629 mm	584 mm	566 mm	545 mm	584 mm
100			700 mm	700 mm	

Figure 7.2. Fragmentation modelling using 5 models.

7.4. Blasting

A comparison of the blasting cost of the current operation practice and the proposed model was done. This was done using both INNOVEX 100^{TM} and INNOVEX 207^{TM} as the main explosive. The results are as follows:

1. There is a 0.35% reduction in the mass charge per hole.
2. There is a 17.6% reduction in the powder factor.
3. There is a 17.6% reduction in the energy factor.
4. There is a 17.4 % reduction in the cost of initiation accessories per tonne.
5. There is a 17.6 % reduction in the cost of bulk explosives per tonne of blasted rock.
6. There is an overall 17.6% reduction in the total blasting cost per tonne/BCM of blasted material.

These result are because there is an increase in the tonnes produced per drill hole, coupled with an increase in the stemming height, the total charge length is reduced. This means that there will be less explosive in a blast hole but producing a higher quantity of blasted material. Because powder factor is a function of the mass charge and the total blasted material, there is a subsequent reduction in the powder factor. Figure 7.3 shows a graphical representation of these results.

Bulk Product	INNOVEX 207		INNOVEX 207		
Explosive Density, ρ_{expl}	1.23 g/cc		1.23 g/cc		
Explosive Diameter, D_{expl}	270 mm		270 mm		
Mass of charge per hole, $M_c = V_c \times \rho_{expl}$	809.9 kg		807.1 kg		***-0.35%***
Powder Factor, $PF = M_c / V_r$	2.01 kg/bcm		1.66 kg/bcm		***-17.6%***
Powder Factor, $PF = M_c / T_r$	0.75 kg/tonne		0.61 kg/tonne		
Relative Weight Strength of explosive, *RWS*	75 %		75 %		
Relative Bulk Strength of explosive, *RBS*	115 %		115 %		
Absolute Energy of ANFO, AWS_{ANFO}	2.30 MJ/kg		2.30 MJ/kg		
Explosive Energy, $EE = RWS \times M_c \times AWS_{ANFO} / 100$	1397.04 MJ		1392.18 MJ		
Energy Factor, $EF = EE / V_r$	3.47 MJ/bcm		2.86 MJ/bcm		***-17.6%***
Energy Factor, $EF = EE / T_r$	1.29 MJ/tonne		1.06 MJ/tonne		
Velocity of detonation of explosives, *VoD*	5,000 m/s		5,000 m/s		
Theoretical detonation pressure, $P_d = 0.25 \times \rho_{explo} \times VoD^2 \times 10^{-6}$	7.69 GPa		7.69 GPa		*0.0%*
Blasthole pressure after expansion, P_b	3,844 MPa		3,844 MPa		*0.0%*
Resource	**Quantity/hole**	**Cost**	**Quantity/hole**		**Cost**
Bulk product	810 kg	$890.00 /t	807 kg		$890.00 /t
EDD 20m (Primary)	1	$18.70 /unit	1		$18.70 /unit
EDD 20m (Secondary)	0	$18.80 /unit			$18.70 /unit
Primer 400g (Primary)	1	$5.70 /unit	1		$5.70 /unit
Primer 400g (Secondary)	0	$5.70 /unit			$5.70 /unit
Surface wire	0	$82.50 /Roll			$82.50 /unit
Blasting accessories - Gas-bags	0	$0.39 /unit			$0.39 /unit
Blasting accessories - liners, etc.	1	$5.00 /unit	1		$5.00 /unit
Stemming	0.26 m³	$15.00 /t	0.26 m³		$15.00 /t
Drilling	16.0 m	$10.42 /m	16.1 m		$10.42 /m
Cost	**$/hole**	**$/tonne**	**$/hole**	**$/tonne**	**% Diff. to BC**
Initiating Explosives cost	$24.40	$0.0225	$24.40	$0.0186	-17.4%
Bulk Explosive cost	$720.79	$0.66	$718.29	$0.55	-17.6%
Accessories cost	*$5.00*	$0.0046	*$5.00*	*$0.0038*	*-17.4%*
Blasting cost	*$750.19*	$0.690	*$747.69*	*$0.569*	***-17.6%***

Figure 7.3. Explosive analysis

The reduction in the mass charge per hole means a reduction in the cost of explosives per tonne produced. Also; since fewer holes will be drilled on a particular pattern, there is a corresponding reduction in the amount of accessories (EDDs, Boosters, liners) used on a specific pattern to produce an increased tonnage. This ripple effect leads to an overall reduction in the total blasting cost per hole.

A performance analysis was done on the explosive to compare the results obtained from the use of the two different types of high-energy explosive supplied by the contractor. It was found that the two types of explosive produced very similar results, with INNOVEX^{TM} 207 even producing better results than that of INNOVEX^{TM} Lateral. Because INNOVEX^{TM}

Lateral is a 9.1% more expensive than INNOVEX^{TM} 207, a cost benefit analysis performed shows that the company can make substantial saving if it was to be using only INNOVEX^{TM} 207 as a high-energy explosive and INNOVEX^{TM} 100 as a low-energy explosive.

7.5. Quality Control and Quality Assurance

The results from the QA/QC show that more can be done when it comes to compliance to the designed drilling and blasting parameters. BME Xplolog^{TM} online system is utilised to analyse compliance (Omnia, 2017). This compliance can be achieved by providing more training to the drilling and charging crew. Ample time should be allowed between drilling, charging and blasting to ensure that remedy measures are implemented should there be any need. Figure 7.4 shows XPLOLOG interface used for QA/QC analysis.

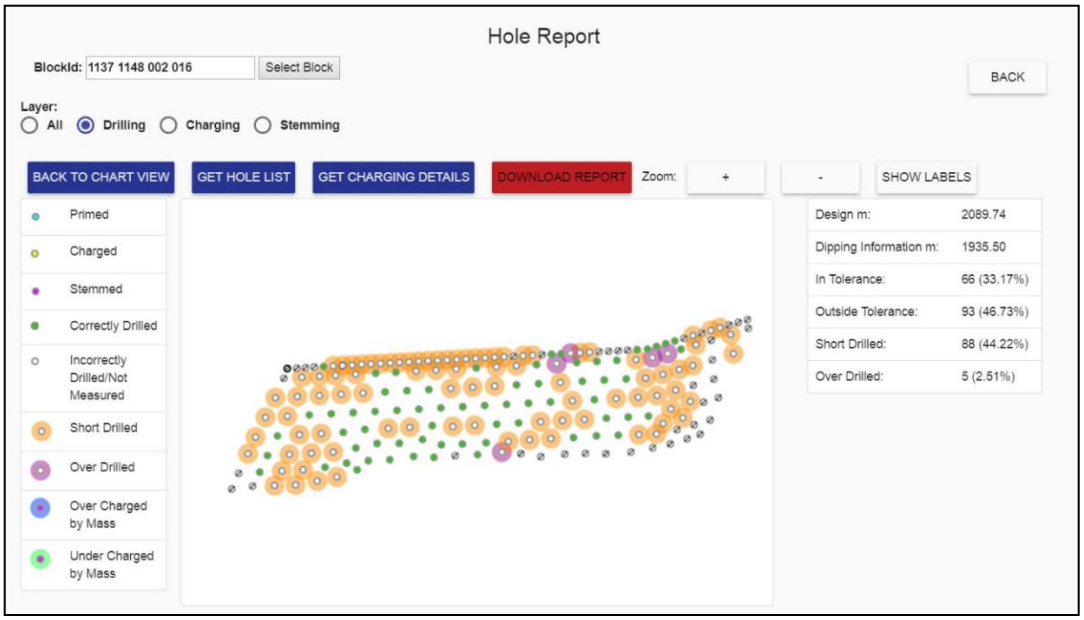

Figure 7.4. XplologTM interface showing hole report.

7.6. Crushing

The monthly crushing quantities for period of 3 months is given in Table 7.2. It should be noted that during this period of time, the crushing target was not met. This was due to several factors including crusher bridging due to feeding of boulders into the crusher and a reduction in crusher efficiency due to an increase in the amount of fines. From the results presented in Table 7.1, and using the crusher modelling conducted in Chapter 6.5, it can be concluded that the crusher performance will increase, and the set targets will be reached.

Table 7.2. Primary crushing data for 3 months

Month	Actual Crushed (Tonne)	Budget (Tonne)	Variance	Specific Energy (kWh/t)	Crushing Cost (electricity, $/t)
August	121,858	156,445	-34,587	0.12	$0.01 /t
September	116,344	133,252	-16,909	0.23	$0.02 /t
October	134,809	120,097	14,711	0.64	$0.06 /t
Average	124,337	136,598	-12,262	**0.33**	**$0.03 /t**

During this period, an average throughput of 3,433t/h was recoded. However; when material from the optimized blast was fed to the crusher, a 4,500tph crusher throughput was achieved. This shows that the crusher throughput will increase by about 13% if the optimised pattern is implemented.

Because the blasted material will contain more fines, secondary crushing can be reduced by 60%, because only material from very hard domain will need to be secondary crushed. Table 7.3 shows secondary crushing data for the 3 months used for analysis.

Table 7.3. Secondary crushing data for 3 months.

Month	Rate (t/h)	Total Crushed (Tonne)	Specific Energy (kWh/t)	Crushing Cost ($/t)
August	2,782	55,710	0.51	0.05
September	4,893	69,659	0.29	0.03
October	4,784	106,408	0.19	0.02
Average	4,153	77,259	0.33	0.03

Monthly electricity cost for this period can be calculated using this data. With the average specific energy of 0.30kWh/t and 77,259 tonnes of ore secondary crushed per month:

Electricity used = Specific energy × Crushed tonnage

= 0.30kWh/t × 77,259

= 23,177.71 kWh

Electricity cost for Secondary crushing = Electricity used × Cost of electricity equals to **$ 2,085.99** (23,177.71 kWh × $0.09/kWh).

Therefore, the company spent $ 2,085.99 on secondary crushing per month. Assuming the same trend continues, in 12 months, $ 2,085.99 × 12 = $ **25,031.93**. However, if secondary crushing is reduced by 60 %, the annual spending will be:

Annual cost at 40% operation= 40% × $25,210.84= **$10,012.77**

Annual saving= $25,031.93 - $10,012.77 = **$15,019.16**

Implementing this strategy will thus result in an annual saving of $15,019.16 from secondary crushing. It should be noted that since the operation hours of the secondary crusher will reduce, even the cost of consumables and the maintenance cost will be reduced. However, these costs were not quantified in this research. Appendix E gives a detailed calculation of the drilling and blasting costs.

7.7. Specific Energy Estimation

Specific comminution was estimated using the formulas and models discussed in Chapter 6.6. Table 7.4 and 7.5 gives the input parameters into the model.

Table 7.4. Operating parameter

Parameter	Value
Crusher feed P_{80}	320 mm
Crusher product P_{80}= SAG mill feed P_{80}	177 mm
SAG product P_{80}	600 µm
Final Product P_{80}= Cyclone overflow	212 µm
P1	300 µm
Pebble crusher feed	52 µm

Table 7.5. Test data; Source: ALS.

Parameter	Value	Unit
Dw_i	6.49	kWh/m^3
M_{ia}	18.2	kWh/t
M_{ic}	6.93	kWh/t
M_{ih}	13.4	kWh/t
G_{pb}	1.69	g/rev
SG	2.8	

Table 7.6. Comminution energy calculation

Pebble	Yes
Crusher in Closed	No
Crusher feed P_{80}	320000 µm
Primary Crusher Product P_{80}=Ball mill feed size, F_{80}, X_1	150000 µm
Ball mill product size, P_{80}	600 µm
Final Product P_{80}, X_3	212 µm
X_2	750 µm
Clossed screen size, P_1	300 µm
Specific gravity, SG	2.8
Constant	4
DW_i	6.5 kWh/t
M_{ia}	18.2 kWh/t
M_{ib}= BW_i (Eq. 6.9)	17.5 kWh/t
M_{ic}	6.9 kWh/t
Gbp	1.69 g/rev
f(X_1)=f(P_{80})	-0.2956
f(X_2)	-0.2958
f(X_3)=f(f_{80})	-0.2952
f(Crusher feed P_{80})	-0.6150
Pebble presence constant, K	1
Open Circuit or Closed Circuit, $K2$	1.19
Coarse Particle Grinding Specific Energy, W_a^*	7.722 kWh/t
Fine Particle Grinding Specific Energy, W_b^{**}	4.518 kWh/t
Conventional Crusher Specific Energy, W_c^{***}	0.960 kWh/t
Total Comminution Specific Energy, W_T^{****}	**13.200 kWh/t**

*Calculated by using Eq. 6.8, **Calculated by using Eq. 6.10, ***Calculated by using Eq. 6.12

****Calculated by using Eq. 6.7.

When these figures are used in the model, a Specific Energy (SE) of **13.20kWh/t** is predicted, which is 8% more than the average specific energy of **12.32 kWh/t** (Table 5.7) for three month period under analysis. This increase can be attributed to factors such as:

1. The proposed models has resulted in an increased mean fragment size as that produced by the current parameters. This mean size is however going to be more consistent as the operation had been optimised.
2. Throughput; Throughput is a main component in the determination of specific energy, so as the throughput increases, SE is expected to increase.
3. Recirculation of feed; As finer material is fed to the crusher (feed less that the crusher CCS), it just runs through the crusher with less or no impact on it. When this material is introduced to the ball mill, it is inherently stronger than that which was in initially crushed or bruised in the crusher and sustained micro-cracking. This new material will thus succumb to more recirculation than the material that has initially sustained some crushing.
4. Ball charge, etc.

7.8. Conclusion

This chapter discussed the results that were achieved from this research. It can clearly be seen that the operating cost of all the activities would reduce. Despite an increase in the cost of drilling per hole, the drilling cost per tonne would reduce significantly and a 20.3% increase in drill productivity can be achieved. This is coupled with a 17.6% reduction in the blasting cost per tonne, mainly due to the replacement of one explosive with the other. The crushing cost will reduce while the specific energy will increase by 8%, this is mainly due to the fact that the mills will be doing a considerable amount of work than before. The overall result is a saving of $0.05 per tonne from the entire process.

8. CONCLUSION AND RECOMMENDATIONS

8.1. Introduction

The aim of this research was to develop a site-specific mine to mill (M2M) operation strategy that will optimise the drilling, blasting, crushing and milling operation for increased throughput and profitability. In order to achieve this, 7 research questions were posed and used to evaluate the current operation situation and achieve the deliverables of the research. These questions are reviewed in this chapter, a summary and conclusion is given, and the recommendations are submitted for implementation.

8.2. Research summary

A mine to mill operation strategy was developed for Kalumbila mine. This strategy was developed through a comprehensive engineering and scientific methodology. The methodology involved a scoping study, ore domain characterization, fragmentation modelling through drilling simulation, blasting modelling and comminution modelling.

During the scoping study, extensive auditing of the current operating practices was done. Blast design, implementation and the initiation sequences on site was reviewed. A survey of the crushing and grinding circuits was conducted in order to identify the source of bottlenecks and opportunities. The information obtained during this stage provided necessary data used in the modelling process.

Ore characterisation work was untaken in order to have a detailed understanding of breakage characteristics of the ore. Despite the researcher not doing test to determine the geotechnical and metallurgical tests, reports submitted by expert contactors were used as a source of these data. The mine regularly contract expert to undertake such tests.

Modelling and simulation works were done using the data collected during the benchmarking and ore characterization phases. Models were developed and used to predict

the blast fragmentation, milling throughput, power consumptions and efficiency of the complete process.

The modelling and simulation stage provided optimised strategies based on mine and processing constraints and a cost/benefit analysis was done. These results were used to determine the alternate designs and operating strategies for each process to improve the overall efficiency of the operation. Validation of the model was done using the data obtained from 2 trial blasts and previous blast and crushing data. By using key performance indicators (KPI) to quantify the improvements, the developed model and strategy was proposed to the mine for implementation.

The full mine to mill optimization shows that there is:

1. 20.3% in drill productivity,
2. 17.1% reduction in the drilling cost per tonne,
3. 17.6% reduction in the blasting cost per tonne,
4. 17.5% reduction in the total drilling and cost per tonne,
5. 8% increase in the specific energy,
6. 4.6% increase in total comminution cost,
7. 1.6% reduction in the overall drilling and comminution cost,
8. 13 % increase in the crusher throughput.

The final result from the mine-to-mill optimisation shows that there is an overall saving of $0.05 per tonne.

8.3. Answers to Research Question

The answers to the research question are presented herewith:

1. *What is the current drilling practice at the mine?*

The ore at Kalumbila mine is divided into 4 ore domains depending on the rock strength. Therefore, each ore domain has its specific drilling patter parameters, which varies with the diameter of the drill being used. The mine uses four different hole diameters for

production holes, these are 270mm, 252mm, 229mm and 165mm. The 270mm and 299mm are the most used diameters with the 165mm mostly used in presplit. These parameters are given in Table 8.1.

Table 8.1. Kalumbila mine drilling pattern parameter

Hole diameter: 270mm					**Hole diameter: 251mm**			
Parameter	Ore Hardness				Ore Hardness			
	Very Hard	Hard	Medium	Soft	Very Hard	Hard	Medium	Soft
Burden	5.4	6.3	7.0	7.5	5.2	6.1	6.8	7.2
Spacing	6.2	7.2	8.1	8.6	6.0	7.0	7.8	8.3
Sub-drill	4.0	4.0	3.0	3.0	4.0	4.0	3.0	3.0
Stemming	5.5	5.5	5.5	5.5	5.0	5.0	5.0	5.0
Hole diameter: 229mm					**Hole diameter: 165mm**			
Parameter	Ore Hardness				Ore Hardness			
	Very Hard	Hard	Medium	Soft	Very Hard	Hard	Medium	Soft
Burden	5.0	5.8	6.4	6.9	4.0	4.5	5.0	5.5
Spacing	5.8	6.7	7.4	7.9	4.6	5.2	5.8	6.3
Sub-drill	4.0	4.0	3.0	3.0	3.0	3.0	3.0	3.0
Stemming	4.5	4.5	4.5	4.5	4.0	4.0	4.0	4.0

2. *What is the current blasting practice at the mine?*

Kalumbila mine has contracted Bulk Mining Explosives (BME) to conduct blasting operations. KML only provide supervision and manpower to a certain level. Electronic blasting is conducted at mine using AXXIS blasting technology. Three type of pumped emulsion is used at the mine site. These are INNOVEX^{TM} 100, INNOVEX^{TM} 207 and INNOVEX^{TM} LATERAL. INNOVEX^{TM} 100 is a low energy explosive which is used mainly in softer rock and sensitive areas like near the pit boundaries or near the mine structures. INNOVEX^{TM} 207 and INNOVEX^{TM} LATERAL are high energy explosives. 400g viper boosters are used for priming and in some instances INNOPAK^{TM} packaged explosive is used in the presplit instead of the pumped INNOVEX explosive and a detonating cord used in order to offer 0ms delay on the presplit.

3. *How is the implementation of the current drilling and blasting plans, is it accurate or not?*

The drilling and blasting compliance were evaluated via conducting quality control and quality assurance (QA/QC) works. The research shows some levels of compliance, but more can be done to improve it. XY drilling accuracy was increased by means of using the modular mining's ProVision Machine Guidance System to guide the drill rigs (Modular, 2019). The rigs that are not fitted with this system rely on signals given by the assistants on the ground.

4. *What is the current crushing and milling trend to the mine? What is the current throughput for the primary and secondary crushers and for the mills?*

Three ThyssenKrupp KB 63 – 89 Gyratory in-pit crushers with a design throughput of 4,000 tph are used for primary crushing. However, this throughput was rarely achieved due to several constraints. The crushed material is then conveyed to the milling stockpile via a system of three overland conveyors. The material from the conveyors passes through the pit-top bin before being dumped on the milling stockpile feed area. The system has two Metso MP2500 secondary crushers having 3,700tph throughput, which is the biggest one in the world. These crushers operate one at a time and only used when the material being fed is too hard so as to generate more finer fragments. By design, only material form Crusher 3 can be re-routed to the secondary crushers. A Metso MP1250 pebble crusher is installed in the system and is used to crusher milling rejects and sent them back to the milling stockpile. The milling circuit has two train of SAG and Ball mills with a total of 6 cyclone clusters and throughput design of 5,000 tph.

5. *What is the cost associated with blasting and milling?*

The cost of drilling, blasting and comminution was modelled and showed that a cost saving of $0.05 per tonne can be achieved.

6. *What are the opportunities to improve in operation efficiency that can result in cost saving?*

Several improvement opportunities to improve the operation efficiency were identified. Expanding the current drilling patterns will result in the production of a well fragmented material. This will increase the crusher throughput and will lead to the reduction of secondary crushing operation. Well fragmented material will reduce the wear and tear on the loading units and increase the load and haul productivity as the loading time, thus, the cycle time will be reduced. Other benefits are the increase in drilling productivity and powder factor. These will all lead to a substantial cost saving from the overall operations.

8.4. Conclusions

Mine to mill optimization is a strategy that if applied effectively can lead to increase in productivity and a reduction in the total operating costs. In order for this strategy to succeed, management commitment is important. There should be willingness on the part of the top company management to allocate finances and manpower to such a department. A spirit of collaboration and inter-departmental optimisation between the mining and processing departments should be promoted as opposed to departmental operation and cost optimization. It has been concluded that for Sentinel mine to increase the productivity of the mining and processing operations, the following steps must be taken:

1. Clean-ups should be done after a blast muckpile has completely been loaded to provide ready and sufficient areas for marking and drilling.
2. QA/QC should be done and compliance to design specification be adhered to, both during drilling and blasting. Shortcuts when doing QA/QC must be avoided and all work should be done as per standard operation procedure.
3. More blocks must be designed with INNOVEX^{TM} 207 instead of INNOVEXTM LATERAL, as it will result in cost saving while giving the same blast performance and output. In the long run, only INNOVEX^{TM} 207 should be used as a high energy explosive.
4. Pattern expansion must be undertaken, and the model must be used to ensure that the desired results are achieved.
5. More geological and geotechnical logging should be conducted so as to provide enough data to be used in the fragmentation prediction models.
6. Crusher stockpile should be introduced to provide a constant feed to the crusher in case there is hauling stoppage, especially during blasting.

7. Secondary crushing should be reduced to less than 50% and only used when extremely hard ore is fed to the crushers.

The M2M optimization that was carried out at Kalumbila Mineral Limited has demonstrated that instead of each department optimising their operations, an inter-departmental optimisation should be done, as this it will result in marginal increase in company's productivity and a reduction in cost spending.

8.5. Recommendations

As the sentinel pit goes deeper, hard rock formation will be encountered. For efficiency operations, more geological and geotechnical works must be done at the mine so as to have a clear understanding of these geotechnical aspect of blasting. This will provide an advantage to the drill-and-blast team to further optimise the drilling and blasting operations. This will also allow the processing engineers to optimise their operations so as to be able to process effectively such a kind of material. Continuous improvement in the pattern size should regularly be done to accommodate new geological features in different domains and levels. The mine management can also commission a study on the impact this increased mill throughput will have on flotation and recovery.

Deeper pits, hard-ore couple with low grades possess a new challenge to mining operations in most of the mine. Explosive engineering technology has advance to a level of being to ascertain the exact energy and ideal density of an explosive. This make the distinction between high-energy and low-energy explosive more vivid than ever. Thus, the effect of hard-ore and the use of new explosive technology presents a new face to M2M and calls for further research. Sentinel ore grades are low; thus, any level of dilution is detrimental to the operation. The effect of dilution on both the current operation and the life of mine needs to be studied and documented.

REFERENCES

Adebola, J.M., Ajayi, O.D., Peter, E.O., 2016. Rock Fragmentation Prediction using Kuz-Ram Model. Journal of Environment and Earth Science. Volume 6, No.5, 2016. ISSN 2224-3216 (Paper) ISSN 2225-0948 (Online).

AEISG, 2007. Australian Explosives Industry and Safety Group Incorporated, Elevated Temperature and Reactive Ground – Code of Practice. [Online] Available: http://www.dmp.wa.gov.au/documents/Code_of_Practice/DGS_COP_ElevatedTempReactiveGround.pdf (10.12.2018).

ALS Metallurgy, 2018.Report No. A19173. Report to Kalumbila Minerals Ltd.

Ash, 1963. The mechanics of rock breakage-Part 2: Standards for blasting design. Pit and Quarry 56(3): 118-122

ASTM, 1995. Designation: D 5731 – 95. Standard Test Method for Determination of the Point Load Strength Index of Rock. American Society for Testing and Materials. 100 Barr Harbor Dr., West Conshohocken, PA 19428.

ASTM, 1996. Designation: D 6032 – 96. Standard Test Method for Determining Rock Quality Designation (RQD) of Rock Core. American Society for Testing and Materials. 100 Barr Harbor Dr., West Conshohocken, PA 19428.

Australian Explosives Industry And Safety Group Inc. 2007. Code of Practice. Elevated temperature and reactive ground. ISBN 978-1-921308-18-5

Barratt, D.J., Allan, M.J., 1986. Testing for autogenous and semiautogenous grinding: a designer's point of view. Minerals and Metallurgical Processing, 65– 74 (May).

Bennett, D., Tordoir A., Walker, P., La Rosa, D., Valery, W., Duffy K., 2014. Throughput Forecasting and Optimisation at the Phu Kham Copper-Gold Operation. 12th AUSIMM Mill Operators' Conference / Townsville, Qld.

BME, 2019. BME website. http://www.bme.co.za/ (25.01.2019).

Bond, F.C., 1952.The third theory of comminution. Transaction of AIME.193 (2).p.484 – 494.

Bond, F.C., 1961. Crushing and grinding calculations. British chemical engineering, Part I, 6 (6), 378– 385, Part II, 6 (8), 543– 548.

REFERENCES (continued)

Botha, G.L., 2014. Management of reactive ground at the Goedgevonden opencast Coal mine in the Witbank coalfields of South Africa. Master's thesis. University of the Witwatersrand, Johannesburg, South Africa.

Burger, B., McCaffery, K., Jankovic, A., Valery, W., McGaffin, I., 2007. Batu Hijau Model for Throughput Forecast, Mining and Milling Optimisation and Expansion Studies. Metso Minerals Process Technology Asia-Pacific, Brisbane, Australia.

Chatziangelou, M., Christara, B., 2013. Rock mass blastability dependence on rock Mass quality. Bulletin of the Geological Society of Greece, vol. XLVII, pp 1694-1705.

Chiappetta, R F, and Treleaven, T, 1997. Expansion of the Panama Canal. Blasting Analysis International, Inc. (BAI). Proceedings of the 7th High-Tech Blasting Seminar: State-of-the-Art Blasting Technology Instrumentation and Explosives Application, Vol 2, p867**.**

Cho, S.H., Kaneko, K., 2004. Rock Fragmentation Control in Blasting. Transactions of the Mining and Materials Processing Institute of Japan. Volume 45, No. 5 (2004) pp. 1722 to 1730 2004.

CSA Global (UK) Ltd, 2012. NI 43-101 Technical Report, Sentinel Prospect, Trident Project, North West Province, Zambia. Report to First Quantum Minerals Ltd. May 2012.

Cunningham, C., 1983. The Kuz-Ram Model for the Prediction of Fragmentation from Blasting. In Proceedings of the first International Symposium on Rock Fragmentation and Blasting, Lulea, Sweden, August 22–26.

Cunningham, C., 1987. Fragmentation Estimations and the Kuz-Ram Model – Four Years on. In Proceedings of the Second International Symposium on Rock Fragmentation by Blasting, Keystone, Colorado, August 23–26.

Cunningham, C., 2005. The Kuz-Ram fragmentation model – 20 years on. Brighton Conference Proceedings. European Federation of Explosives Engineers, ISBN 0-9550290-0-7.

Deere, D.U., 1964. Technical description of rock cores for engineering purposes. Rock Mechanics and Engineering Geology 1964;1(1):16e22.

REFERENCES (continued)

Deere, D.U., Hendron, A.J., Patton, F.D., 1967. Cording EJ. Design of surface and near surface construction in rock. In: Proceedings of the 8th U.S. Symposium on Rock Mechanics Failure and Breakage of Rock. New York: American Institute of Mining, Metallurgical and Petroleum Engineers, Inc.; 1967. p. 237e302.

Dey, A. 1995. Drilling machine. Latest development of heavy earth moving machinery, Annapurna Publishers, pp.120-228.

Djordjevic, N., 1999. A two-component of blast fragmentation. Proceedings of the Sixth International Symposium on Rock Fragmentation by Blasting (Fragblast-6), Johannesburg, South Africa, 8–12 August 1999. Southern African Institute of Mining and Metallurgy, Johannesburg. pp. 213–222.

Dyno Nobel, 2010. Blasting and Explosives Quick Reference Guide. Dyno Nobel Asia Pacific Pty Limited (ACN 003 269 010).

Esen, S., Bilgin, H.A.,2000. Effect of explosive on fragmentation. The 4th Drilling and Blasting Symposium.

Esen, S., La Rosa, D., Dance, A., Valery, W., Jankovic, A., 2007. Integration and Optimisation of Blasting and Comminution Processes. Metso Minerals Process Technology Asia-Pacific, Brisbane, Australia.

Esen, S., Onederra, I., Bilgin, H.A., 2003. Modelling the size of the crushed zone around a blasthole. International Journal of Rock Mechanics and Mining Sciences, vol. 40, no. 4. pp. 485–495.

Explosive act, 1995. Ministry of Legal Affairs, Government of the Republic of Zambia.

Faramarzi, F., Mansouri, H., Ebrahimi, M.A., 2013. A rock engineering systems-based model to predict rock fragmentation by blasting. International Journal of Rock Mechanics & Mining Sciences. Volume 60, pages 82–94.

Fickett, W., Davis, W., 1979. Detonation Theory and Experiment. Berkeley: University of California Press, 1979. p. 16, 54.

First Quantum Minerals Ltd, 2013. Sentinel IPCC Implementation. Internal report. January 2013. Kalumbila, Zambia.

First Quantum Minerals Ltd, 2015. NI 43-101 Technical Report. May 2015. North West Province, Zambia.

REFERENCES (continued)

Gomes, M.P., Junior L.T., Filho, E.S.N., Colacioppo, J., Jankovic, A., Valery, W., 2010. Optimization of the SAG mill circuit at Kinross Paracatu Brazil. https://www.researchgate.net/publication/310954092 .

Gray, D., Lawlor M., Briggs, A.,2015. NI43-101 Technical Report. Trident Project, North West Province, Zambia. Report to First Quantum Minerals Ltd. May 2015. Kalumbila, Zambia.

Hakami, A., Mansouri H., Ebrahimi, M,A., Farsangi, M. R., Faramarzi, F., 2015. Study of the Effect of Blast Pattern Design on Autogenous and Semi-Autogenous Mill Throughput at Gol-e-Gohar Iron Ore Mine. 11th International symposium on Rock Fragmentation by Blasting. 24-26 August 20015, Sydeney, Australia.

Hariparsad, N., 2015. RG-AFR-001, Kalumbila Sentinel Mine Bucket Test Reactive Ground Testing. Orica Africa Pty Ltd internal report to Kalumbila Mine management. Kalumbila, Zambia.

Hart, S., Rees, T., Tavani, S., Valery, W., Jankovic, A., 2011. Process Integration and Optimisation of Boddington. SAG 2011 Conference Proceedings, Vancouver, Canada, 25-28 September 2011.

Hettinger, M. R., 2015. The effects of short delay times on rock fragmentation in bench blast. Master's Thesis, Missouri University of Science and Technology. htp://scholarsmine.mst.edu/masters_theses/.

Hudson, J. A., Harrison, J.P., 2000. Engineering Rock Mechanic., p. 113-138. Published by Elsevier Science Ltd.

Hukki, R.T., 1962. Proposal for a solomnic settlement between the theories of von Rittinger, Kick and Bond. Trans. AIME 223, 403–408.

Hustrulid, W,.1999. Blasting Principles for Open Pit Mining. Vol. I. A.A. Balkema, Rotterdam. pp 27- 31,854- 855.

II'yushin, A.A., 1999. The mechanics of a continuous medium. Izd-vo MGU. Moscow. (Translated in Hustrulid W. Blasting principles for open pit blasting, vol. II. Rotterdam: Balkema, p. 964–1009 [Chapter 21]), 1971 [in Russian].

ISEE Blasters' Handbook, 2011. International Society of Explosives Engineers, p.741. Cleveland, Ohio.

REFERENCES (continued)

Isokangas, E., Valery, W., Jankovic, A., Sönmez, B., 2012. Using Process Integration & Optimization to Provide Integrated Process Solutions for Mining Operations, From Mine to Mill. 26th IMPC conference, New Delhi, India.

ISRM,1978. Suggested methods for the quantitative description of discontinuities in rock masses. International Journal of Rock Mechanics and Mining Sciences & Geomechanics Abstracts 1978;15(6):319e68

Itävuo, P., Vilkko, M., 2011. Simulation and advanced control of transient behaviour in gyratory cone crushers. 8th International Mineral Processing Seminar (Procemin 2011), Santiago, Chile. p. 63 – 72.

Jankovic, A., Valery, W., 2002. Mine to Mill Optimisation for Conventional Grinding Circuits – A Scoping Study. Journal of Mining and Metallurgy, 38 (1-4) A (2002) 49-66.

Jimeno, C. L., Jimeno, E.L., Francisco, J. A. C., 1995. Drilling and Blasting of Rock. A.A. Balkema. Rotterdam. De Ramiro, Yvonne Visser translated to English. pp 30, 56-61, 179-183, 190.

JKTech , 2019 JKTech Laboratory Services, JK Drop Weight Test .40 Isles Road, Indooroopilly, QLD 4068, AUSTRALIA.

Johansson, D, 2011. Effects of confinement and initiation delay on fragmentation and waste rock compaction. Results from small scale tests. Doctoral thesis, Luleå University of Technology, Luleå.

Johansson, D., Ouchterlony, F., 2013. Shock Wave Interactions in Rock Blasting: the use of Short Delays to Improve Fragmentation in Model-Scale. Rock Mechanics and Rock Engineering, Volume 46, Issue 1, pp. 1-18.

Johnson, C. E., 2014. Fragmentation Analysis in the Dynamic Stress Wave Collision Regions in Bench Blasting". Theses and Dissertations--Mining Engineering. 16. https://uknowledge.uky.edu/mng_etds/16.

Kanchibotla, S.S., Valery, W., Morrell, S. 1999. Modelling fines in blast fragmentation and its impact on crushing and grinding. Proceedings of Explo'99, Kalgoorlie, Western Australia, 7–11 November 1999. pp. 137–181.

Karra, V.K., 1982. A process performance model for cone crushers. In: Proceedings of the 14th International Mineral Processing Congress, Ontario, Canada, III. pp. 6.1–6.14.

REFERENCES (continued)

Katsabanis, P.D., Liu, L., 1996. Delay Requirements for Fragmentation Optimization. Measurement of Blast Fragmentation. Balkema, 1996.

Katsabanis, P.D., Omid,i O., 2015. The Effect of Delay Time on Fragmentation Distribution through Small- and Medium-scale Testing and Analysis. 11th International Symposium on Rock Fragmentation by Blasting / Sydney, Nsw, 24–26 August 2015.

Katsabanis, P.D., Omidi, O., Rielo, O., Ross, P., 2014a. A review of timing requirements for optimization of fragmentation, presented to ISEE Annual Conference on Explosives and Blasting Technique, Denver, 9–12 February.

Katsabanis, P.D., Omidi, O., Rielo, O., Ross, P., 2014b. Examination of timing requirements for optimization of fragmentation using small scale grout samples. Blasting and Fragmentation, Volume 8 İssue 1, pages 35–54.

Katsabanis, P.D., Tawadrous A., Braun A., Kennedy C., 2006. Timing effects on the fragmentation of small blocks of granodiorite. FRAGBLAST International Journal for Blasting and Fragmentation, 10(1–2):83–93.

Kick, F.,1885. Das Gesetz der proportionalen Widerstande und seine anwendung felix, Leipzig.

Krause, V., 2016. Kalumbila Minerals reactive ground. BME Internal report to Kalumbila Mine management. Kalumbila, Zambia.

Kuznetsov, V. M., 1973. The Mean Diameter of the Fragments Formed by Blasting Rock. Soviet Mining Science. Volume 9(2) , pp. 144–148. USSR.

Kwangmin, K., 2006. Blasting Design Using Fracture Toughness and Image Analysis of the Bench Face and Muckpile. Master's thesis. Virginia Polytechnic Institute and State University. Virginia, USA.

Lam, M., Jankovic, A., Valery, W., Kanchibotla, S., 2001. Maximizing Sag Mill Throughput at Porgera Gold Mine by Optimizing Blast Fragmentation. SAG 2001 Conference, University of British Columbia Vancouver, B. C., Canada.

Levin, J., 1992. Indicators of grindability and grinding efficiency. Southern African Institute of Mining and Metallurgy, Johannesburg 92 (10), 283–289.

Lilly, P.A., 1986. An Empirical Method of Assessing Rock Mass Blastability. Large Open Pit Mining conference, AusIMM/EAAust, Newman, pages 89-92.

REFERENCES (continued)

Lilly, P.A., 1994: The use of the blastability index in the design of blasts for open pit mines.

Lu, W., Leng, Z., Chen, M., Yan, P., Hu, Y., (2016). A modified model to calculate the size of the crushed zone around a blast-hole. The Journal of The Southern African Institute of Mining and Metallurgy. Volume 116 pages 413-422.

McKee, D. J., 2013. Understanding Mine to Mill. The Cooperative Research Centre for Optimising Resource Extraction (CRC ORE), Sir James Foots Building, University of Queensland St Lucia, Brisbane Australia.

Modular, 2019. Modular mine system, http://www.modularmining.com/product/provision/#tab-3 (25.01.2019).

Monjezi, M., Rezaei, M., Yazdian, V.A., 2009. Prediction of rock fragmentation due to blasting in Gol-E-Gohar iron mine using fuzzy logic. International Journal of Rock Mechanics & Mining Sciences. Volume 46, pages 1273–1280.

Morrell, S., 2004a. An alternative energy-size relationship to that proposed by bond for the design and optimisation of grinding circuits. International Journal Mineral Process. 74, 133–141.

Morrell, S., 2004b. Predicting the specific energy of autogenous and semi-autogenous mills from small diameter drill core samples. Minerals Engineering (17/3), 447–451.

Morrell, S., 2008. A method for predicting the specific energy requirement of comminution circuits and assessing their energy utilisation efficiency. Minerals Engineering 21 (2008) 224–233.

Morrell, S., 2009. Predicting the overall specific energy requirement of crushing, high pressure grinding roll and tumbling mill circuits. Minerals Engineering 22 (2009) 544–549.

Napier-Munn, T.J., Morrell, S., Morrison, R.D., Kojovic, T., 1996. Mineral Comminution Circuits Their Operation and Optimisation. Brisbane, Queensland: University of Queensland.p.66 - 99.

Omnia Group (Pty) Ltd, 2017. Xplolog™ Surface, Software & Information Technology.

REFERENCES (continued)

Onederra, I., Esen, S., Jankovic, A., 2004 Estimation of fines generated by blasting – applications for the mining and quarrying industries. Article in Transactions of the Institution of Mining and Metallurgy, Section A: Mining Technology.

Orica, 2013a. Drill and Blast Study Report, Sentinel Open Cut. Kalumbila, Zambia.

Orica, 2013b. A briefing note on reaction ground - version 6. [Online] Available:https://www.oricaminingservices.com/uploads/Briefing_Note_Reactive_Ground_Vers_6.pdf (10.12.2018).

Orica, 2015. Drill and Blast Review, Sentinel Mine. Kalumbila, Zambia.

Otterness, R. E., Stagg, M.S., Rholl, S.A., 1991. Correlation of shot design parameters to fragmentation. In Proceedings ISEE Annual Conference on Explosives and Blasting Research, pp 179–191. International Society of Explosives Engineers: Cleveland.

Ouchterlony, F., 2005. The Swebrec function: linking fragmentation by blasting and crushing. Mining Technology. Transaction of the Institute of Mineral and Metal. Volume 114, pages A29–A44.

Ouchterlony, F., 2010. Fragmentation characterization; the Swebrec function and its use in blast engineering Rock Fragmentation by Blasting – Sanchidrián (ed). © 2010 Taylor & Francis Group, London, ISBN 978-0-415-48296-7.

Palmström, A., 1974. Characterization of jointing density and the quality of rock masses. Internal report. Norway: A.B. Berdal; 1974 (in Norwegian)

Palmström, A., 2002. Measurement and characterization of rock mass jointing. In: Sharma VM, Saxena KR, editors. In-situ characterization of rocks. Lisse: A.A. Balkema; 2002. p. 49e98.

Priest, S.D., Hudson, J., 1976. Discontinuity spacing in rock. International Journal of Rock Mechanics and Mining Sciences & Geomechanics Abstracts 1976; 13(5): 135–48.

Renner, D., La Rosa, D., DeKlerk, W., Valer, W., Sampson, P., Noi, S.B., Jankovic, A., 2006.. AngloGold Ashanti Induapriem mining and milling process integration and optimisation. International Conference on Autogenous and Semi-autogenous Grinding Technology, Vancouver, Canada. Volume: Volume 1, 249 – 256.

REFERENCES (continued)

Rossmanith, H.P., 2003. The Mechanics and Physics of Electronic Blasting. In Proceedings of the 33rd Conference on Explosives and Blasting Technique. ISEE, Nashville, TN.

Rossmanith, H.P., Uenishi, K., Hochholdinger-Arsic, V., 2009. Waves, fractures and boundary effects associated with blast experiments conducted in cylindrical and block type specimens. Proceedings of the Ninth International Conference on Rock Fragmentation by Blasting – Fragblast 9 (ed: J A Sanchidrián), pp 407–414. Taylor and Francis Group: London.

Rowland, Jr., C.A., Kjos, D.M., 1978. Rod and ball mills. In: Mular, Bhappu, (Eds.), Mineral Processing Plant Design. SME, New York, pp. 239– 278. revised 1980, Chapter 12.

Rusnak, J.A., Mark, C., 2000. Using the point load test to determine the uniaxial compressive strength of coal measure rock. Research gate article, (10.09.2018).

Rybinski E., Ghersi, J., Davila, F., Linares, J., Valery, W., Jankovic, A., Valle, R., Dikmen, S., 2011. Optimisation and Continuous Improvement of Antamina Comminution Circuit. Compañía Minera Antamina S.A Derby 055, torre 1, piso 8, oficina 801, Santiago de Surco Lima 33, Perú.

Sen, Z., Kazi, A., 1984. Discontinuity spacing and RQD estimates from finite length scanlines. International Journal of Rock Mechanics and Mining Sciences & Geomechanics Abstracts 1984;21(4):203e12.

Simmons, M., 2015. Kalumbila Mine Reactive Ground Testing. RG-14-0062. Orica Australia Pty Ltd Internal Report to Kalumbila Mine Management. Kalumbila, Zambia.

SMC Testing, 2019a. The most widely-used comminution test in the world for AG & SAG Mills, HPGRs and Crushers. https://www.smctesting.com/tools (10.02.2019).

SMC Testing, 2019b. Using the SMC Test® to predict comminution circuit performance.

Spathis A.T., 2004. A Correction relating to the Analysis of the Original Kuz-Ram Model. Fragblast, Volume 8, No 4, pp 201-205.

Spathis, A.T., 2013. A three-parameter rock fragmentation distribution. Measurement and Analysis of Blast Fragmentation – Sanchidrián & Singh (Eds).© 2013 Taylor & Francis Group, London, ISBN 978-0-415-62140-3.

REFERENCES (continued)

Split online system 2019. . https://www.spliteng.com/products/split-online-systems/ (28.02.2019).

Stagg, M.S., Nutting, M.J., 1987. Blast delay influence on rock fragmentation; one-tenth scale tests. USBM IC 9135, pp 79–95.

Stagg, M.S., Rholl, S. A., 1987. Effects of accurate delays on fragmentation for single-row blasting in a 6.7 m (22 ft) bench. Proceedings of the Second International Conference on Rock Fragmentation by Blasting – Fragblast 2, Keystone, pp 210–223.

Szuladzinski, G., 1993. Response of rock medium to explosive borehole pressure. Proceedings of the Fourth International Symposium on Rock Fragmentation by Blasting-Fragblast-4, Vienna, Austria. p. 17–23.

Valery, W., Jankovic, A., La Rosa, D., Dance, A., Esen, S., Colacioppo, J., 2007. Process integration and optimization from mine-to-mill. Metso Minerals Process Technology Asia-Pacific, Brisbane, Australia.

Valery, W., Jankovic, A., Sonmez, B., 2011. New methodology to improve productivity of mining operations. Metso Minerals Process Technology Asia-Pacific, Brisbane, Australia.

Valery, W., Vale, R., Duffy, K., Jankovic, A., Tabosa, E., (2016). Complete Optimisation from Mine-to-Mill to Maximize Profitability. Hatch, 61 Petrie Terrace, Brisbane 4000, Queensland, Australia.

Van Jaarsveld, P., and Van Greunen, P., 2013. Dealing with reactive ground. BME, a member of the Omnia group. BME conference 2013, Gauteng.

von Rittinger, P., 1867. Lehrbuch der Aufbereitungskunde in ihrer neuesten Entwickelung und Ausbildung systematisch dargestellt.

Vovk, A., Mikhalyuk, A., Belinskii, I., 1973. Development of fracture zones in rocks during camouflet blasting. Soviet Mining Science 1973;9(4):383–7.

Walker, W.H., Lewis, W.K., Mcadams, W.H., Gilliland, E.R. Principles of Chemical Engineering. McGraw-Hill, NY, USA. 1937.

Whiten, W.J., 1972.The simulation of crushing plants with models developed using multiple spline regression. Journal of the South African Institute of Mining and Metallurgy. xx(x). p. 257 – 264.

REFERENCES (continued)

Whiten, W.J., 1974. A matrix theory of comminution machines. Chemical Engineering Science, No. 29: 585 599.

Wines, D., Lilly, P., 2002. Measurement and analysis of rock mass discontinuity spacing and frequency in part of the Fimiston Open Pit operation in Kalgoorlie, Western Australia: a case study. International Journal of Rock Mechanics & Mining Sciences, (pp. 589 -602).

Xstract Mining Consultants.,2012. Preliminary Geotechnical Stability Review of the Sentinel Open Pit Footwall. Report to Kalumbila Minerals Ltd. Kalumbila, Zambia.

Xstract Mining Consultants, 2014. Sentinel Open Pit Geotechnical Design Study. Report to Kalumbila Minerals Ltd. Kalumbila, Zambia.

Xstract Mining Consultants, 2015. Sentinel Open Pit, Geotechnical Design Study. Report to Kalumbila Minerals Ltd.

Yamamoto, M., Ichijo, T., Inabe, T., Morooka, K., Kaneko, K., 1999. Experimental and theoretical study on smooth blasting with electronic delay detonators. 3rd International Symposium on Rock Fragmentation by Blasting.

Zhang, L., 2016. Determination and applications of Rock Quality Designation (RQD). Journal of Rock Mechanics and Geotechnical Engineering, doi:10.1016/j.jrmge.2015.11

APPENDIXES

APPENDIX A

Sentinel Mine drilling fleet

CAT MD6640

EPIROCK PIT VIPER 217

SANDVIK D25K *(Not actual)*

FURUKAWA DRC20 *(Not actual)*

APPENDIX B

Explosives and Blasting accessories used at Sentinel Mine

BME PRODUCTS

INNOPAK Megamite packaged explosive

Viper Booster

INNOVEX™ 100

INNOVEX™ Lateral

INNOVEX™ 207

AXXIS EDD

AXXIS blasting box

AXXIS Logger

AXXIS Line Tester

APPENDIX C

Calculations for fragmentation models

Fragmentation model input parameter

A detailed calculation of the input parameter of the 5 fragmentation models is given below.

Table C.1. Fragmentation models input parameters

Material Hardness	Very Hard
Drill and Blast Parameters	Units
Material density, ρ_{rock}	2.70 g/cc
Hole Diameter, *D = 23 BH*	270 mm
Bench Height, *BH*	12.0 m
Burden, *B = 22D*	5.9 m
Spacing, *S = 1.15 B*	6.8 m
Spacing factor = *S/B*	1.15
Pattern Type (Square or Staggered)	Staggered
Subdrill, *Su = 15 D*	4.1 m
Hole Length, *L = BH + Su*	16.1 m
Stemming, *St = 17D*	4.6 m
Charge Length, C_{leng} *= L - St*	11.5 m
Scaled depth of burial, *SDOB*	1.03
Explosive type	INNOVEX™ 207
Explosive density, ρ_{expl}	1.23g/cc
Relative Weight Strength ,*RWS*	98%
Absolute Energy of ANFO, AWS_{ANFO}	2.30 MJ /kg
Velocity of detonation of explosives, *VoD*	5000m/s
Compressive strength, σ_c	100 Mpa
Youngs Modulus, *E*	42.2 Gpa
Poisson's ratio, *v*	0.25
Insitu Block Size	0.7 m
Rock Mass Description, *RMD*	JF
Joint Spacing, *JS*	0.4 m
Joint Plane Angle, *JPA*	20
Joint Condition Factor, *JCF*	1.5
Joint Plane Spacing, *JPS*	80
Rock correction factor, *C(A)*	0.7

Table C.1. Input parameters (Continued)

Standard deviation of drilling accuracy, *SD*	0.50m
Drill pattern factor	1.1
Inter-hole delay, *T*	51.0 ms
Standard deviation of IS, σ_t	1.0 ms
Dynamic tensile strength factor, f	6
Adiabatic gas expansion coefficient, γ	1.2

Volume of rock per hole, V_r

$V_r = B \times S \times BH$ $V_r = 5.9 \times 6.8 \times 12 = 487\ m^3$

Tonnes of rock per hole, T_r

$T_r = V_r \times \rho_{rock}$ $T_r = 487\ m^3 \times 2.70g/cc = 1{,}315$ tonnes

Drill productivity, *DrillProd*

$DrillProd = \frac{V_r}{L}$ $DrillProd = \frac{487\ m^3}{16.1} = 30m^3/m$

Mass of charge per hole, $\mathbf{M_c}$

$M_c = V_c \times \rho_{exp}$ $M_c = \left(\frac{270^2}{4000}\right)\pi \times 11.5 \times 1.23 = 807.06kg$

Powder Factor, *PF*

$PF = \frac{M_c}{V_r}$ $PF = \frac{807.06kg}{1{,}315\ t} = 0.61kg/t$

Relative Bulk Strength of explosive, *RBS*

$RBS = \frac{\rho_{expl} \times RWS}{0.8}$ $RBS = \frac{1.23g/cc \times 98\%}{0.8} = 151\%$

Explosive Energy, *EE*

$EE = RWS \times M_c \times \frac{AWS_{ANFO}}{100}$ $EE = 98\% \times 807.06kg \times \frac{2.30MJ/kg}{100} = 1819.12MJ$

Energy Factor , *EF*

$EF = \frac{EE}{T_r}$ $EF = \frac{1819.12\ MJ}{1315t} = 1.38MJ/tonne$

Theoretical detonation pressure, P_d

$P_d = 0.25 \times \rho_{exp} \times VoD^2 \times 10^6$ $P_d = 0.24 \times 1.23g/cc \times 5000m/s \times 10^6 = 7.69GPa$

Tensile Strength ,T_s

$T_s = \frac{\sigma_c}{12}$ $T_s = \frac{100}{12} = 8.3$ Mpa

Joint Factor, *JF*

JF = (JCF ×JPS) + JPA *JF* = (1.5 ×80) +20 = 140

Rock Density Influence, *RDI*

RDI = (25 × ρ_{rock}) – 50 *RDI* = (25 × 2.7g/cc) – 50 = 17.5

Hardness Factor, *HF*

HF = if E<50, $\frac{E}{3}$ *; if E>50,* $\frac{\sigma_c}{5}$ HF= $\frac{42.2}{3}$ = 14.07

Rock Mass Factor, *A*

A = 0.06 × (RMD + RDI + HF) - C(A) A= 0.06 × (140 +17.5 + 14.07) – 0.7 = 9.59

p-wave velocity , *PWv*

$$PW_v = \frac{E}{\upsilon}\left(\frac{1-\upsilon}{(1+\upsilon)\times(1-2\upsilon)}\right)^{0.5} \times 1000$$

$$PW_v = \frac{42.2}{2.7\text{g/cc}} \times \left(\frac{1-0.25}{(1+0.25)\times(1-(2\times0.25))}\right)^{0.5} \times 1000 = 4{,}331 \text{ m/s}$$

s-wave velocity , *SWv*

$$SW_v = \frac{E}{\upsilon}\left(\frac{1}{2(1+\upsilon)}\right)^{0.5} \times 1000 \qquad SW_v = \frac{42.2}{0.25}\left(\frac{1}{2(1+0.25)}\right)^{0.5} \times 1000 = 2{,}500\text{m/s}$$

Optimum delay for maximum fragmentation, T_{max}

$$T_{max} = \left(\frac{15.6}{\frac{PW_v}{1000}}\right) \times B \qquad T_{max} = \left(\frac{15.6}{\frac{4{,}331}{1000}}\right) \times 5.9 = 21.4\text{ms}$$

Timing factor, A_t

$$A_t = 0.90 + \left(0.1 \times \left(\frac{T}{T_{max}} - 1\right)\right) \qquad A_t = 0.90 + \left(0.1 \times \left(\frac{51\text{ms}}{21.4\text{ms}} - 1\right)\right) = 1.04$$

Scatter ratio, R_s

$$R_s = 6 \times \left(\frac{\sigma_t}{T}\right) \qquad R_s = 6 \times \left(\frac{1.0\text{ms}}{51\text{ms}}\right) = 0.12$$

Timing uniformity factor, n_s

$$n_s = 0.206 + \left(\frac{1-R_s}{4}\right)^{0.8} \qquad n_s = 0.206 + \left(\frac{1-0.12}{4}\right)^{0.8} = 1.18$$

2. Fragmentation Models calculations

<u>Kuz-Ram Parameters, after Cunningham (1983, 1987)</u>

Uniformity index, *n*

$$n = \left[2.2 - 14\left(\frac{B}{D}\right)\right]\left[0.5\left(1 + \frac{S}{B}\right)\right]^{0.5}\left[1 - \frac{Z}{B}\right]\left[0.1 + \text{Abs}\left(\frac{(BCL_b - CCL_t)}{L}\right)\right]^{0.1}\left[\frac{L}{H}\right]C(A)$$

$$n = \left[2.2 - 14\left(\frac{5.9}{270}\right)\right]\left[0.5\left(1 + \frac{6.9}{5.9}\right)\right]^{0.5}\left[1 - \frac{0.5}{5.9}\right]\left[0.1 + \text{Abs}\left(\frac{11.5}{11.5}\right)\right]^{0.1}\left[\frac{11.5}{12}\right] \times 0.7 = 1.91$$

Energy per blasthole, Q

$$Q = M_c \times \frac{RWS}{100} \times 0.87 \qquad Q = 807.06\text{kg} \times \frac{98\%}{100} \times 0.87 = 688$$

Mean Fragment Size, x_m

$$x_m = A \times \left(\frac{V_r}{Q}\right)^{\frac{4}{5}} \times Q^{\frac{1}{6}} \qquad x_m = 9.59 \times \left(\frac{487}{688}\right)^{\frac{4}{5}} \times 688^{\frac{1}{6}} = 21.6\text{cm}$$

Characteristic Size (Uncorrected), xc

$$x_c = \frac{10 \times x_m}{\frac{Loge21}{n}} \qquad x_c = \frac{10 \times 21.6}{\frac{\text{Loge}2}{1.91}} = 262\text{mm}$$

Kuz-Ram Paramaters, after Spathis (2004)

Gamma function = $\Gamma(1+\frac{1}{n})$

$\Gamma(1+\frac{1}{1.91}) = 0.89$

Characteristic Size (Corrected), x_{c1} = dK/Γ(1+1/n)

$$x_{c1} = \frac{x_m}{\Gamma\left(1+\frac{1}{n}\right)} \qquad x_{c1} = \frac{21.6}{\Gamma\left(1+\frac{1}{1.91}\right)} = 244\text{ mm}$$

Swebrec Parameters, after Ouchterlony (2005)

Shifting Factor - Calculated, g(n)

$$g(n) = \frac{(\text{In}2)^{\frac{1}{n}}}{\Gamma\left(1+\frac{1}{n}\right)} \qquad g(n) = \frac{(\text{In}2)^{\frac{1}{1.91}}}{\Gamma\left(1+\frac{1}{1.91}\right)} = 0.93$$

50% Passing size (g(n) = 1), x_{50}

$$x_{50} = g(n) \times A \times Q^{\frac{1}{6}} \times \frac{\left(\frac{115}{RWS_{ANFO}}\right)^{\frac{19}{30}}}{PF^{0.8}} \times 10$$

$$x_{50} = 1 \times 9.59 \times 688^{\frac{1}{6}} \times \frac{\left(\frac{115}{98\%}\right)^{\frac{19}{30}}}{1.66^{0.8}} \times 10 = 216\text{mm}$$

Fragment size upper limit, x_{max}

$x_{max} = 1000 \times Insitu\ block\ size$ $\qquad x_{max}$ = 1000×0.7= 700mm

Curve-undulation parameter, *b*

$$b = \left[2\text{In}2\text{In}\left(\frac{x_{max}}{x_{50}}\right)\right]n \qquad b = \left[2\text{In}2\text{In}\left(\frac{700mm}{216mm}\right)\right] \times 1.91 \ = 3.10$$

Swebrec Parameters, after Ouchterlony (2005)

50% Passing size , with calculated g(n), x_{50}

$$x_{50} = g(n) \times A \times Q^{\frac{1}{6}} \times \frac{\left(\frac{115}{RWS_{ANFO}}\right)^{\frac{19}{30}}}{PF^{0.8}} \times 10$$

$$x_{50} = 0.93 \times 9.59 \times 688^{\frac{1}{6}} \times \frac{\left(\frac{115}{98\%}\right)^{\frac{19}{30}}}{1.66^{0.8}} \times 10 = 201\text{mm}$$

Curve-undulation parameter, *b*

$$b = \left[2In2In\left(\frac{x_{max}}{x_{50}}\right)\right] \times n \qquad b = \left[2\text{In}2\text{In}\left(\frac{700}{201}\right)\right] \times 1.91 \ = 3.30$$

JKMRC Crush Zone Model, after Esen et al., (2003) and Onederra et al., (2004)

Crushed Zone

Rock stiffness, *K*

$$K = \frac{E_d}{1+\nu_d} \qquad K = \frac{42.2\text{GPa}}{1+0.25} \ = 33,760,000,000\text{Pa}$$

Borehole Pressure, P_b

$P_b = P_d \times 0.85$ $\qquad P_b = 7.69\text{GPa} \times 0.85 = 6,534,375,000\text{Pa}$

Crushing zone index, *CZI*

$$CZI = \frac{(P_b)^3}{(K) \times \sigma_c^2} \qquad CZI = \frac{(6,534,375,000)^3}{33,760,000,000 \times (100 \times 1,00,000)^2} = 826.4$$

Radius of crush zone, r_c

$r_c = 0.812 \times r_o \times (CZI)^{0.219}$ $\qquad r_c = 0.812 \times \frac{270}{2} \times (826.4)^{0.219} = 477\text{mm}$

Volume of fines in crushed zone, V_{fine}

$$V_f = \left[\pi\left(\frac{r_c}{1000}\right)^2 - \pi\left(\frac{D}{2000}\right)^2\right] \times C_{leng}$$

$$V_f = \left[\pi\left(\frac{477}{1000}\right)^2 - \pi\left(\frac{270}{2000}\right)^2\right] \times 11.5 = 7.54m^3$$

Breakage Zone

Pressure decay factor, φ

$$\varphi = [(0.0083E) + 0.9955] \times \left(\frac{PW_v}{VOD}\right)^{-0.33}$$

$$\varphi = [(0.0083 \times 42.2) + 0.9955] \times \left(\frac{4{,}331}{5{,}000}\right)^{-0.33} = -1.42\text{mm}$$

Equilibirum pressure, P_{eq}

$$P_{eq} = P_b \left(\frac{r_c}{\frac{D}{2}}\right)^{\emptyset}$$

$$P_{eq} = 6{,}534{,}375{,}000 \times \left(\frac{477mm}{\frac{270mm}{2}}\right)^{-1.42} = 1{,}087{,}581{,}725\ Pa$$

Length of cracks, C_l

$$C_l = \frac{D}{2} \times \left(\frac{T_S \times 1{,}000{,}000}{P_{eq}}\right)^{\frac{1}{\emptyset}} - r_c$$

$$C_l = \frac{270}{2} \times \left(\frac{8.3 \times 1{,}000{,}000}{1{,}087{,}581{,}725}\right)^{\frac{1}{-1.42}} - 477 = 3{,}694\text{mm}$$

Dynamic tensile strength, T_d

$$T_d = T_s \times f \qquad T_d = 8.3 \times 6 \times 1{,}000{,}000 = 50{,}000{,}000\ \text{Pa}$$

Strain at borehole wall, $\mathcal{E}_s$

$$\varepsilon_s = \frac{P_b \times (1-\upsilon)}{2\{[(1-2\upsilon)] \times (1000 \times \rho_{rock}) \times PW_v^2\} + [3P_b \times \gamma \times (1-\upsilon)]}$$

$$\varepsilon_s = \frac{6{,}534{,}375{,}000 \times (1 - 0.25)}{2\{[(1 - (2 \times 0.25))] \times (1000 \times 2.7) \times 4{,}331^2\} + [3 \times 6{,}534{,}375{,}000 \times 1.2 \times (1 - 0.25)]}$$

$$\varepsilon_s = 0.07$$

Number of near field radial cracks, C

$$C = \varepsilon_s \times \frac{P_b}{T_d} \qquad C = 0.07 \times \frac{6{,}534{,}375{,}000}{50{,}000{,}000} = 9.4$$

Volume of fines in breakage zone, V_b

$$V_b = \left\{\left[\left[\frac{\left(\left(\cos\left(\frac{360}{2C}\right)\times\left(\frac{r_c}{1000}\right)\right)\times\left(\sin\frac{320}{2C}\times\frac{r_c}{100}\right)\right)}{2}\right]+\left[\frac{\left(\left(\left(\sin\left(\frac{360}{2C}\right)\times\frac{r_c}{1000}\right)\times\left(\frac{C_l+r_c}{1000}\right)\right)-\left(\cos\left(\frac{360}{2C}\right)\times\left(\frac{r_c}{1000}\right)\right)\right)}{2}\right]\right]\times\left(\frac{r_c}{1000}\right)^2\right\}\times CL$$

$$V_b = \left\{\left[\left[\frac{\left(\left(\cos\left(\frac{360}{2\times9.4}\right)\times\left(\frac{477}{1000}\right)\right)\times\left(\sin\left(\frac{320}{(2\times9.4)}\right)\times\frac{477}{100}\right)\right)}{2}\right]+\left[\frac{\left(\left(\left(\sin\left(\frac{360}{(2\times9.4)}\right)\times\frac{477}{1000}\right)\times\left(\frac{11.5+477}{1000}\right)\right)-\left(\cos\left(\frac{360}{(2\times9.4)}\right)\times\left(\frac{477}{1000}\right)\right)\right)}{2}\right]\right]\times\left(\frac{477}{1000}\right)^2\right\}\times 11.5$$

$$V_b = 26.97m^3$$

Fines inflection point (% fines <1 mm), f_c

$$f_c = \frac{V_c+V_b}{V_r} \qquad f_c = \frac{7.54+26.97}{487} = 7.1$$

Uniformity index of fines, n_f

$$n_f = \frac{LN\left[\frac{-LN(1-f_c)}{LN(2)}\right]}{LN\left[\frac{0.001}{\frac{x_m}{100}}\right]} \qquad n_f = \frac{LN\left[\frac{-LN(1-7.1)}{LN(2)}\right]}{LN\left[\frac{0.001}{\frac{21.6}{100}}\right]} = 0.42$$

APPENDIX D

Drill productivity

Table D.1. Drill productivity input parameters

Parameters	**Value**
Burden, *B*	5.9m
Spacing, *S*	6.8m
Subdrill,*Su*	4.1m
Diameter, *D*	270mm
Hole length, *HL*	16.1m
Volume of rock per hole, V_r	402 bcm
Scheduled work hours, Sch_{hr}	8,448 hours
Availability, *A*	90%
Utilisation, *U*	80%
Redrill allowance, R_a	5%
Penetration rate, Pen_{Rate}	25 m/ophr
Required material production, *Tag*	50,000,000 bcm

Utilisation of Availability, $U_{of}A$

$U_{of}A = A \times U$ $U_{of}A$= 90% ×80% = 72%

Drill Operating Hours, ophr

$ophr = Sch_{hr} \times U_{of}A$ $ophr$ = 8,448 ×72% = 6,083 ophr/drill

Number of meters/drill, m_{Drill}

$m_{Drill} = ophr \times Pen_{Rate} \times (1+R_a)$ m_{Drill} = 6,038 × 25×(1+5%)= 159,667.20

Number of holes/drill,

$$No.Holes_D = \frac{\left(\frac{No.meters/drill}{1+R_a}\right)}{HL} \qquad No.Holes_D = \frac{\left(\frac{159{,}667.20\text{m}}{1+5\%}\right)}{16.1\text{m}} = 9{,}474 \text{ hole}$$

Material produced/drill, Mat_{Drill}

$Mat_{Drill} = No.Hole_D \times V$ Mat_{Drill} = 9,474 holes × 485bcm = 4,592,276 bcm

Required blast holes, Req_B

$$Req_B = \frac{Tag}{V_r} \qquad Req_B = \frac{50{,}000{,}000 \text{ bcm}}{485 \text{ bcm/hole}} = 113{,}471 \text{ holes}$$

Drill Productivity, $Prod_{Drill}$

$$Prod_{Drill} = \frac{V_r}{HL} \qquad Prod_{Drill} = \frac{458}{16.1} \times 100 = 3{,}020\%$$

Required drill meters, Req_m

$$Req_m = \frac{Tag}{Prod_{Drill}} \times (1 + R_a) \qquad Req_m = \frac{50{,}000{,}000}{3{,}020\%} \times (1 + 5\%) = 1{,}912{,}275\text{m}$$

Number of drills required (Rounded up)

$$No.Drill = \frac{Tag}{Mat_{Drill}} \qquad No.Drill = \frac{50{,}000{,}000\ \text{bcm}}{4{,}592{,}276\ \text{bcm/drill}} = 12\text{Drills}$$

APPENDIX E

Drilling and Blasting Cost

Table E.1. Blasting accessories prices

Resource	Quantity/hole	Cost
Bulk product (INNOVEX^{TM} 207)	810 kg	$890.00 /t
EDD 20m	1	$18.70 /unit
Primer 400g	1	$5.70 /unit
Surface wire	0.005	$82.50 /Roll
Blasting accessories - liners, etc.	1	$5.00 /unit
Stemming	0.26 m³	$15.00 /t
Drilling	16.0 m	$10.42 /m
Total Comminution Cost		$2.28/tonne

Bulk Explosive cost

$$\frac{810\text{kg/hole} \times \$890/\text{t}}{1000} = \$718.29/\text{hole} \qquad \frac{\$718.29/\text{hole}}{1{,}315\text{t/hole}} = \$0.55/\text{tonne}$$

Initiating Explosives cost

$18.70 + $5.70 + (0.005 × $82.50) = $24.81/hole

$$\frac{\$24.81/hole}{1{,}3145t/hole} = \$0.0189/\text{tonne}$$

Total Blasting cost

Bulk explosive cost + Initiation explosive cost+ Accessories cost

$718.29 + $24.81 + $5 = $748.10/hole

$0.55 + $0.0189 + $0.0038 = $0.57/tonne

Stemming

0.263 m³ × $15.00/t = $3.94/hole $\qquad \frac{\$3.94/\text{hole}}{1{,}315\text{t/hole}} = \$0.0030/\text{tonne}$

Drilling Cost

16.1m × $10.42/m = $167.76/hole $\qquad \frac{\$167.76/\text{hole}}{1{,}315\text{t/hole}} = \$0.13/\text{tonne}$

Total Drilling Cost

Stemming + Drilling Cost = $3.94+ $167.67= $171.61/hole

$0.0030 + $0.13 = $0.133/tonne

Total Drill and Blast cost

Total Blasting cost + Total Drill cost = $748.10 + $171.61 = $924.8/hole

$$= \frac{\$924.8/\text{hole}}{1{,}315\text{t/hole}} = \$0.71/\text{tonne}$$

Total Operating Cost

Drill cost, Blast blasting + Comminution cost = $0.71 + $2.28 = **$2.99/tonne**

APPENDIX F

Specific Energy calculations

Table F.1. Operating parameter

Parameter	**Value**
Pebble	Yes
Crusher product P_{80}= SAG mill feed P_{80}	177 mm
SAG product P_{80}	600 µm
Final Product P_{80}= Cyclone overflow	212 µm
Closed screen size, P_1	300 µm
Pebble crusher feed	52 µm
X_2	750 µm

Table F.2. Test data; Source: ALS.

Parameter	**Value**
Dw_i	6.49 kWh/m^3
M_{ia}	18.2 kWh/t
M_{ic}	6.93 kWh/t
M_{ib}= BW_i	17.5 kWh/t
M_{ih}	13.4 kWh/t
G_{pb}	1.69 g/rev
SG	2.8

Table F.3.Comminution energy calculation

Parameter	**Value**
f(X_1)=f(P_{80})	-0.2956
f(X_3)=f(f_{80})	-0.2952
f(Crusher feed P_{80})	-0.6150
Pebble presence constant, K	1
Open Circuit or Closed Circuit, $K2$	1.19
Coarse Particle Grinding Specific Energy, W_a^*	7.722 kWh/t
Fine Particle Grinding Specific Energy, W_b^{**}	4.518 kWh/t
Conventional Crusher Specific Energy, W_c^{***}	0.960 kWh/t
Total Comminution Specific Energy, W_T^{****}	**13.200 kWh/t**

$f(X_i) = -\left(0.295 + \frac{x_i}{1{,}000{,}000}\right)$

$f(X_1) = \text{f(P80)} = -\left(0.295 + \frac{600}{1{,}000{,}000}\right) =$ **-0.2956**

$f(X_2) = -\left(0.295 + \frac{750}{1{,}000{,}000}\right)$ **= -0.2958**

$f(X_3)\text{f(f80)} = -\left(0.295 + \frac{212}{1{,}000{,}000}\right)$ = **-0.2955**

Coarse Particle Grinding Specific Energy, *Wa*

$W_a = 0.95 * M_{ia} 4\left(X_2^{f(x_2)} - X_1^{f(x_1)}\right)$

$W_a = 0.95 \times 18.2 \times 4(750^{-0.2958} - 177{,}000^{-0.2956})$ = **7.82 kWh/t**

Fine Particle Grinding Specific Energy, *Wb*

$W_b = M_{ib} 4\left(X_3^{f(x_3)} - X_2^{f(x_2)}\right)$

$W_b = 17.5 \times 4 \times (212^{-0.2952} - 750^{-0.2958})$ = **4.52 kWh/t**

Conventional Crusher Specific Energy, *Wc*

$W_c = K_2 M_{ic} 4\left(X_2^{f(x_2)} - X_1^{f(x_1)}\right)$

$W_c = 1.19 \times 6.9 \times 4 \times (750^{-0.2958} - 320{,}000^{-0.6150})$ = **0.91 kWh/t**

Total Comminution Specific Energy

$W_T = W_a + W_b + W_c$

W_T= 7.82 + 4.52 + 0.91 = **13.25 kWh/t**